

**ESTIMATION OF NATURAL RADIOACTIVITY AND HEAVY METAL  
CONCENTRATION IN SOIL SAMPLES FROM RAYFIELD - DU MINING SITE JOS,  
NIGERIA**

**BY**

**ATIPO, Michael Kolawole**

**MTech/SPS/2017/7213**

**DEPARTMENT OF PHYSICS  
SCHOOL OF PHYSICAL SCIENCE  
FEDERAL UNIVERSITY OF TECHNOLOGY  
MINNA**

**SEPTEMBER, 2021**

**ESTIMATION OF NATURAL RADIOACTIVITY AND HEAVY METAL  
CONCENTRATION IN SOIL SAMPLES FROM RAYFIELD - DU MINING SITE JOS,  
NIGERIA**

**BY**

**ATIPO, Michael Kolawole**

**MTech/SPS/2017/7213**

**A THESIS SUBMITTED TO THE POSTGRADUATE SCHOOL FEDERAL  
UNIVERSITY OF TECHNOLOGY, MINNA, NIGERIA IN PARTIAL FULFILLMENT  
OF THE REQUIREMENTS FOR THE AWARD OF THE DEGREE OF MASTER OF  
TECHNOLOGY IN (APPLIED NUCLEAR PHYSICS)**

**SEPTEMBER, 2021**

## ABSTRACT

Mining of tin and other related activities have been active and thus leading to economic growth in the Jos area of Nigeria for more than a century. However, mining of minerals has been confirmed to enhance the concentrations of heavy metals and natural radioisotopes in the soil, air and water bodies in the environment. In an attempt to evaluate the radiological impact of NORM and heavy metals (HM) burdens resulting from tin mining activities at Rayfield-Du area of Jos. Specific activities of natural occurring radioactive nuclei ( $^{238}\text{U}$ ,  $^{232}\text{Th}$  and  $^{40}\text{K}$ ) and HM concentrations were evaluated in soil samples collected from the mining site. The soil samples were classified as normal soil (S), tailings (T) and mineral soils (M) and their corresponding mean activities for  $^{238}\text{U}$ ,  $^{232}\text{Th}$  and  $^{40}\text{K}$  were analysed using a well calibrated HPGe detector based gamma spectrometric system. While the HM concentrations in the soils were evaluated using Energy Dispersed X-ray Fluorescence spectrometric system. The mean activity concentration for  $^{238}\text{U}$ ,  $^{232}\text{Th}$  and  $^{40}\text{K}$  were 323.44, 877.63 and 864.99 Bqkg<sup>-1</sup>; 138.84, 469.31 and 578.65 Bqkg<sup>-1</sup>; and 168.83, 436.08 and 346.1 Bqkg<sup>-1</sup> respectively for M, T and S samples. The calculated radiation dose parameters for the soil samples were all higher than the recommended safety limit. For all the collected soil sample, the external hazard risk  $H_{ext}$  were 2.21, 2.81 and 4.44 for S, T and M respectively while the mean calculated radium equivalent was 819, 1057 and 1645 Bqkg<sup>-1</sup> for S, T, and M respectively. The excess life cancer risk (ELCR) estimated for the mine was more than the world average value. The radio ecological dose rate estimate for non-human biota in the mine revealed that all non-human species except lichen and bryophyte had absorbed dose rate less than the 10  $\mu\text{Gyh}^{-1}$  screening dose. Generally, the potential of developing radiation induced health defects as a result of high radiation absorbed dose rate by the miners and dwellers around the mine is very high. The analysis of eight HM (Cr, Cu, Zn, Pb, Co, As, Cd, and Ni) concentrations showed that they were above the Nigerian reference level except for Co and Ni. For S, T, and M soil classification, the pollution index of the considered HM concentration was 0.67, 1.49, and 0.71 respectively. The corresponding ecological risk indices was 102,172, and 56 for S, T, and M. These can be classified as low pollution except T soil with moderate potential ecological risk index.

## **TABLE OF CONTENTS**

Title Page	i
Declaration	ii
Certification	iii
Acknowledgements	iv
Abstract	v
Table of Contents	vii
List of Tables	x
List of Figures	xi
List of Plates	xiii
Abbreviation, Glossaries and Symbols	xiv

### **CHAPTER ONE**

1.0 INTRODUCTION	1
1.1 Background to the Study	1
1.2 Statement of the Problem	2
1.3 Aim and Objectives of the Study	4
1.4 Justification	4
1.5 Scope	6

### **CHAPTER TWO**

2.0 LITERATURE REVIEW	7
2.1 Ionising Radiation	7
2.2 Sources of Ionizing Radiation	9

2.2.1 Natural source of ionizing radiation	9
2.2.2 Human activities	9
2.2.3 Consumer products	10
2.2.4 Ionizing radiation in building materials	10
2.2.5 Monitoring natural radiation	11
2.3 Effect of Radiation in Biological System	11
2.3.1 Interaction of radiation with biological cells	13
2. 4 Chemistry of Direct Consequence of Irradiation	14
2.4.1 Physical stage	15
2.4.2 Physio – chemical stage	15
2.4.3 Chemical stage	16
2.4.4 Biological stage	17
2.5 Biological Effect	18
2.5.1 Stochastic and non-stochastic effects	19
2.6 Bio Effects on Human Embryo	22
2.7 Protection of Human from Radiation	23
2.8 Radiation Detectors	25
2.8.1 Gas filled detector	25
2.8.2 Scintillator detector	27
2.8.3 Scintillator detector principle	28
2.8.4 Semiconductor detector	30
2.9 Background Principle of Gamma Spectroscopy	32
2.9.1 Detector efficiency	34
2.9.2 Detector resolution	34
2.10 Radioactive Decay Kinetics and Equilibrium	34

2.11 X-Ray Fluorescence Spectrometry	41
2.12 Tin Mining in Nigeria	42
2.13 The Study Area	44
2.14 Geology of the Study Area	46
2.14.1 Basement complex	46
2.14.2 The younger granites	48
2.14.3 The basalts	51
2.14.4 Economic geology	13
2.15 Review of Previous Studies	52
2.15.1 Natural radioactivity in mines soils and environment	52
2.15.2 Heavy metals toxicology	57

### **CHAPTER THREE**

3.0 MATERIALS AND METHODS	60
3.1 MATERIALS	60
3.2 Methods	60
3.2.1 Site survey	60
3.3 <i>In-situ</i> Gamma Radiation Measurement	62
3.4 Gamma Spectrometric Analysis	64
3.4.1 Sample collection	64
3.4.2 Sample preparation	65
3.4.3 Gamma – activity measurement and spectra analysis	67
3.5 Evaluation of Radiological dose and risk Parameters	70
3.5.1 Absorbed dose rate ( $D$ )	70
3.5.2 Radium equivalent ( $R_{eq}$ )	70
3.5.3 Annual outdoor effective dose rate ( $E_{out}$ (mSv/y))	71

3.5.4 The external hazard index	71
3.5.5 Excess life cancer risk	71
3.6. Method of Radiological Impact Assessment	71
3.7 Heavy Metal Measurement	73
3.7.1 Energy dispersive X-ray fluorescence analysis	74
3.7.2 Sample analysis	74
3.7.5 Determination of analytes of interest using EDXRF spectrometric analysis	76
3.7.6 Calculation of concentrations	76

## **CHAPTER FOUR**

4.0 RESULTS AND DISCUSSION	77
4.1 <i>In- Situ</i> Gamma Radiation Level	77
4.2 Specific Activities Concentrations of NORM in Mine Soil Samples	84
4.3 Assessment of Radiological Hazard Parameters due to NORM Concentration	93
4.4 Radiological Impact of NORM Concentration on Non- human Biota	99
4.5 Heavy Metals Concentrations and Pollution Indices	102
4.5.1 Soil heavy metal pollution indices	103

## **CHAPTER FIVE**

5.0 CONCLUSION AND RECOMMENDATIONS	107
5.1 Conclusion	107
5.2 Recommendations	108
REFERENCES	110
APPENDIX	118

## LIST OF TABLES

Table	Page
2.1 Classification of ionising radiation	7
2.2 Average effective dose equivalent to adult man per year due to the different source of radiation worldwide	13
2.3 Somatic effects due to different level of Radiation	21
2.4 Acute Radiation syndrome due to different level of Radiation	22
2.5 Stages and effect of radiation on human embryo	23
2.6 Occupational and public exposure as recommended	25
2.7 Geological succession in Naraguta Area	46
2.8 Toxicology of Heavy Metal	59
4.1. Measured ADR, elevation, coordinate and calculated dose parameters of contaminated soil	77
4.2. Measured ADR, elevation, coordinate and calculated dose parameters in tailing areas	78
4.3. Summary of measured <i>in-situ</i> ADR, AEDR, ELCR and effective organ doses	83
4.4. Comparison of ADR with earlier research in other places	83
4.5 Specific activities of NORM in S soils	85
4.6 Specific activities of NORM in T soils	85
4.7 Specific activities of NORM in M soils samples	86
4.8. Summary of activity Concentrations in soil due to mining in Jos and other places in Nigeria	91
4.9. Radiological hazard indices due to NORM concentration in S samples	94
4.10. Radiological hazard indices due to NORM concentration in T samples	94
4.11. Radiological hazard indices due to NORM concentration in M samples	95
4.12. Correlation coefficient between NORM and radiation safety indices	97
4.13. Risk quotients for considered terrestrial organisms	102
4.14. Heavy metal concentration in S, M and T soil samples and pollution indices	103

## LIST OF FIGURES

Figure	Page
2.1: Schematics of a Gas Filled Detector	27
2.2: Block Diagram of Scintillating Detector	28
2.3: Schematic Diagram of Semi-Conductor Detector	32
2.4: Schematic Diagram of HPGE Detector	33
2.5: Decay chain of $^{238}\text{U}$ (4n+2 series)	37
2.6: Decay chain of $^{235}\text{U}$ (4n+3 series)	38
2.7: Decay chain of $^{232}\text{Th}$ (4n series)	39
2.8: Decay chain of $^{237}\text{Np}$ (4n+1 series)	40
2.9: Schematic diagram of EDXRF	42
2.10: Map of the Study Area Rayfield – Du Jos, Plateau	44
2.11: Digitised Geological Map of Jos	47
2.12: Digitised Geological Map of Naraguta Sheet	47
3.1: Location Map of the Study Area with sampling points identified	61
3.2: Soil, Mineral Soil, and tailings collection point	64
3.3: Energy Calibration Curve of the Detector	68
3.4: Efficiency Calibration Curve of the Detector System	68
3.5: ERICA (Version 1.2.1) Graphic User Interface	73
4.1: Spatial Distribution (a) Elevation (b) ADR (c) ELCR, (d) AEDR Across mine	80
4.2: Mean distribution of $^{238}\text{U}$ , $^{232}\text{Th}$ , and $^{40}\text{K}$ specific activity concentrations in soil samples	88
4.3: Spatial distribution of $^{238}\text{U}$ , activities for the sample location	92
4.4: Spatial distribution of $^{232}\text{Th}$ activities concentration of sampled location	92
4.5: Spatial distribution of $^{40}\text{K}$ activities concentration of sample location	93
4.6: Variation of the mean radiological parameters of all the soil classes	97

4.7: Spatial distribution of ADR due to NORM concentration in the mine	98
4.8: Relationship between In – situ ADR and Ex – situ ADR	99
4.9: Total dose rate per organism calculated from ERICA	101
4.10: Pollution index of HM in the S, T, and M Soils	105
4.11: Potential Ecological Risk Index of the HM in Soils	106

## LIST OF PLATES

Plate	Page
I: Multipurpose Survey Meter RDS – 30	63
II: GPS Map 76CSX	63
III: Raw Soil Sample	65
IV (a) Agate Mortar	66
IV (b) Sieve (500 nm mesh)	66
V: Marinell Beakers (500g)	
VI: HPGe setup at the National Institute of Radiation Protection and Research (NIRPR), Ibadan, Nigeria	67
VII: Pellet Beaker 20g	73
VIII: EDXRF Machine	75

## ABBREVIATIONS AND ACRONYMS

Cu	Copper
Fe	Iron
U	Uranium
Th	Thorium
Sn	Tin
K	Potassium
Ni	Nickel
GUI Graphic	Graphic User Interface
NORM	Naturally Occuring Radioactive Material
Pb	Lead
UNSCEAR	United Nations Committee on Effects of Atomic Radiations
Zn	Zinc
Cd	Cardium
As	Arsenic
Co	Cobalt
RQ	Risk Quotients
EDXRF	Energy Dispersive X-ray Fluorescence
NGRL	Nigerian Geoscience Research Laboratory
IR	Ionising Radiation
ELCR	Excess Life Cancer Risk
AEDR	Annual Effective Dose Rate
ADR	Annual Dose Rate
AGDR	Annual Gonadal Dose Rate
T	Tailing
S	Normal Soil Sample
M	Mineral Soil
BDL	Below Detection Limit
NNRA	Nigerian Nuclear Regulatory Authority
UV	Ultra Violet

NCRP	National Council on Radiation Protection
NRCCBEIR	National Research Council Committee on Biological Effect of Ionising Radiation
IAEA	International Atomic Energy Agency
ICRP	International Commission on Radiation Protection
IARC	International Agency for Research on Cancer
CDC	Centre for Disease Control
UNSCEAR	United Nations Scientific Committee on Effect of Atomic Radiation
USDoE	United State Department of Education
DPR	Department of Petroleum Resources
WHO	World Health Organisation
SIPRI	Stockholm International Peace Research Institute

## APPENDIX

Appendix	Page
A1. Active Mining site1	118
A2. Residential house 150 m away from active mine site 2	118
A3. Active mine site3	119
A4. Sample of extracted tin product	119
A5. Abandoned mine site	120
A6. Goggle earth map of the study area	120
A7. Active mine site 4	121
A8. Active mine site 5	121

## CHAPTER ONE

### 1.0

### INTRODUCTION

#### 1.1 Background to the Study

The exposure of man and his environment to natural source of ionising radiation is a continuous process (United Nations Scientific Committee on the Effect of Atomic Radiation (UNSCEAR), 2000). These sources are mainly from external primordial radionuclide which include Uranium ( $^{238}\text{U}$ ), Thorium ( $^{232}\text{Th}$ ), Potassium ( $^{40}\text{K}$ ) and from radionuclide within man himself. Of major concern from the perspective of radiological health is the external (terrestrial) source. Although many radionuclide of natural origin exists, only few have relative abundance and radioactive intensity to contribute largely to the total absorbed dose from natural sources. Long lived radioisotopes of concern, which contribute mostly to radiation dose from terrestrial sources include; radioactive uranium ( $^{238}\text{U}$ ), thorium ( $^{232}\text{Th}$ ), potassium ( $^{40}\text{K}$ ) and their radioactive decay daughters such as radium ( $^{226}\text{Ra}$ ) and Radon ( $^{222}\text{Rn}$ ), (UNSCEAR, 2000). Figure 1.1a and b show the decay chains of the primordial radioisotopes- uranium ( $^{238}\text{U}$ ) and thorium ( $^{232}\text{Th}$ ). These radionuclides are sometimes known as Naturally Occurring Radioactive materials (NORM). The absorbed doses from NORM are directly linked to their distribution in the environment. The distribution of NORM in undisturbed environment is however not uniform and their concentration in natural soils and rocks are largely dictated by geological composition and the geography of the location (Olarinoye *et al.*, 2010). Consequently, the distribution of natural radiation dose differs from one location to another.

Some human activities have also been recognised to enhance the distribution of NORM in the physical environment. These activities include nuclear accidents, oil and gas

prospecting, minerals mining and milling processes (Dowdall *et al.*, 2004; Musa and Jiya, 2011; IAEA, 2005). The environmental effect of these anthropogenic activities can be accessed via the measurement of radiation dose within the vicinity where the activities are carried out. In Nigeria, unregulated mining of solid minerals are on-going in different parts of the country. Consequently, mining sites are scattered all over the country where illegal and uncontrolled mining are taking place. For more than a century the Nigerian Mining industry has been very active. One of the oldest mining area in Nigeria is the Jos Plateau in Northern part of Nigeria where mining has been going on for more than a century (Masok *et al.*, 2015).

## **1.2 Statement of the Research Problem**

The negative impact of mining tin or any other minerals on man and his environment cannot be over emphasised. Although, mining brings a lot of economic and sometimes infrastructural benefits to the immediate mine community and the nation at large, it however, brings threat to human and animal lives. This threat emanates from the pollution the mining activities bring to the ecological habitats and also the changes in the landscape. Abandoned and active mining pits affect the water table by changing the upstream course brought about by lowered base level. The lowered base level is a major cause of gully erosions. The pits may also serve as snares for unsuspecting animals and humans. These hazards are mostly suffered by the immediate community and the mine workers. Furthermore, the environmental pollution that accompanies tin mining stems from the chemo toxic and radiotoxic chemicals that are released to the environment during mining and milling of minerals. Waste products such as mine tailings and sludge rich in heavy metal and radioactive bearing mineral are the major cause of the environmental pollution resulting from mining. The tin ore itself is a radioactive mineral that contains Zircon, Monazite, Xenotime and thorite (Ibeanu 2003). These are uranium, thorium and heavy

metal bearing minerals. Heavy metals associated with tin mine tailings include: Zn, Pb, Cu, Sn, and Ni. These metals are toxic to plants and animals when their concentration in farm soil surface and underground water is more than their natural distribution in geological formations.

Research conducted and concluded internationally at different mine area have all come to the conclusion that crops, soil, water and the air of mining areas and their environment are contaminated by NORM and heavy metals (Arogunyo *et al.*, 2009, Ademola, 2008, Jibiri *et al.*, 2007, Jwanbot *et al.*, 2012, Masok 2015a,b Isikalu *et al.*, 2011). Consequently, it can be concluded that tin mining increases the distribution of these radioactive and chemotoxic substances in the environment to a large extent. As a result, the background gamma, alpha, and beta, radiation is increased in mining field and vicinity (Ibeanu, 2003; Funtua, 2005; Ademola, 2008; Arogunyo, 2009). Another issue of concern is that these toxic materials are not only concentrated in the mining vicinity. They are dispersed in the soil, air, and water from the source to other areas through weather factors such as wind, surface run off and soil water. They are also re-distributed by man through the transportation of contaminated soil for building and farming purposes.

Mining activities may thus be a major threat to ecological habitat of man and animals. In this regard, continuous monitoring of the extent of contamination of soil in mining area is very important. Mineral extraction negatively impacts the environment, miners and the general public health of the people living around the mine field at Rayfield- Du area of Jos South local government area of Plateau State. Previous research on radiological impact of tin mining in Jos Plateau region has paid little attention to the dose received by non-human biota. However, measured doses in other research has compared with high background radiation regions where noticeable radiation induced defects has been recorded. Dose levels have been set by international organisations towards protecting the non-human

biotas (IAEA, 2011; ICRP, 2003; UNSCEAR, 2008). The level of radiation burden to non-human species in an active mine is thus very necessary.

### **1.3 The Aim and Objectives of the Research**

The aim of this research is to assess the radiological hazard and heavy concentration due to Natural Occurring Radioactive Material (NORM) and heavy metal concentration in an active tin mining field at Rayfield – Du, Jos South Local Government area of Plateau state, Nigeria.

The objectives of the research are to:

- (i) measure the *in situ* terrestrial gamma radiation dose in the mining field in Rayfield – Du, Jos South, Nigeria.
- (ii) determine the activity concentrations of  $^{40}\text{K}$ ,  $^{232}\text{Th}$ , and  $^{238}\text{U}$  in mine soils, tailings and mineral soils collected from the mine field.
- (iii) calculate radiological hazard indices associated with the measured radioisotopes concentrations.
- (iv) evaluate the concentrations of selected heavy metals (Chromium (Cr), Copper (Cu), Zinc (Zn), Lead (Pb), Cobalt (Co), Arsenic (As), Cadmium (Cd), and Nickel (Ni)) in the soils, tailings and minerals soils from the mine.
- (v) evaluate the dose to non-human biota based on the measured radionuclide concentrations.

### **1.4 Justification of the Study**

In view of the health hazard associated with uncontrolled increase in radiation exposure to man and his environment, it has become greatly important for continuous environmental impact assessment of mining activities whenever they are carried out. This will reveal the

extent of damage done to the environment and the health risk associated with the mining and milling processes. Such impact assessments include the measurement of NORM and heavy metals within the mining company's vicinity. Also  $^{226}\text{Ra}$  another radionuclide of concern is a decay product of  $^{238}\text{U}$  which is also widely distributed in many geological formations such as soils, water and rocks. It decays to  $^{222}\text{Rn}$  (-a gas) with a half-life of about 4 days). This gas has been reported to be a major cause of lung cancers among non-smokers (IARC 2012). The fact that many active and abandoned mining sites in Jos are located around residential area is a cause for concern. It has thus become important that the radiological risk parameters of the population in the said area be evaluated.

This research will report the concentrations of  $^{238}\text{U}$ ,  $^{232}\text{Th}$  and  $^{40}\text{K}$  in the soils around a mining site at Rayfield – Du, area of Jos Plateau. The radiological risk parameters associated with the NORM distribution will be presented. Data from this research is important to government, mining company, and individuals who work or live around the area under study. This will give the level of environmental hazard caused by the mining operations; provide basic radiological data for evaluating environmental impact and for judgment of future impacts. Data on the future health risk such as cancer associated with working and living in the area will also be provided. The data from this report could be used by government and policy maker to create awareness and legislation in the risk associated with using contaminated soils for building and farming. Also since mining has been established to be a major factor contributing to enhanced radiation exposure in the environment, it is important for baseline studies to be carried out prior to the commencement of mining procedure and routinely from time to time so as to ascertain the impact of mining activities on the environmental radiation level, of the environment. Generally environmental radiation measure are also important for future exploration of minerals, problem of nuclear waste management, location of orphan sources, and

processing of radioactive material. Consequently data from this study will reveal if regulations and standard practice procedure with respect to radiation protection mechanism is adhered to in the selected mine area. The growing international concern with the ecological impact of mining in the environment has made this research relevant and timely.

### **1.5 Scope of the Study**

The research was conducted at an active mine site at the Rayfield – Du area of Jos south in Plateau state in Nigeria. Radiological burden of the mining and tailings of contaminated soil would be restricted to the measurement of the three primordial radionuclide  $^{40}\text{K}$ ,  $^{232}\text{Th}$  and  $^{238}\text{U}$  using a High Pure Germanium (HPGe) detector. The heavy metal analysis will be done using Energy Dispersive X-Ray Fluorescence (EDXRF) spectrometer and restricted to (8) eight major poisonous heavy metals. Furthermore, terrestrial dose to non-human elements in the biota would be calculated for birds, amphibians, reptiles, trees mammals and other organisms using the ERICA 1.2 computer simulation.

## CHAPTER TWO

### 2.0

### LITERATURE REVIEW

#### 2.1 Ionising Radiation

The transmission of energy or energetic particles through space or a specific medium is termed radiation. Radiations with enough energy to remove bound electron in the atom they pass through (ionisation) are termed Ionising Radiation (IR) (James, 1995). Ionising radiations include nuclear radiations such as  $\alpha$ ,  $\beta$  particles, electromagnetic radiation e.g. X-ray,  $\gamma$ -rays and heavy charged particles such as  $^2\text{H}$ ,  $^3\text{H}$ , and other heavy metals. IR are sometimes classified using charge (i.e. charged and uncharged); have no electric charge (IAEA, 2009). The massive type of IR may be seen as rest mass ionisation projectile with energy in excess of the binding energy of atoms in chemical compound mode (directly and indirectly using radiation) (ICRP, 2009). Table 2.1 show examples that they are in the various classification and capable of breaking chemical bonds and ionising the molecules. When X- rays and  $\gamma$ - rays are absorbed, high-energy electrons are released in the irradiated materials, and it is these electrically charged particles that are save as the ionising agents (ICRP, 2007).

**Table 2.1:** Classification of ionising radiation

S/NO	Classification	Type of Radiation
1	Rest Mass Corpuscular radiation Electromagnetic radiation	Neutrons, proton, electron, positron, pious and other heavy metal ions X-ray and $\gamma$ -ray
2	Electric charge Charged Uncharged	Heavy ions, protons and electrons X-ray, $\gamma$ -ray and neutrons
3	Ionization mode Direct ionization Indirect ionization	Protons, electron, positrons and heavy ions X-ray, $\gamma$ -ray and neutrons

Source: James (1995)

The interaction of neutrons with material medium is more complex. When they interact with the nuclei of hydrogen atoms, these nuclei are set in motion and produce ionisation. Neutrons upon entering an atomic nuclei can cause an instability such that the atoms themselves may disintegrate and emit radiation which results in ionization (ICRP, 2003). It is common between all the types of radiation, whether electromagnetic or corpuscular, to produce charged particles which are responsible for the ionisation effects they ultimately produce. The biological impact of these kinds of radiation which are not unconnected to the consequent ionisation in living tissues are essentially similar. However, the distribution of damage caused by these radiations in the body varies with respect to the type, energy and penetrating power of the radiation in picture.

IAEA report (1974), gave the ranges of alpha and beta particles in soft tissue particles to be about 0.01 to 0.07 mm and order of several millimeters greater than those of alpha particles in such tissues respectively. In human beings, radiation exposure is responsible for the cause of disease such as blood cancer. Its effect may be somatic and genetic. In the somatic effects, the victim carries the only faces the consequence without a posterity effect which genetic effects of ionising radiation exposure is seen in the offspring of the exposed human being. In order to avoid such negative effects, various organisations worldwide have come up with standards and regulations on radiation safety guidelines. Among them are: International Commission on Radiological Protection (ICRP), International Atomic Energy Agency (IAEA), International Labour Organisation (ILO), International Commission on Radiological Units and Measurements (ICRU), United States' National Council on Radiation Protection and Measurements (NCRP) and the Nigerian Nuclear Regulatory Authority (NNRA).

## **2.2 Sources of Ionising Radiation**

Ionising radiation comes from two major sources – natural and artificial.

### **2.2.1 Natural source of ionizing radiation**

The main natural sources of IR are extra-terrestrial which is known to comprise of cosmic radiation and Cosmogenic radionuclides, and terrestrial radiation which are basically due to the primordial radionuclides (Stockholm International Peace Research Institute (SIPRI), 1981). The magnitude of exposures to cosmic is largely dependent on the geographical location and altitude. For instance, altitude is a directly proportional to the exposure one can get from these radiations. Cosmogenic radionuclides refers to those designed as a result of the interaction of the major cosmic ray with elements on earth's atmosphere. Primordial radionuclides are those simply those radionuclides which are attributed to the 'bigbang'. They include  $^{235}\text{U}$ ,  $^{238}\text{U}$ ,  $^{232}\text{Th}$ , and  $^{40}\text{K}$  decay series). They have by long half-lives in towering to hundreds of thousands of years.

Furthermore, exposures can also result from the technologically enhanced natural exposure. They are exposures to natural sources of radiation that are caused by human activities. Examples include exposure to cosmic radiation during air and space travels; For example, it is estimated that at 10 km height, aircraft crews and frequent travelers are subjected to from 1 to 2.5  $\mu\text{Sv/h}$  close to the equator and 4 to 6  $\mu\text{Sv/h}$  directly above 50°N. (Kraus and Kendall 1999). Other sources of enhanced exposures include mining activities in phosphate industry, processing of monazite sands for rare earths extraction, oil and gas industry and coal-fired work stations.

### **2.2.2 Human activities**

Activities of man such as mining, medical application of IR for diagnostics and therapeutics, electricity generation from nuclear power, nuclear weapons viability testing,

and the production of varieties of common products like smoke detectors which are known to contain radioactive materials, can cause further exposure to IR. For medical exposures, exposure from X-ray diagnostics is perhaps the largest source of medical exposure including chest, limb X-ray examinations and dental X-rays. Other sources are categorized under nuclear medicine. They comprise diagnostic procedures used for nuclear tracers and also for treatment of disease. Some examples of radionuclides used here are cobalt irradiation for the management of cancers, or the injection of radioactive iodine which concentrates in the thyroid for management of Graves' disease (James 1995).

### **2.2.3 Consumer Products**

Ionising radiation has also found application in the engineering of some consumer products. Also, it can be used to sterilize products which comprise cosmetics and medical materials used in surgeries or other applications and for shrink-wrap packaging. This can be used for the determination of material thicknesses, the extent of how full cans are before being sealed, and the crack presence or quality of welds in structures such as bridges and buildings. This usage of IR can lead to the exposure of factory workers although it doesn't make the consumer product radioactive. Radioactive materials also are used in many consumer products. The most common is smoke detectors which uses radioactive  $^{241}\text{Am}$  to detect smoke particles in the air (National Research Council Committee on Biological Effect of Ionising Radiation (NRCCBEIR), 1990 and James, 1995).

### **2.2.4 Ionising radiation in building materials**

Several building materials possess low levels of radioactive material. Such building materials which include brick, sandstone, gypsum, natural stone, concrete, or granite are most likely to emit low levels of radiation. Radioactive materials in concrete, brick,

natural stone, sandstone, gypsum, and granite contain naturally-occurring radioactive substances like radium, uranium, and thorium which can decay into the radioactive Radon gas depending on the amount of these substances present and may also cause small increases in radiation levels. The energy per unit mass of radiation in building materials depend on the type and amounts of materials used (CDC, 2015).

### **2.2.5 Monitoring natural radiation**

Due to effects from ionising radiation on human beings, monitoring of natural radiation has gained significant attention by the scientific community for several decades. The oldest of the scientific organizations in this area is the International Commission on Radiological Protection (ICRP) formed in 1928. ICRP has maintained continuous studies in radiation monitoring and protection problems that are of special relevance to the radiation control programs. UNSCEAR, established in 1955, presents to the United Nations General Assembly, and thereby to the global community, its latest evaluation of the sources of ionizing radiation and effects of its exposures. IAEA was established in 1957 within the United Nations family as the global center of cooperation in the nuclear field to promote safe, secure and peaceful nuclear technologies. IAEA, in its part, while responding to the needs of its member states, recently launched an environmental remediation project dealing with problems of radioactive contamination globally (IAEA, 2006b). Its aim is to collate and disseminate information concerning the key problem affecting the environment and remediation of contaminated sites. The techniques employed world-wide in radiation monitoring include intermittent physical examinations and estimation of internally deposited radioactivity by bioassay and total body counting. Personnel monitoring, radiation and contamination surveys, and constant environmental monitoring are other methodologies employed in radiation monitoring.

### **2.3 Effect of radiation in biological system**

The fundamental difference between ionising radiation and other common types of radiation in the environment such as heat is its ability to undergo ionisation. Considering that water is largely composed of cell, ionisation can lead to molecular changes and to the formation of chemical species of a type which are damaging to the chromosome material of the human cell. Radiation ranks amid the most thoroughly examined agents associated with disease (Herman, 1996). The damage caused by the irradiation of human tissue stems from atomic and molecular interaction by way of ionization, excitation and dissociation, which may ultimately lead to clinical symptoms. The ensuing biological effects of exposure of man to radiation are well known from experiments; observations on occupation exposure of workers (this includes: scientist, medical personnel, industrial radiographers, atomic energy worker, miners), patients exposed to radiation for diagnosis and therapy, people exposed to fallout of nuclear weapons debris accidents such as the wind scan accident in England in 1956 and Chernobyl disaster of 1986 (Hiroshima and Nagasaki (1981)).

Ionizing radiation injury is dependent on a number of factors including: the shielding, nature ( $\alpha, \beta, \gamma$ ) and energy of the radiation, the dose, homogeneity of dose and time of exposure. When the dose and dose rate is within the accepted level, the effect of radiation is small and most time no effect is observed, though the effect of low level radiation are not yet entirely understood (IAEA 1982, ICRP 1990, ICRP 1975). Human body is permanently irradiated from ionizing radiation externally and internally. Outdoor radiation are from natural sources (earth, cosmic) and human sources (radiation generators), they are commonly termed environment ionizing radiation (Bek-Uzaov *et al*, 2003). In the body, the K-40 is by its nature existent all through human life. In the case that anyhow

(inhalation, ingestion, etc), other radionuclide (like radon in air) enter inside the body, the body becomes internally contaminated.

External radiation sources, natural or man-made, are of equal risk to man. Their sources and corresponding effective dose equivalent are given in Table 2.2 below. The total natural background radiation (cosmic, earth and internal radiation from radionuclide in human body) leads to an effective dose equivalent for an individual of about 1 to 2 mSv per year at sea level. This value is rough world mean based on the data from many sources (IAEA 1983b, ICRP 1975, NCRP 1975).

**Table 2.2:** Average effective dose equivalent to adult man per year due to the different source of radiation worldwide

<b>Radiation Source</b>	<b>Effective Dose Equivalent (mSv)</b>
Total natural radiation	1 to 2
Cosmic	0.3
Terrestrial	0.4
Total internal (inhalation included)	≤ 1
K – 40	0.2
U Series (Rn – 220 + daughters)	0.65
Others (C – 14 e.t.c.)	0.01
Fall – out	0.01
Medical application	1
Industrial application	≤ 0.01
Coal and Nuclear energy	0.001

Source: NCRP (1975)

### **2.3.1 Interaction of radiation with biological cells**

When a biological cell is exposed to ionizing radiation subject to the energy of the radiation, the radio sensitivity of the tissue, and time of exposure, the following are probable effects on the cells.

#### **(i) Cells are undamaged by the radiation**

Ionization may form chemically active substances which now and again change the structure of the cells. These modifications might be equivalent to those progressions that happen normally in the cell and may have no negative impact. Cells that are damaged; fix the damaged and work typically. Some ionizing events produce substances not regularly found in the cell. This can prompt breakdown of the cell structure and its parts. The cell can fix the damage in the event that it is limited. Indeed, even damage to chromosome is normally fixed. A huge number of chromosomes distortion happens in human body. The human body has a compelling system to fix these changes.

**(ii) Cells are damaged, repair the damage and operate abnormally (cell mutation)**

On the off chance that a damaged cell needs to perform a function before it has had the opportunity to fix itself, it will either be not able to play out the fix or perform function erroneously or not completely. The outcome might be a cell that can't play out their typical capacities or they presently become damaging to other cells. These adjusted cells might be not able to recreate themselves or may create at an uncontrolled rate. Such cells can be the hidden reason for malignant growth (James 1995, Herman 1996).

**(iii) Cell death (as a result of the damage)**

If a cell is extensively damaged by radiation, or damaged in such a way that reproduction is affected, the cell may die.

**2.4 Chemistry of direct consequence of irradiation**

Every one of the above four events occur between four phases of direct consequence of irradiation. Ionization and excitation are vague and may happen anywhere in the body. At the point when the legitimately influenced particle is in protein atom or in a particle of chemically toxic, at that point certain particular impacts because of the damage atom may guarantee. In any case, the greater part of the human body is water and a large portion of

the immediate activity of radiation is consequently on water. The consequence of this energy absorption by water is the generation in the water of highly reactive free radicals that are synthetically poisonous and which may apply their harmfulness on different atoms. Ionizing radiation produces plenteous secondary electrons in matter (James 1995), the energies of these electron in water is in the scope of 10-70 eV. The creation of electron in water with some other radiation (chemical changes) subsequently offers rise to watched biological impact. These chemical changes happen in the following stages.

#### 2.4.1 Physical stage

At the point when the radiation transfers energy to a biological cell, the water substance of the cell absorbs the energy bringing about excitation and Ionization consuming 20% and 80% of the all the energy individually. This stage keep going for around 10-15secs at most.



At the end of this stage  $\text{H}_2\text{O}^+$ ,  $\text{H}_2\text{O}^*$  and an electron ( $e^-$ ) are produced.

#### 2.4.2 Physio – chemical stage

The positive ion ( $\text{H}_2\text{O}^+$ ) dissociates immediately according to the equation



While the electron of the initial stage is gotten by a neutral unadulterated water particle to become watery electron which is a transient specie with an actual existence time of about 1min in unadulterated water (Bier, 1970)



The  $\text{H}_2\text{O}^\cdot$  dissociation immediately:



The ions  $\text{H}^+$  and  $\text{OH}^-$  are of no outcome, since all body liquids as of now contain a significant concentration of these ions. The free-radical  $\text{H}$  and  $\text{OH}$  may join with like radicals or they react with different molecules in the solution. Essentially the direct energy transfer (LET) of the radiation determines their most likely destiny. On account of a high pace of LET, for example, from a section of a  $\alpha$  - particle or other particle of explicit high ionisation (SI), the free  $\text{OH}$  radicals are framed close enough to empower them to join with one another prompting the creation of hydrogen peroxide)



While the free- $\text{H}$  radical join to form gaseous hydrogen this stage typically last 10-12s (James, 1995). The  $\text{H}_2\text{O}$  being a generally steady compound endure sufficiently long to diffuse to point very remote from their place of origin. It is an exceptionally ground-breaking oxidizing agent and would thus be able to influence molecules or cells that didn't endure radiation damage legitimately (Indirect effect). On the radiated cell (water) contains broke down oxygen, the free hydrogen radical may join with oxygen to form the hydroperoxyl radical:



This is increasingly steady and not so reactive. It's more prominent strength permits the  $\text{HO}_2$  radical to join with free  $\text{H}$  radical to form  $\text{H}_2\text{O}_2$  thereby further upgrading the toxicity of the radiation.

### 2.4.3 Chemical stage

The receptive species (free radicals and peroxides) assault the organic molecule of the cell, for the most part the biological, significant molecule Deoxyribonucleic acid (DNA) and Ribonucleic corrosive (RNA) which may prompt the breakage of the long-chain molecule. Fundamental molecules are accordingly annihilated and freak molecules are produced. This function less or even harmful and are foreign to the functioning cell (Herman, 1996). Right now, fundamental life function of the cell might be smothered and the hereditary material might be damaged. It keeps going for around  $10^{-6}$ s (James, 1995)

#### **2.4.4 Biological stage**

With a time scale that varies from minutes to quite a while the chemical changes can affect the individual cell in various manners. The ionization and excitation brought about by radiation therefore prompts separation of atom of DNA molecules in the cell. Since the DNA molecule is broken, an unexpected, irregular change in the nucleotide arrangement of the DNA will happen, bringing about modification of the hereditary code that subsequently may cause the cell and all cells got from it vary in appearance or conduct. This change, known as transformation can be of two kinds:

Point transformation – this is the substitution of one nucleotide by another and Clastogenic change – This incorporate inclusion or cancellation, which is the expansion or evacuation of any bit of DNA from one base pair to very broad part and reversal, which is the extraction of a number of the twofold helix followed by its reinsertion in a similar point however in turnaround the direction.

Almost certainly, if a point change happens only one base of one DNA strand fix would be simple as the corresponding base in the other strand obviously can go about as a layout for the fix (DNA decadence) for transformation happening in a similar area of both strand or

if lactogenic damage happens, mistake-free fixes are more outlandish. There is constantly an opportunity of dilapidation even in a solitary strand point change.

Un-fixed change is answerable for the negative destiny of a transformed cell. On the off chance that a transformation isn't appropriately fixed the cell either gets by as a practical however changed cells or the cell dies for example through Apoptosis, (an orderly systematic and programmed process of self-destruction of the cell).

## **2.5 Biological Effect**

Depending upon the dose, sort of radiation and observed endpoint, the biological impacts of radiation can contrast generally. Some happen moderately quickly while others may take a long time to get obvious. Contingent upon the class of cell (autosomal or germ) influenced, the biological impact can be arranged into somatic impacts (which shows in the uncovered individual itself either quick or late) and hereditary impact (which by and large are transmitted to descendants) (Herman, 1996).

The Depending on the dose, the kind of radiation and observed endpoint, the biological effects of radiation can differ widely. Some occur relatively rapidly, while others may take years to become apparent. Depending on the class of cell (autosomal or germ) affected, the biological effect can be classified into somatic effects (which manifests in the exposed individual itself either immediate or late) and genetic effect (which in general are transmitted to descendants) (Herman, 1996).

The hereditary damage to a population brought about by radiation is for similar reasons, likewise hard to evaluate. An unpleasant worldwide gauge can in this manner just be given, to be specific that the common foundation radiation is answerable for a couple of percent (< 10 %) of all gene change in man and that additional radiation exposure prompts extensively short of what one genuine hereditary impact for each 100 man (ICRP, 1975,

NCRP, 1971). Radiation can modify the hereditary data contained in a germ cell or zygote, which can be transmitted to a group of people yet to come. In grown-up male, the advancement of develop sperm from stem cell takes about 10weeks; they are created consistently having gone through a few stages. In this way a grown-up male who gets a moderate dose of radiation won't encounter a prompt abatement in fertility. Be that as it may, as his develop sperm cells are drained a diminishing in fertility or even sterility will happen (James, 1975). An acute X-ray dose of 0.15 Gy to the testicles hinders spermatozoa creation (temporary infertility). An X-ray dose of 3 to 5 Gy either acute or partial, more than a little while can cause permanent sterility (Beir, 1970). In the female human, all germ cells are available as oocytes not long after birth. There are no stem cells, and there is no cell division. An acute dose of 0.65 to 1.5 Gy to the human ovary impedes fertility temporarily. The limit for perpetual sterility in the grown-up human female (irradiation of the ovaries) is in the scope of 2.5 to 6 Gy for acute exposure and is about 6 Gy for extended exposure (Beir, 1970)

The hereditary impact because of transformation in germ cells may run from mild changes in the eye or skin color to serious deformation, for example, hindered development, little head size, and impeded mental limit (Herman,1996).

### **2.5.1 Stochastic and non-stochastic effects**

Observed radiation effects might be extensively grouped into two classifications, to be specific, stochastic, and non-stochastic effects. Stochastic effects are those with no connection with seriousness, the likelihood of their event increment with dose without threshold (ICRP 1975), for example effect happens by some coincidence. They happen among unexposed and exposed people. The frequency of the event of a stochastic effects has a linear relationship with the dose. With regard to radiation protection, stochastic

effects mean cancer and hereditary impact. The consequence of the introduction to a cancer-causing agent or mutagen is an expansion in the likelihood of an event of the effects, with the increment in the likelihood being corresponding to the amount of the dose. In this manner the development of disease (cancer) doesn't particularly rely upon radiation introduction, anyway exposure to a cancer-causing agent to improve the probability of cancer and the more noteworthy the dose, the more prominent the probability. The commonest kinds of radiation induced cancer growth are leukemia, lung cancer, breast cancer, thyroid, and bone cancer growth. The dormant time of leukemia is around two years, while for other people, it is between 10 and 25 yrs (Paul *et al.*, 1999). Non-stochastic effects are those for which the severity increases with increasing dose and may therefore have a threshold (ICRP, 1975). Most biological effect falls into the category of deterministic effects. Deterministic effects are portrayed by three characteristics, a specific, dose must be surpassed before the effect is observed, the size of the effect increment with the dose, and there is an unmistakable, unambiguous causal connection between exposure to the noxious agent and the observed effect.

At the point when the entire body is irradiated, some non-stochastic effects may develop with increasing dose. These effects are called Acute Radiation Syndrome (ARS). Acute radiation happens at the high dose level for the most part from mishaps. They are effects of a single accidental exposure to a high dose radiation during a brief timeframe (acute exposure). Acute entire body radiation of exposure influences all the organs of the body. Anyway various organs have various degrees of sensitivity to radiation, the example of response or disease syndrome in overexposures/individual, relies upon the extent and homogeneity of the dose. The acute radiation syndrome is separated into three classes.

Hematopoietic syndrome, gastrointestinal syndrome, and the focal sensory system syndrome in order of increasing severity. Their symptoms and comparing dose range are given in Table 2.3 and 2.4.

**Table 2.3:** Somatic effects due to different level of Radiation

<b>Dose Equivalent Received (Sv)</b>	<b>Radiation Effect</b>
0 – 0.25	No detectable clinical effects; late effects very improbable.
0.25 – 0.5	slight transient blood changes (reduction in lymphocyte number etc) late effects improbable
0.5 – 1.0	Marked changes in the blood picture with postponed recovery; brief nausea and weariness; late effect not impossible, yet no genuine shortening of expectancy
1.0 to 2.0	The nausea, and fatigue with conceivable vomiting within 24hrs; checked changes in the blood picture; following idle time of 1 to about fourteen days, pavers, general weakness with entirely plausible recuperation; some death conceivable in 2 to about a month and a half; shortening of life expectancy because recently effects by about 1%
2.0 to 3.0	The Nausea, vomiting, and conceivable diarrhea of the bowels inside scarcely any hrs; solid changes in blood picture; following dormant time of about 1week,, loss of hunger, pallor, sore throat, general weakening, and fever; when all is said in done, recuperation within 3 months, however some likelihood of death within 2 to about a month and a half around a couple of percent shortening of life expectancy because of postponed effect (cancer)

Source: ICRP (1975)

**Table 2.4:** Acute Radiation syndrome due to different level of Radiation

<b>Dose Equivalent Received (Sv)</b>	<b>Radiation Effect</b>
3.0 – 6.0	<p>Hemopoietic syndrome</p> <p>The Nausea, vomiting, and diarrhea in 1 to 2 hours; solid changes in the blood picture; after idle time of as long as multi-week, fever, general weakness, extreme incendiary of mouth and throat, emaciation, hemorrhage, at about 4.5sv half demise likelihood, at 6sv almost unavoidable death within 2 to 6 wks. Because of coming up short of blood framing organs; arrangement postponed effects of survivors.</p>
6.0 -12	<p>Gastrointestinal Syndrome</p> <p>As above; queasiness and so forth within 60 minutes; redness of skin, and so on. Within a couple of days; death within 2 to 3 weeks. Because of loss of body liquid from damaged intestinal walls.</p>
Above 12	<p>Central Nervous System Syndrome</p> <p>As above; death within a few due to damage to central nervous system; peeling of skin.</p>
Above 100	<p>As above; immediate coma death within hours</p>

Source: ICRP (1975)

## **2.6 Biological Effects on Human Embryo**

Quickly partitioning cells and tissues in which cells are consistently being supplanted are among the most radiosensitive: the gonads, gastrointestinal tract, and blood forming organs, lymphatic system, and skin. The creating embryo shows more effects of a similar dose of radiation which has appeared to deliver catastrophic consequences for the creating undeveloped embryo. The traditional effects are development hindrance, embryonic, fetal, or neonatal death, and gross inherent distortion. Elements of significance are the stages and likely teratogenicity effects as organized in Table 2.5. The embryo is considerably sensitive to being executed when in the pre-implantation arrange than later. Notwithstanding, development impediment and teratogens are not commonly found because of an exposure during this stage (James, 1995). Some biological effects of radiation regulated either acutely or over an all-encompassing period may set aside a long effort to create and get clear. Such changes are considered deferred or late somatic effect these effects incorporate cancer, shortening of life expectancy and radiation induced cataract.

**Table 2.5:** Stages and effect of radiation on human embryo

<b>Stages of Development</b>	<b>Radiation effects</b>
Pre-implantation	Prenatal death, abortion
Organogenesis	Prenatal death, growth retardation congenital abnormalities
Fetal stage	Growth disorders, mental retardation, structural anomalies

Source: James (1995)

## **2.7 Protection of Human from Radiation**

- (i) The genuine danger related with the utilisation of radiation has offered ascend to lawful protection regulation in various nations. The fundamental guideline

set breaking points for the absorbed doses equivalent got by various gatherings of the populace is the essential radiation protection quantity. The point of the dose restriction idea is to limit the ingested dose equal got by the various gatherings of the populace while as yet permitting helpful utilisation of radiation (IAEA, 1982d).

- (ii) This suggests the avoidance of non-stochastic effects and the constraint of the event of stochastic effects to an adequate level. This is accomplished by clinging to three significant standards (Beir, 1970).
- (iii) Justification of Training: No practice on including exposure to radiation (after examination with accessible elective strategies, as to dose) will be allowed by the capable authorities except if it delivers a net advantage evaluated on a hazard advantage investigation for the individual or cost-benefit analysis for society.
- (iv) Optimization of protection: Any radiation work must be performed in such a manner that exposure are As Low As Reasonably Achievable (ALARA principle) (IAEA, 1983b)

Dose Impediment: the dose proportional to people will not surpass the points of confinement prescribed for the fitting conditions by the ICRP. On a basic level, one's dose in the region of an external radiation source can be diminished by expanding the distance from the source, by limiting the hour of exposure, and by the utilisation of protecting. Accidental inhalation and ingestion of radionuclides can be forestalled if customary observing of the earth is done with the goal that coincidental release can be distinguished early and the earth cleaned. For therapeutic admission of radio nuclide, it ought to be exposed to the most reduced portion feasible for the equivalent clinical reason to be accomplished. The ICRP suggested that exposure of individual ought to be exposed as far

as possible (ICRP 1977). The word-related portion limit is planned for guaranteeing that no individual is exposure to inadmissible hazard just as forestalling any non-stochastic impacts and limiting the opportunity of stochastic impacts. Word-related dose breaking points and open portion limit apply to introduction coming about because of practices and barring medicinal exposure and common foundation are given in Table 2.6

**Table 2.6: Occupational and public exposure as recommended by ICRP**

<b>Dose</b>	<b>Occupational Exposure</b>	<b>Public Exposure</b>
Effective Dose	50 mSv	1 mSv;
Annual	100 mSv in 5yrs	5-y annual average $\leq$ 1mSv
Cumulative		
Annual	150 mSv lens of eye; 500 mSv	15 mSv lens of the eye;
Equivalent Dose	skin, hands, feet	50 mSv skin, hands, feet

Source: ICRP (1990)

## **2.8 Radiation Detectors**

There are numerous kinds of detectors normally utilized for ionising radiation detection the decision of detector relies here and there upon the radiation type, energy range and goals, fluency, exactness and effectiveness of detection required. By and large, detectors can be classified as:

- a. Gas filled Detectors
- b. Scintillation Detectors
- c. Semiconductor Detectors

### **2.8.1 Gas filled detector**

At the point when gas-filled detectors which are operated in the current mode are considered, there is normally no inherent pulse amplitude uniqueness. Along these lines, all the wellsprings of foundation radiation which are available will subsequently add to the foundation current estimated from an ion chamber. For instance, the ionisation which

results from cosmic rays at sea level amounts to around two-ion sets for each second, per cubic centimeter of STP air. Foundation at sea level amounts springing forward from terrestrial radiation and radioactivity of materials from the encompassing can be about a similar request of greatness, though the current from characteristic alpha movement of basic divider materials is typically a request for size lower. As an unmistakable component which separate Gas multiplication detectors from the conventional proportional and Geiger systems, method of operation has been created for gas detectors.

This element is alluded to as the constrained streamer or self-extinguished streamer (SES) mode and has since discovered application essentially in position-sensitive multi wire chambers. In similitude with corresponding or Geiger-Mueller detectors, the SES gadgets depends on the Townsend avalanches slides development in a gas to causing the multiplication of the measure of charge recovered from ion sets which are birthed along the track of ionizing particles that are incident on it. It can anyway be noticed that the SES method of incident exceptionally contrasts in the spread technique for these avalanches slides through the gases. Ultraviolet (UV) photons assume an indispensable role in the spread of avalanches in the Geiger mode because of the way that they are transmitted by energized atoms framed by electron collisions during the progression of an avalanche slide. Thus in the proportional mode, avalanche slide gets forestalled either by means of keeping the avalanche slide little or by the utilisation of a \"quench\" gas which appropriately ingests the UV photons without causing an electron discharge. Because of the way that just one avalanche slide gets created per unique ion pair, the size of the pulse delivered as yield stays corresponding to their number.

This anyway isn't the situation in the Geiger mode where the UV photons transmitted in one avalanche proliferates all through the gas volume, making extra avalanches which in the end spreads all through the length of the anode wire however gets ended by the build-

up of space charge which encompasses the anode. Therefore, the enormous yield pulse size never again has a reliance on the quantity of unique ion sets. Figure 2.1 shows the schematic diagram of gas-filled detector.

In the SES mode, the created avalanches get a fairly controlled opportunity of propagation. This is accomplished by utilizing gas mixtures which strongly absorbs the UV photons, subsequently forestalling the development of extra avalanches a long way from the first site. Empirically, it is observed that given legitimate conditions, the recently birthed avalanches will develop appearing as a restricted "streamer" expanding radially away from the anode wire surface (Knoll, 2010).

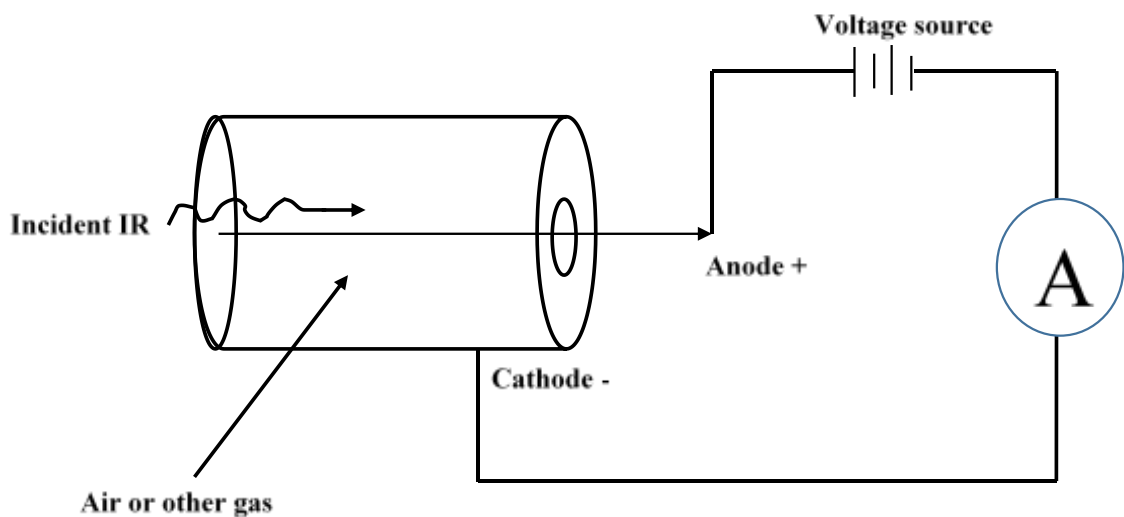


**Figure 2.1: Schematics of a gas filled detector**

### 2.8.2 Scintillator detector

The abundance of thallium-activated sodium iodide scintillation detectors (NaI[Tl]) in the early 1950s gave easy of way to the spectroscopy of gamma rays to be undertaken in its debut with small, portable instruments. Subsequently, a practical detector was accessible which had the option to give a high efficiency for the detection of gamma and X-rays and at the same time give adequately decent energy resolution which will be valuable while

isolating the contributions of multi - energetic gamma-ray sources. Gamma-ray spectroscopy by means of the guide of scintillators has advanced into an experienced science having applications in assorted specialized fields. Figure 2.2 shows the square outline of a scintillator detector.

In spite of the fact that it was for all intents and purposes the first practical solid detection medium which was applied in gamma-ray spectroscopy, NaI (Tl) remains ostensibly the most incomprehensibly known scintillation material for this purpose. This is inferable from its amazingly good light yield, magnificent linearity, and the high atomic number of its iodine constituent. It very well may be noticed that cesium iodide alongside more current inorganic scintillators likewise have recorded some achievements in gamma-ray spectroscopy in spite of the fact that the consolidated utilization of every single other material reaches out to just a little division of the cases in which sodium iodide is discovered (Knoll, 2010).

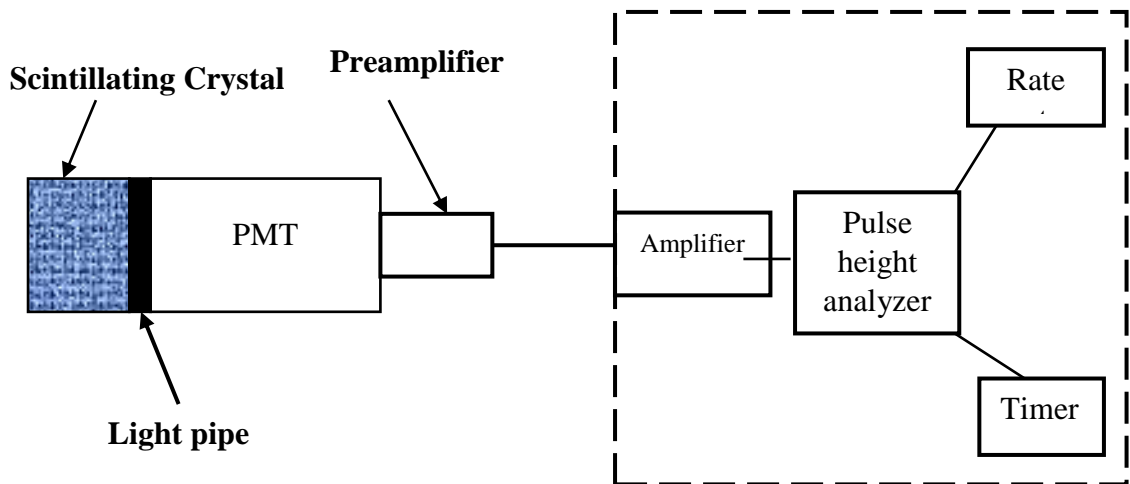


**Figure 2.2:** Block diagram of scintillating detector

### 2.8.3 Scintillator detector principle

The IR detection utilising the scintillation light created in certain target materials is an old technique among others. This scintillation procedure anyway remains relatively one of the

most viable techniques utilised for the viable and spectroscopy of a wide range of radiations.

The perfect scintillation material ought to have the accompanying properties:

1. Change of the kinetic energy of charged particles to detectable light with a high scintillation effectiveness.
2. The yield because of this change ought to have direct proportionality with the deposited energy.
3. The medium's emission wavelength must seem transparent to it to guarantee great light collection.
4. For quick signal pulse to be produced, the decay time of the induced luminescence ought to be short.
5. The material ought to have great optical quality and subject to bulk production in enormous sizes with the end that it becomes of interest as a practical detector.
6. Its index of refraction ought to be near that of glass (1.5) in order to permit the effective coupling of the scintillation light to light sensors.

It tends to be noticed that it is practically impossible to have a material which would at the same time meets every one of these criteria, which is the reason the decision of a specific scintillator is a function of permitting compromise among these factors and more. The scintillators which have been generally applied includes the inorganic alkali halide crystals (sodium iodide is the favourite), organic-based fluids, and plastics. The inorganics have the inclination of having both the best light output and linearity factor, despite the fact that there are a few special cases which are moderately delayed in their reaction time. Organic scintillators by and large have speed as a merit however unfortunately yields less light.

The application additionally expected impacts significantly the scintillator decision. Moreover, the high unfortunately of the constituents and high density of inorganic crystals are a quality in their choice for gamma-ray spectroscopy, while organics are regularly in chosen in preference for beta spectroscopy and fast neutron detection because of their hydrogen content.

Fluorescence is described by the prompt emission of obvious radiation from a material substance attributable to excitation of its atoms by certain methods. It is appropriate to make a distinction between a few different processes which can likewise prompt the emission of noticeable light. Phosphorescence refers to the emission of a longer wavelength of light as compared to fluorescence with a characteristic, lower time of emission. Deferred fluorescence brings forth a similar emission spectrum as prompt fluorescence in any case, it is portrayed by a much longer time of emission after the excitation. It is normal that for any material to be a good scintillator, it ought to convert a large fraction as possible of the incoming radiation energy to prompt fluorescence, and simultaneously limit the by and large undesirable contributions of phosphorescence and deferred fluorescence (Knoll, 2010).

#### **2.8.4 Semiconductor detector**

Simple junction joined with surface-barrier detectors in semiconductor diode detector has recorded boundless use for the detection of alpha particles and different radiations aside from long ranged radiation. Significantly, their confinement is found in the greatest depletion depth (active volume) which can be made. The utilisation of silicon or germanium of normal semiconductor purity and depletion depths more noteworthy than 2 or 3 mm are hard to accomplish in spite of the application of bias voltages which are close

to the breakdown level. For gamma-ray spectroscopy, a lot more noteworthy thicknesses are required for the detectors and this thickness of the depletion region is given by:

$$d = \left( \frac{2EV}{eN} \right)^{1/2} \quad (2.8)$$

where  $V$  is the reverse bias voltage, and  $N$  is the net impurity concentration in the bulk semiconductor material,  $E$  is the dielectric constant and  $e$  is the electronic charge. At a thought about applied voltage, it is conceivable to accomplish greater depletion depths just by bringing down the  $N$  by means of further decreases in  $N$ . Two general methodologies exists which can be taken to achieve this objective. Right off the bat, further refining is looked for after which is fit for decreasing the impurity concentration to approximately  $10^{10}$  atoms/cm<sup>3</sup>. With this degree of impurity in germanium, it is conceivable to arrive at a depletion depth of 10 mm by the utilisation of a reverse bias voltage which is under 1000V. Nevertheless, such a low impurity concentration connotes levels which is typically uncommon while thinking about material purity. Different Procedures have risen to accomplish this objective in germanium yet silicon remains a bug. Detectors manufactured from a ultrapure germanium are alluded to as intrinsic germanium or high-purity germanium (HPGe) detectors and their availability accompanies several centimeters of depletion. Additionally, another methodology planned for diminishing the net impurity concentration is to make a compensated material where the residual impurities containing opposite dopant type to to strike a balance. This anyway can't be attempted by including the appropriate amount of dopant to the semiconductor before the development of the crystal because of the way that there may never be an outright balance between acceptors and donors. Figure 2.3 shows the schematic diagram of a semiconductor detector device.

Along these lines, a material is termed as either n or p-type depending upon the dominant impurity regardless of how slight the distinction might be. Rather, the process involved in lithium ion drifting has been utilised in silicon and germanium crystals to reward the material after the tone. The explanation given to clarify this distinction is that the melting point of silicon (1410°C) which is incredibly higher than that of germanium (959°C) makes excluding impurities during the refining process increasingly strenuous. It is conceivable that germanium gamma-ray detectors crystal is developed to such an extent that the residual acceptor impurities are actually balanced utilising a thickness of about 2 cm of interstitial lithium donor atoms put on top. The resulting material has more intrinsic than extrinsic properties. Indeed, even in an imperfect compensation, the remaining net impurity level may at present be sufficiently low to consider the depleting of drifted region over its whole thickness. Germanium detectors produced through the process of lithium drifting are assigned as Ge (Li). The HPGe broad availability in the early 1980s gave an option in contrast to lithium drifting and now beats the creation of Ge (Li) (Knoll, 2010).

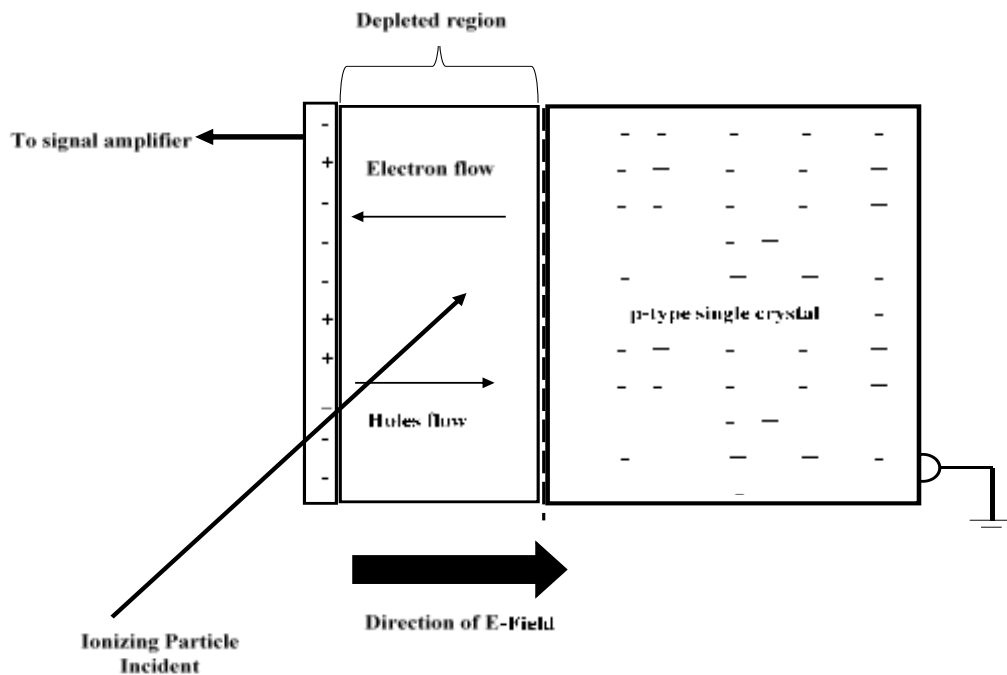


**Figure 2.3:** Schematic diagram of Semiconductor detector

## 2.9 Background Principle of Gamma Spectroscopy

Gamma decay is the most applicable kind of decay applied in gamma-ray spectroscopy. At whatever point a nucleus undergoes radioactive decay ( $\alpha$  or  $\beta$ ), the resulting nucleus produced is alluded to as a daughter nucleus. This daughter nucleus is every now and again in an energized state. In gamma decay, the energized nucleon after decaying to a lower energy state emits energy as a quantized photon. Inferable from the way that nuclear energy levels are discrete, the transitions between energy levels are fixed for a given transition. This emitted photon from a nuclear transition is known as a gamma-ray. Gamma-ray ( $\gamma$ -ray) spectroscopy is a quick and non-destructive analytical technique which can be utilised for the identification of several radioactive isotopes within a sample. In gamma-ray spectroscopy, a detector measures the incident gamma-ray energy. The measured energy of the radioisotopes is then contrasted and the energy of a realized energy to identify it nature. This procedure has assorted applications, especially where a rapid non-destructive analysis is wanted. Figure 2.4 shows the block diagram of HPGe detector.

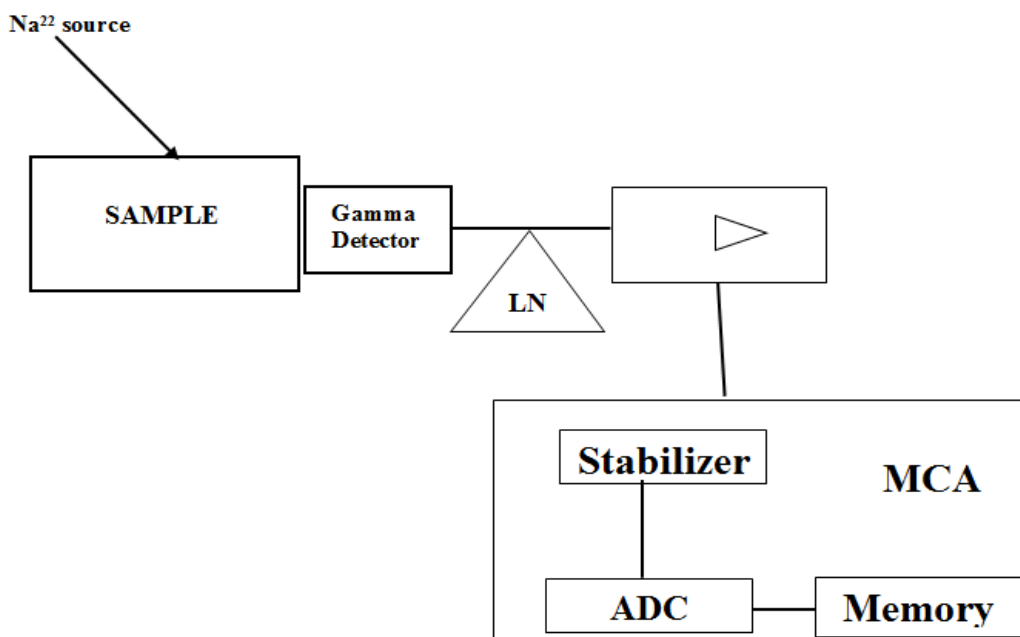


**Figure 2.4:** Schematic diagram of HPGe detector

### **2.9.1 Detector efficiency**

Detector efficiency refers to the measure of how many pulses happen per given number of gamma rays. Detector effectiveness can be named as:

- a. Total Efficiency: refers to the ratio of the number of counts produced by the detector to the number of gamma rays given out by the source (every which way).
- b. Intrinsic Efficiency: The ratio of the number of pulses which are created by the detector to the number of gamma rays which strike the detector.
- c. Relative Efficiency: Refers to the general comparison of the efficiency of one detector with another

Full-Energy Peak (or Photo-peak) Efficiency: This refers to the productivity for creating just full-energy peak pulses and an extraordinary size of the pulse for the gamma ray.

Unmistakably, a suitable detector must be capable of absorbing a huge fraction of the gamma ray energy (Knoll, 1989).

### **2.9.2 Detector resolution**

Resolution refers to the measure of the width (full width at half limit) of a single energy peak at a given energy, which can be communicated either in total keV (Germanium Detectors) or as a level of the thought about the energy (Sodium Iodide Detectors). Better resolution makes the system separate plainly the peaks within a spectrum.

## **2.10 Radioactive Decay Kinetics and Equilibrium**

Radioactive decay, (special case of a couple), is independent of the ambient conditions around a radioisotope. Subsequently, the likelihood of decay at any given moment is constant for that specific radioisotope. The equation one can be differentiated to learn how

the number of parent nuclei present advances with time. The time constant,  $\lambda$ , shows the rate of decay for a given nuclei.

$$\frac{dN}{N} = \lambda dt \quad (2.9)$$

Given that the symbol  $N_0$  represents the number of radioactive nuclei initially present at  $t = 0$ , along these lines the number nuclei present at some given time is given as:

$$N = N_0 e^{-\lambda t} \quad (2.10)$$

This equation can be applied while estimating radiation with a detector. In that the count rate will show a reduction from some initial count rate in a similar way that the number of nuclei will diminish from some initial number of nuclei (Choppin *et al.* 2006; Reilly *et al.* (1991), Loveland *et al.* (2006), and Moody *et al.* (2005).

Additionally, the decay rate can likewise be represented in terms of half-life as ( $T_{1/2}$ )

$$T_{1/2} = \frac{\ln 2}{\lambda} \quad (2.11)$$

The half-life is estimated as far as the units of time and refers to what extent it takes for the number of radioactive nuclei in an offered test to diminish to half of the initial quantity by decaying. Relatively, for a short lived, and a long lived, the count rate will be higher for the radioisotope with the short half-life, the same number of more decay occasions must happen per unit time all together for the half-life to be shorter.

Radioactive decay likewise produces a radioactive daughter product. Contingent on the relative half-existences of the parent and daughter, there can emerge a few situations of equilibrium viz: zero equilibrium, transient equilibrium, or secular equilibrium. Secular equilibrium happens when the half-lives of the parent is any longer than the half-lives of

the daughter. In a given equilibrium, the proportion of atoms of every daughter and parent nuclide can be depicted as:

$$\frac{N_P}{N_D} = \frac{\lambda_D - \lambda_P}{\lambda_P} \quad (2.12)$$

Attributable to the relative higher value of the parent half-life, the observed measure of activity is as little as the parent decays thus

$$\frac{N_P}{N_D} = \frac{\lambda_D}{\lambda_P} \quad (2.13)$$

Which can be modified to show the equality between the activity of the daughter and that of the parent.

$$A_P = A_D \quad (2.14)$$

This point came to is called secular equilibrium, the proportion of the activities of both nuclides is fixed.

The decay chains of the isotopes  $^{238}\text{U}$  (Radium series),  $^{235}\text{U}$  (Actinium series),  $^{232}\text{Th}$  (Thorium series) and  $^{237}\text{Np}$  (Neptinium series) are illustrated Figures 2.5, 2.6, 2.7 and 2.8 respectively.

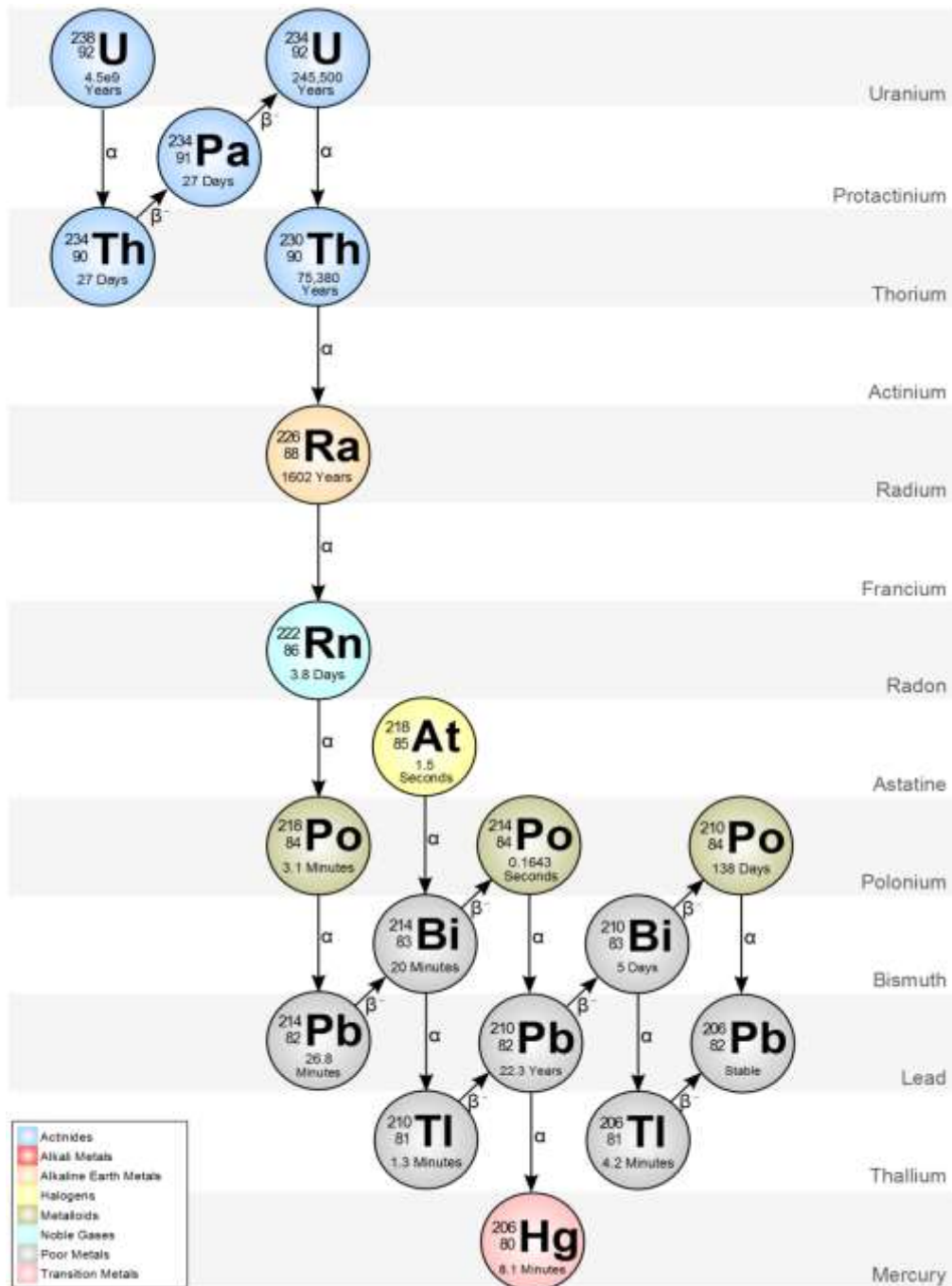
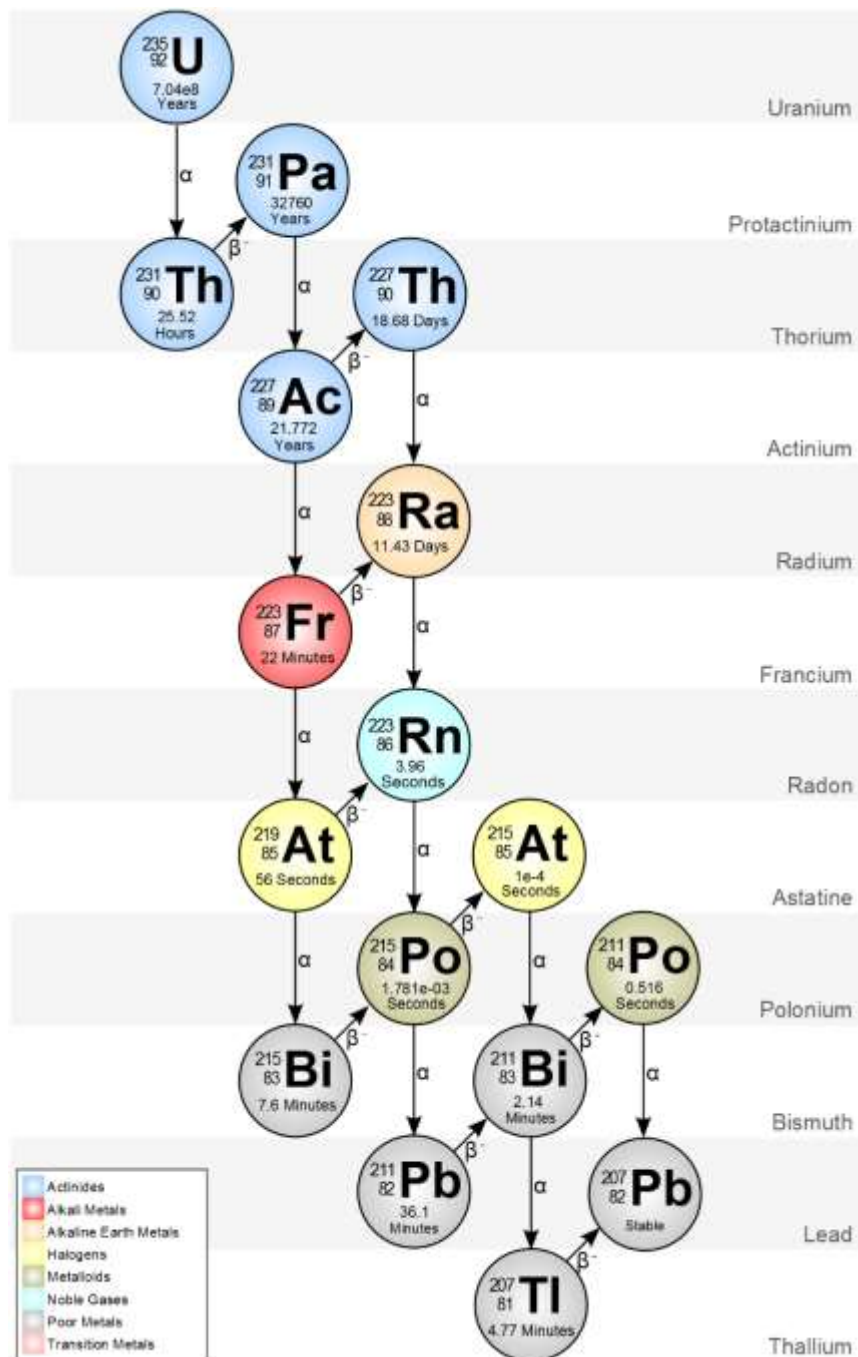
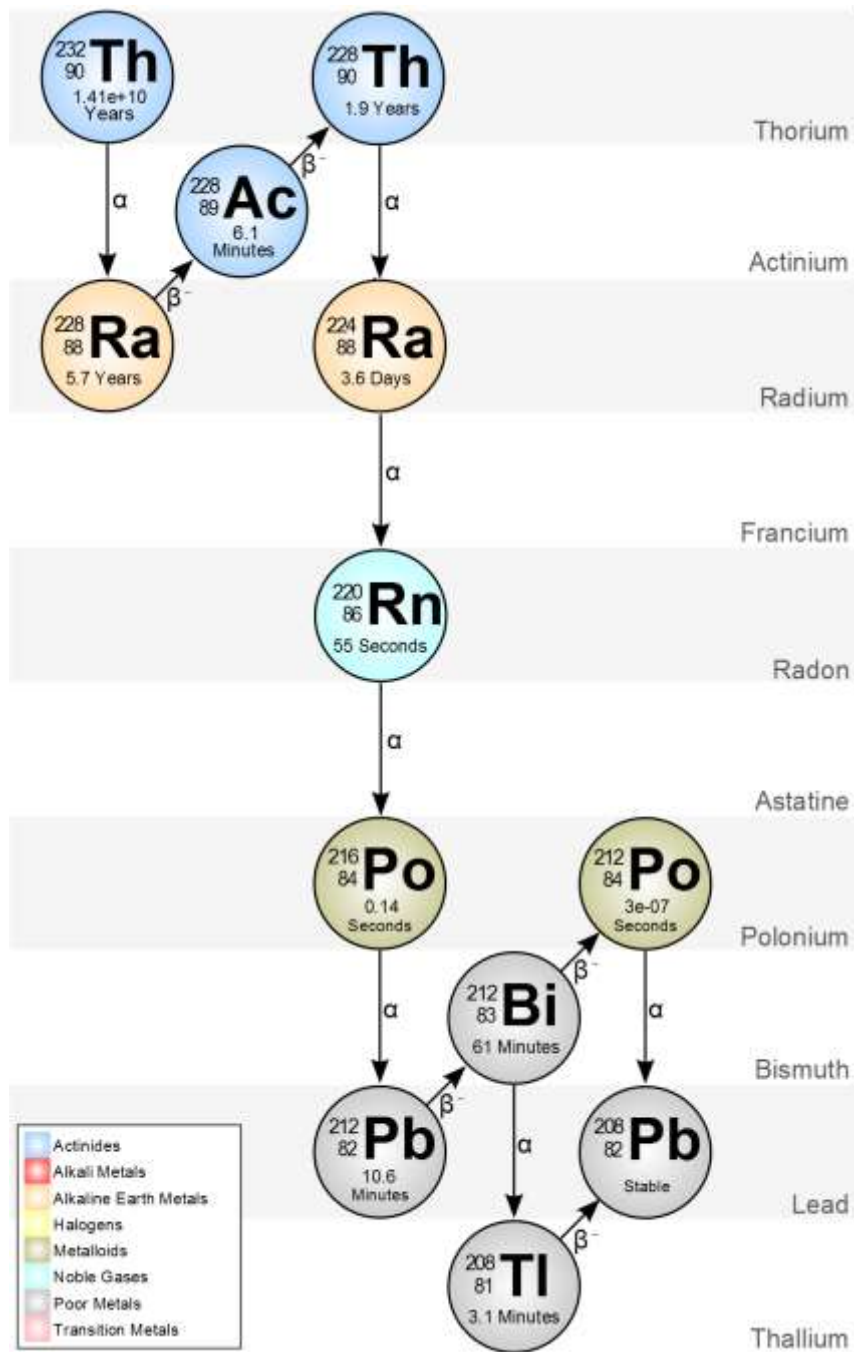


Figure 2.5: Decay chain of  $^{238}\text{U}$  (4n+2 series) (<https://metadata.berkeley.edu/nuclear-forensics/Decay%20Chains.html>)



**Figure 2.6:** Decay chain of  $^{235}\text{U}$  (4n+3 series) (<https://metadata.berkeley.edu/nuclear-forensics/Decay%20Chains.html>)



**Figure 2.7:** Decay chain of  $^{232}\text{Th}$  (4n series) (<https://metadata.berkeley.edu/nuclear-forensics/Decay%20Chains.html>)

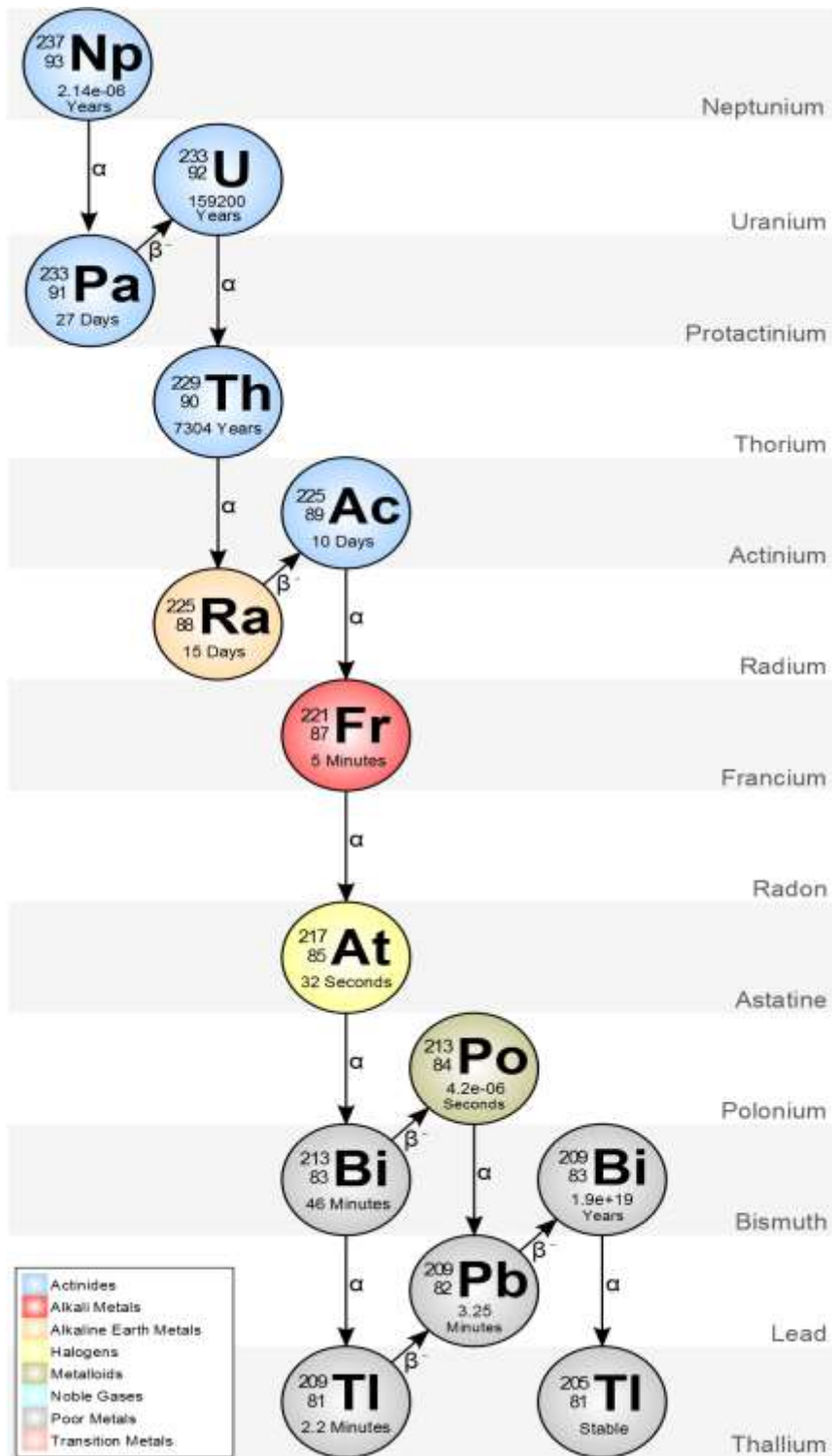


**Figure 2.8:** Decay chain of  $^{237}\text{Np}$  (4n+1 series) (<https://metadata.berkeley.edu/nuclear-forensics/Decay%20Chains.html>)

## 2.11 X-Ray Fluorescence Spectrometry

X-ray fluorescence spectrometry is a technique for quantitative examination which utilises X-ray energy. The laws of electromagnetic radiation, which expresses that the surface of a body can absorb the incident radiation and later reflect the incident radiation simply like a mirror with spherical symmetry which can transmit the incident radiation and emit the radiations likewise applies to X-rays.

X-rays are known to start from the loss associated with the interaction of high-energy electrons with atoms. The incident electrons from the X-rays tube undergo movement towards the electronic field of the electrons contained inside the different shells of the atom in the targeted material. The electrons which are incident gets decelerated and lose energy. In any case, high-energy electrons enter the external orbital of the target's atoms and collide in the process with an electron found in the inner orbital.

In any case, it is conceivable that these inner electrons are completely expelling subsequently leaving the atom in an unstable state. While Electron rearrangements going on to restore stability, there is a resulting arrival of energy in a type of X-ray. Figure 2.5 shows the schematic diagram of EDXRF. These generated X-rays possess have discrete wavelength which has a relationship with the atomic number of the atoms producing them and along these lines they are alluded to as 'characteristic X-rays'. This concept forms the possibility of X-ray spectrometry.

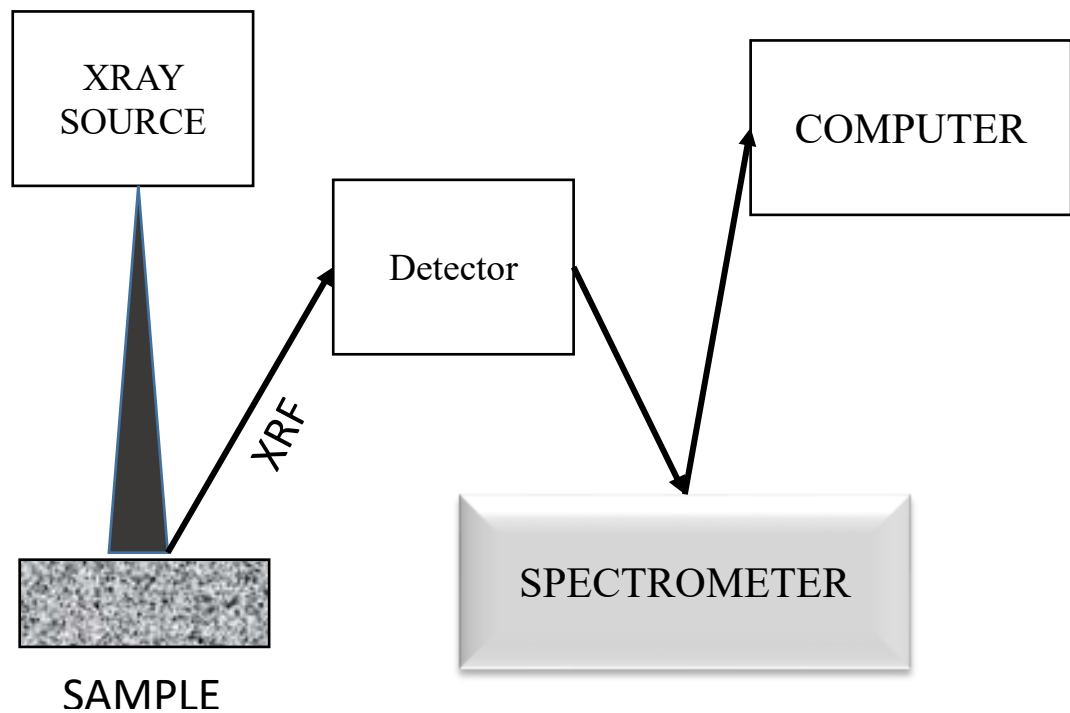


**Figure 2.9: Schematic diagram of EDXRF**

### 2.12 Tin Mining in Nigeria

Historically, discovery of tin in the Jos Plateau can be traced to the years between 1700 and 1750 in an area called Kuza along the Delimi river channel (Mackay *et al.*, 1949). During this period, the local farmers needed superior agricultural tools beside their bare hands and sticks for their subsistence agricultural practice. They immediately noticed that when iron and tin were mixed, a stronger and more durable agricultural implement can be constructed. The local populace referred to the discovery as a gift from their God thereafter (Cooper, 2002). The mining of tin in the modern day Jos Plateau thus started to develop in the clusters of villages in and around Kuza. The economy of the area also started developing at a fast rate due to the discovery and the influx of traders from across the Nile and Sahara to buy smelted tin rods. Also by 1770 the number of local smelters (blacksmiths) rose considerably in Naraguta (as the plateau area was fondly called). Small

scale local mining was thus flourishing during this period. Organised and mechanised mining was however never to begin until the survey of mineral in Northern Nigeria was conducted between 1904 and 1909. The survey revealed the abundance of tin ore over a wide space of the modern day Jos Plateau of Nigeria (Hodder, 1959).

The British company then known as the Royal Niger Company (RNC) was birthed in 1848 and obtained licenses from the British government to mine tin in the Plateau in 1908 as Nigeria was still under the British Colonial occupation. By 1909, the RNC began mining and through the British government placed a ban on all local mining. In 1913 the RNC started giving licenses to other mining companies to operate. This led to rapid increase in Nigeria's tin output. The RNC in 1909 was producing about 458 tons of tin which rose to 8174 tons after 1919 when more companies were licensed. Consequently, licensed area after mining also increased from 373 km<sup>2</sup> to about 900 km<sup>2</sup>. This brought workers of many tribes and nationality to the Jos Plateau and eventual revolution to the technical skills of the people and the organization of mining labour and management. Furthermore, the economic and infrastructure fortune of the Plateau and Northern Nigeria soared (Hodder 1959). Rail lines were built from Lagos to Zaria for the sole purpose of exporting tin. By independence in 1960, Nigeria was the sixth largest producer of tin worldwide (Hodder 1959).

Throughout the pre independent era, unfortunately, no law was enacted by the colonial leaders to control mining activities in Nigeria. Large area of mining land were consequently devastated due to mining activities. The environmental destruction slowed down due to the discovery of oil in Oloibiri in 1956 (Idowu 2013). This discovery led to the diversion of government interest away from solid mineral mining to oil exploration. Consequently, the fortune of the tin mining and milling industry began to decline and presently remained so to a. In addition, the decrease in the global demand for tin, and the

almost three year of civil war leading to the departure of foreign expatriate in the tin mining companies were other factors that led to the decrease in production of tin and dwindling fortune of the industry (Adekoya 2005, Idowu 2013). Presently solid mineral account for less than 1% of Nigeria gross domestic products. The lack of government interest in tin mining over the years has made mining regulations in the Plateau inadequate, thus, many unregulated and illegal mining are, scattered across the Plateau. The devastating impact of these unregulated mining in the environment is unquantifiable. This has led to a host of ecological problems such as flood, erosion and loss of farm lands. These present untold hardship and economic loss to the inhabitants of the Jos Plateau area.

### 2.13 The Study Area

The area now known as Jos is the capital of the north central state of Plateau in Nigeria (Figure 2.10).

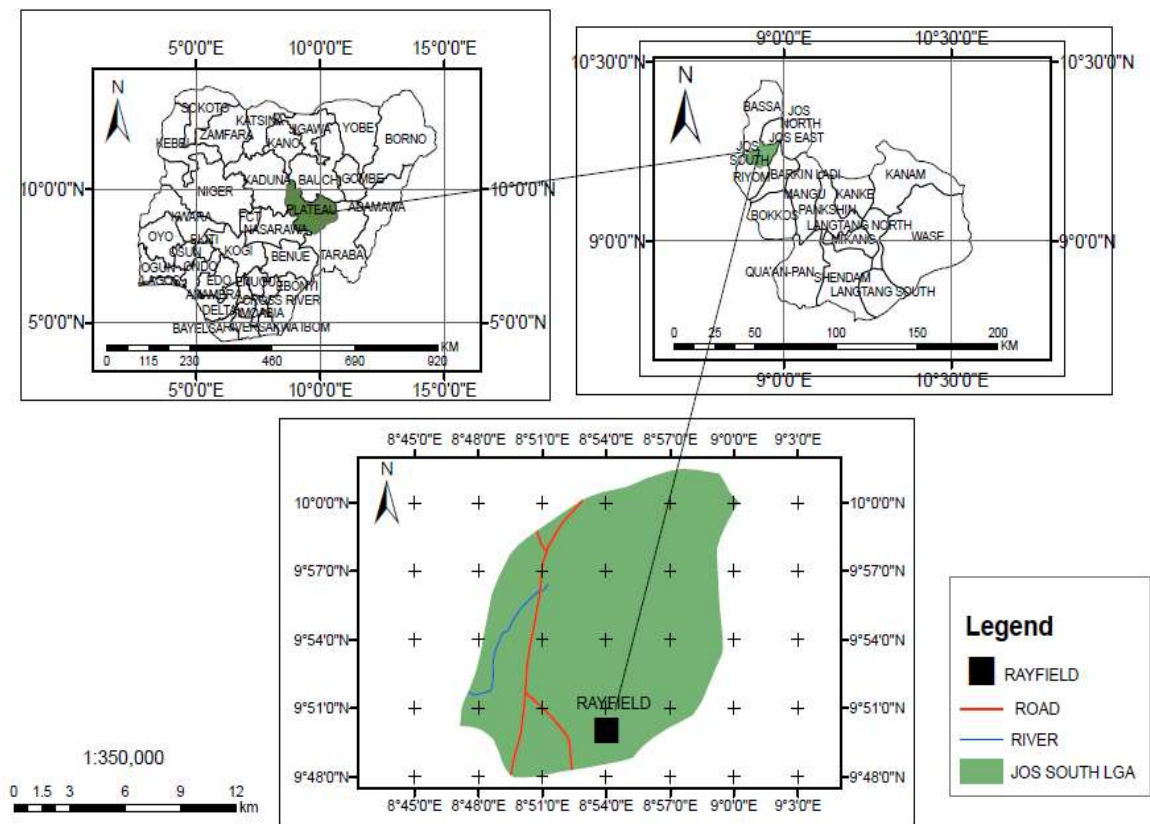


**Figure 2.10:** Map of the study area Rayfield-Du, Jos

The area is bounded by longitudes 8°15' and 9°15' E and latitudes 9°30' and 10°10' N and about 4062 feet above sea level (Figure 2.10). Climatically, it is dominated by tropical dry and wet conditions with annual rainfall and temperature ranging between 1500 – 2000 mm and 20°C – 25 °C respectively (Wapwera *et al.*, 2015). The topography is characterised by series of highlands of varying heights and flat topography. The vegetation consists of stunted trees, tall grasses and shrubs. The geological sequence of the area is predominantly made up of volcanic and plutonic rocks belonging to four main age groups. Sediments are limited to valley alluvium. A general succession according to Macleod *et al.* (1971) is in Table 2.7 Most of the area is underlain by rocks of the Basement Complex. The oldest rocks include the granulitic gneisses in small widely scattered outcrops and a few small bodies of dioritic rocks. The rest of the Basement Complex (migmatites, granite- gneisses and granites) are members of a single orogenic cycle. The area is dominated by Younger Granites a series of non-orogenic intrusive and associated acid volcanoes. The Jos-Plateau forms the centrepiece of the area of Younger Granite province and is the principal centre of the associated tin and columbite mineralization. Figure 2.11 shows the digitised geological features of the study area.

Du, Vwang, Kuru, zawon and Gyel are the five major districts of Jos south local government area with Bukuru as it headquarters. According to the 2006 census data, its population is about 307,000 (NPC, 2006) and a total land area covering about 1,037 km<sup>2</sup>. The average altitude of the area is about 1,100 m thus the climatic condition of the area is always cool. November is the onset of the coldest period in the Jos Plateau and it lasts for four months before the raining season begins in March. The major occupation of the local people in Jos is farming, hunting and mining related activities. The mining activities has led to devastation of estimated total area as large as 316 km<sup>2</sup> (Adegboye 2012). The devastated area are characterized by erosion gullies, mine pit and paddocks, mine dumps,

ponds, and abandoned mining with a lot of potentials in the mining ponds equipment scars. The vegetation of the area include dense and close foliage trees.

## 2.14 Geology of the Study Area

### 2.14.1 Basement complex

The rocks of the Basement Complex cover some two thirds of the Jos Plateau (Macleod *et al.* 1971) as shown in Figure 2.11 and 2.12. The general sequence according to Macleod *et al.* (1971), comprises a collection of older granulitic gneisses succeeded by a series of migmatites, granite- gneisses and granites starting a single petrogenic unit.

**Table 2.7: Geological Succession in Naraguta Area (After Macleod *et al.*, 1971)**

Geologic Time	Rock Type	Occurrence
Tertiary-Quaternary	Newer Basalts	volcanic cone and Lava flows while lava  Flows now largely decomposed, overlying alluvium.
Jurassic	Younger Granite	Porphyries, granites and rhyolites
Precambrian to Lower Palaeozoic	Crystalline Basement	Migmatites, Older Granite and Gneisses

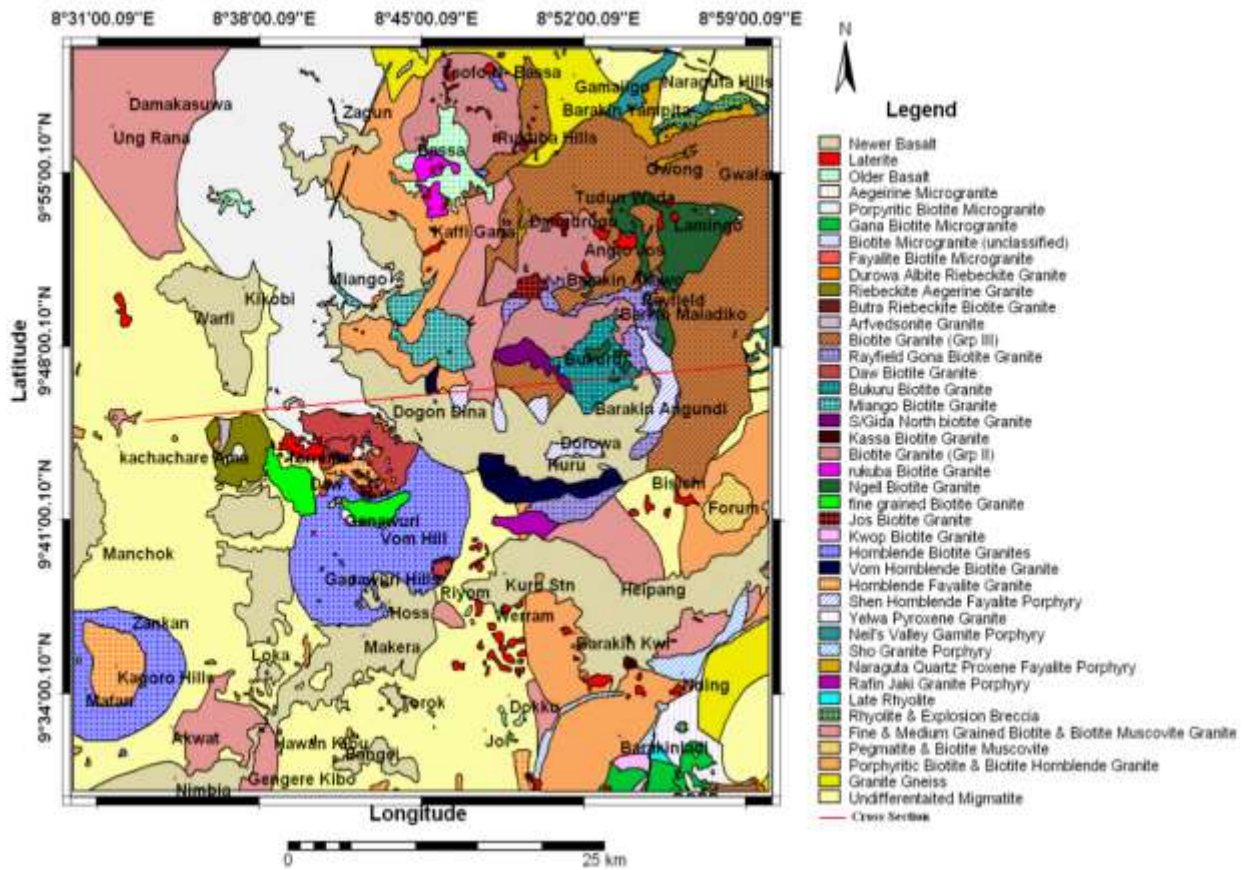


Figure 2.11: Digitised geological map Jos Plateau

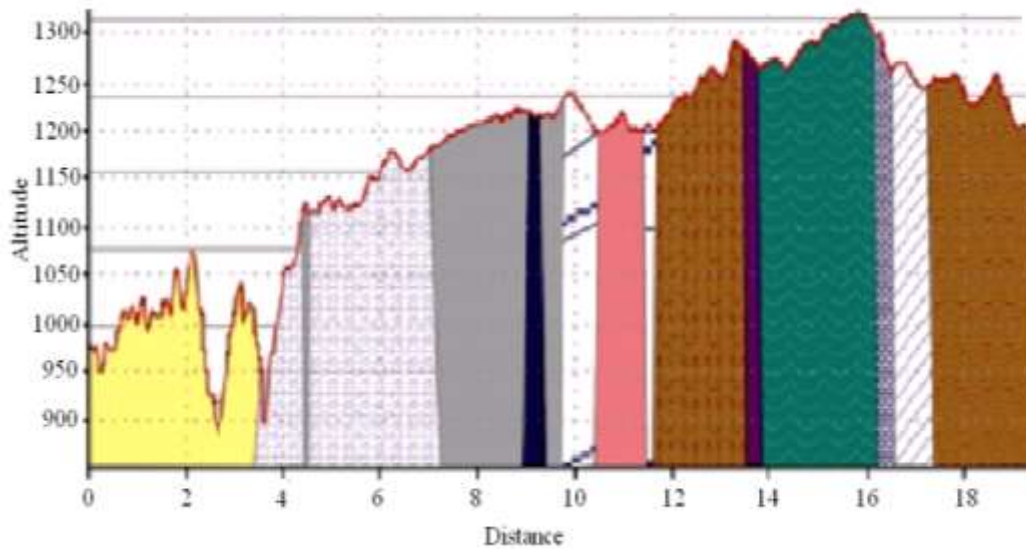


Figure 2.12: Digitised Geological Map of Naraguta Sheet 168 (Compiled and Published by the Geological Survey of Nigeria, 1963). Line AB is a cross section shown above (After Akanbi (2014))

### 2.14.2 The younger granites

The Younger Granites are clustered in the North-Central part of Nigeria and spread from the Benue valley to the Southern Kano province. Granites from the same petrographic province occur to the north in Matsena area of Bornu, around Zinder and the Air Plateau in Niger republic. Related rock types are prominent in the Sahara, Cameroun and the Sudan. The Younger Granites are discordant, high level intrusions which transgress all units of the Basement Complex. They have been preceded by extensive acid volcanism and emplaced by ring faulting and rock subsidence. The suite is mostly acidic, with granites and rhyolites underlying more than 90% of the total area of the province (Macleod *et al.*, 1971). Transitional and basic rocks happen in most of the complexes, but peak of the syenites are quartz-bearing and gabbro, microgabbro and dolerites occupy less than 1% of the total area and comprise only a minor part of any complex in which they occur (Macleod *et al.*, 1971).

Continuation of the same mechanism at greater depth beneath the lava accumulations has localized the peripheral ring-dykes and the granite plutons. The lavas owe their preservation at the present level to the extensive subsidence during the plutonic stage. It is probable that many of the granite plutons, now deeply eroded, were once covered by a volcanic hood (Macleod *et al.*, 1971) by the way, a great variety and number of Younger Granite Complexes exist in Nigeria; different grades of erosion have resulted in the entire range of igneous structural patterns being clearly exhibited. The early volcanic structures are demonstrated in Younger Granite Complexes such as Liruei, Buji, Banke and Saiya-Shokobo. At Ropp and Dagga Allah the segmentation of the Basement Complex and differential subsidence of extensive block is shown. In these two Complexes erosion has proceeded to such a depth that the upper, sub-horizontal sections of the granite intrusions have been partly removed and the network of polygonal feeder ring- dykes is exposed. In

the larger complexes of Jos-Plateau such as Jos-Bukuru and Sha- Kaleri, where much greater volumes of magma are involved, the intricate pattern of the emplacement of the granite plutons has been unravelled. Since the study area is located in the Younger Granite province and these granites host cassiterite a brief discussion of the rock types will be discussed. Three major kinds of granite have been acknowledged and classified on the basis of dominant mafic minerals. These include (Macleod *et al.*, 1971).

(i) Hornblende-granites and porphyries

This important group frequently forms the conspicuous ring-dykes of the region and in many of the complexes has introduced the cycle of granite intrusion. The group contains a wide choice of coloured minerals including fayalites, hedenbergite pyroxene, hornblende, arfvedsonite and biotite and can be subdivided on the basis of texture and mineralogy. In common with the biotite- and riebeckite-granites the hornblende-granites sometimes appear as large plutons with a truly granitic structure, but in the ring-dykes they commonly assume a porphyritic texture and to this facies the term granite-porphyry is applied. In the Jos-Plateau province the early ring-dyke is frequently of a bristly hornblende-biotite-granite or granite-porphyry, and this rock-type is also abundant as large plutons; fayalite-bearing granites do occur but are relatively restricted in extent. The appearance of hornblende- biotite-granite can be correlated with the greater volume of magma and greater depth of erosion in the Complexes of the Plateau area.

(ii) Biotite-granites

Biotite-granite is the most rich and prevalent rock-type in the Younger Granite area and it forms some of the largest individual intrusions. It sporadically occurs as ring-dykes but is more frequently found in the form of large circular and crescentic plutons and as minor stocks. Certain important intrusions of biotite granite exceeds 50 sq.miles (129.5 km<sup>2</sup>) in

the area. The most wide-spread of these occur on the Jos plateau where Jos-Bukuru and Sha-Kaleri developments together include over 400 sq. Miles (1036 km<sup>2</sup>) of this granite. The biotite-granites are divided into three groups whose type examples are intrusions in the Jos-Bukuru complex. Group I (Jos type) are coarse-grained biotite-granites, generally pink in colour and with widely spaced jointing so that they weather to extensive slabs and extremely large boulders. Group II (N'gell type) are medium-grained granites, pinkish in colour and grading into the white, even textured, medium-grained granites of group III. The last group the (Rayfield-Gona type), in its most typical development, is highly distinctive, with biotite growing in separate flanks rather than in clusters, and small flecks of red staining clearly visible in the hand specimen. In thin sections, albite is more apparent than normal, as discrete crystals as well as patchy perthitic intergrowths, and this led to the members of this group being termed as albite-biotite-granites (Jacobson *et al.*, 1958). Chemical analysis show, however that with few exceptions the actual abundance of the albite molecule is a little higher than normal and is never comparable to that in the more aptly named albite-riebeckite-granites, so the term has been now abandoned (Macleod *et al.*, 1971).

Tin mineralization is practically fully confined to the biotite granites. More than three-quarters of the Nigerian tin production is derived from alluvial concentrations shed from the biotite-granites of the Jos-Bukuru and Ropp massifs on the Jos-Plateau. Comprehensive mapping of the biotite-granites has exposed that the mineralized greisens and quartz veins are concerted near the roofs of the intrusions and that the richest alluvial concentrates are found only in the vicinity of, or on the drainage systems from, granite impositions which have undergone light erosion (Macleod *et al.*, 1971).

(iii.) Riebeckite-granites

Riebeckite-granite appears in the mainstream of the Younger-Granite complexes. They occasionally appear such as ring-dykes but are more commonly establish as elliptical plutons and as smaller-sheet like intrusions. Granites containing both riebeckite and biotite are fairly common and form a well characterized group of intrusions. But they may show fairly regular variations in the proportion of riebeckite to biotite. The albite-riebeckite-granites are a distinctive type of the riebeckite-bearing group and are categorized by a high proportion of late albite which substitutes most of the earlier crystallized minerals.

### **2.14.3 The basalts**

Volcanic activity has taken place occasionally from Tertiary to a modern times; the products are almost entirely basaltic and have been further divided into three groups: lateritised Older Basalt, Older Basalt and Newer Basalt. The lateritised Older Basalts represent lavas now decomposed to clays and usually overlain by a thick cap of lateritic ironstone. Organized with essential river sediments they were termed the Fluvio-volcanic Series in the early survey of the Plateau (Falconer 1921). The later extension of the survey in to the southern Plateau (Falconer *et al.*, 1926) suggested that fresh basalts also belong to this lateritised series. However, in the re-survey of the Plateau tin fields (Mackay *et al.*, 1949) these unaltered basalts were grouped with the Newer Basalts and the term Fluvio-volcanic Series was restricted to the completely decomposed basalts and their accompanying sediments. The survey carried out by Macleod *et al.* (1971) found it useful to distinguish an older group- generally small eroded remnant- from a newer group, typically large valley-filing flows which can be traced to reasonably well preserved-cones. The Older group the authors said is restricted to areas in which the lateritised basalts are abundant and in some cases are overlain by lateritised basalt. In other cases, however, 'Older Basalt' maybe later than adjacent lateritised basalts, resting in valleys eroded into the laterite.

#### **2.14.4 Economic geology**

The most common economic mineral in the area is cassiterite. Other minerals in the area include columbite, mite, pyrochlore, fergusonite, thorite, zircon, monazite, xenotime, beryllium minerals, molybdenite, cryolite and other minor minerals such as topaz, galena, pyrite, arsenopyrite, bismuthinite, and chalcopyrite (Macleod *et al.*, 1971).

### **2.15 Review of Previous Studies**

#### **2.15.1 Natural radioactivity in mines soils and environment**

Many researches have been conducted and concluded on the assessment of NORM concentrations in the environment (typical undisturbed soils, mineral soils, tailings) in Nigeria and past.

Ibeanu (1999) researched the radionuclide content level of abandoned heaps of tin mine tailings in Jos, Nigeria. The activity concentration was assessed via a calibrated NaI (TI) detector. The mean activity concentrations acquired for  $^{40}\text{K}$ ,  $^{226}\text{Rn}$ , and  $^{232}\text{Th}$  and determined dose rates in sixty soil and tailing samples collected were  $1251.7 \text{ Bqkg}^{-1}$ ,  $3867.5 \text{ Bqkg}^{-1}$  and  $8301 \text{ Bqkg}^{-1}$  and  $7.2 \mu\text{Gyh}^{-1}$  respectively. The examination concluded that early stage radionuclide concentration and dose rates in the area were very high and beyond the safety limit. Moreover the cancer growth mortality chance for external and internal exposure situations for  $^{226}\text{Rn}$  and  $^{232}\text{Th}$   $1.67\text{E}$  and  $3.41\text{E}-6$  respectively. The researcher concluded that intervention is required in the area in order to save people in general from radiation initiated disease, for example, cancer.

In 2008, Ademola estimated the NORM levels in the mine tailings in Jos territory. In spite of the fact that the research didn't geographically describe the specific area of the mine, in any case, it was expressed that the tailing samples were collected from heaps within a mining field in Jos City. Radiological estimate of the following utilising gamma

spectrometer investigation dependent on a HPGe detector revealed the mean activities of  $^{238}\text{U}$ , and  $^{232}\text{Th}$  to be  $7220 \text{ Bqkg}^{-1}$  and  $16800 \text{ Bqkg}^{-1}$  respectively. In spite of the relative high concentration of  $^{40}\text{K}$  in natural soil, it was not detected in any of the eleven-tailing samples collected and analysed. The measured  $^{238}\text{U}$  and  $^{232}\text{Th}$  levels were seen as around 7220/33 and 16800/45 times greater than their respective world average values in soil based on UNSCEAR (2000) reports. The reported mean effective dose rate, absorbed dose, and radium equivalent were  $9.4 \mu\text{Svh}^{-1}$ ,  $13.5 \mu\text{Gyh}^{-1}$  and  $31200 \text{ Bqkg}^{-1}$  respectively. All were pronounced to be higher than their respective safety and world-average levels. Ademola concluded that the enhanced radiation burden in the studied area was high and miners and inhabitants around the miners were potential candidates for biological effect because of the upgraded external radiation level. The research prescribed further research be done to discover the degree of internal contamination because of internal contamination with  $^{222}\text{Rn}$  a daughter of the uranium decay chain.

The Uranium and Thorium concentrations in the soil of Bitsichi mining region of Southern Jos Level was examined by Arogunjo *et al.* in 2009 with a HPGe detector. The mean concentration acquired were  $8.7$  and  $16.8 \text{ Bqkg}^{-1}$  for  $^{238}\text{U}$  and  $^{232}\text{Th}$  respectively. The qualities were repeated to be higher when compared to their natural values in soil and even places assigned as high natural background areas for example, the Plateau of Pocos de Caldas in Brazil.

The activity concentrations, external gamma dose rates, and internal gamma because of natural radionuclides  $^{226}\text{Ra}$ ,  $^{232}\text{Th}$ ,  $^{40}\text{K}$  in soil and dust of old tin mines being changed over to farmland in Bitsichi, Bukuru and Ropp area of Jos assessed by Jibiri *et al.* (2009). The assessment of the activity of primordial activities were done by means of a  $76 \times 76 \text{ mm}$  NaI(Tl) detector with a resolution of 8% at  $0.662 \text{ MeV}$  gamma energy. They obtain activity in the scope of  $67 \pm 22$  -  $471 \pm 11$ ;  $93 \pm 7$  -  $2190 \pm 19$ ; and  $\text{BDL}-906 \pm 47 \text{ Bqkg}^{-1}$  for  $^{226}\text{Ra}$

$^{232}\text{Th}$  and  $^{40}\text{K}$  respectively. The most noteworthy  $^{40}\text{K}$  concentration was gotten from soil samples from Ropp while highest  $^{226}\text{Ra}$  and  $^{232}\text{Th}$  concentration were acquired from Bitsichi soil samples. They likewise revealed that the activities of all the three radionuclides were higher than their respective world average values in soils. The external absorbed dose rate due to the radionuclide concentrations extended from 0.07 to 2.02  $\text{mSvy}^{-1}$  while the mean annual internal effective dose because of inhalation and ingestion of soil particles during cultivating practices were evaluated to be 16.9 $\mu\text{Sv}$ , 8.8  $\mu\text{Sv}$  and 8.1  $\mu\text{Sv}$  for Bitsichi, Ropp and Bukuru respectively. In any case, the authors failed to acknowledge the mining activities that preceded the cultivating activities in the area as a potential factor liable for the high distribution of radionuclides in the soils. The high radionuclide activities were attributed to the farming practices embedded at the different farms, for example, application of fertilisers.

The Estimation of Radionuclides in processed tin mine tailings in Jos were made using NaI(Tl) detector by Mangset and Sheyin 2009. The outcomes shows that the mean activity concentration ranged from 364  $\text{Bqkg}^{-1}$  - 27930  $\text{Bqkg}^{-1}$  in the tailings. So also HPGe detector was used to determine the radioactivity in mine tailings in Jos, the outcomes revealed that  $^{226}\text{Ra}$  have mean activity concentration ran between 51.36  $\text{Bqkg}^{-1}$ –512.24  $\text{Bqkg}^{-1}$  while  $^{232}\text{Th}$  mean focuses went between 378.02  $\text{Bqkg}^{-1}$ –2635.78  $\text{Bqkg}^{-1}$  (Isikalu *et al.*, 2011).

Likewise farm soil samples were examined for radioactivity levels because of  $^{226}\text{Ra}$ ,  $^{232}\text{Th}$  and  $^{40}\text{K}$  using gamma-ray spectroscopy in Jos territory by Jibiri *et al.* in 2011. The majority of the physical and chemical properties of farm soils indicated low values in heavy-mined area (Bitsichi) and generally high values in low-mined territories (Bukuru and Ropp). The farm soils over the areas were basically acidic. Results also showed no obvious correlation between physical-chemical properties and the radionuclide

concentration of  $^{226}\text{Ra}$ ,  $^{232}\text{Th}$  and  $^{40}\text{K}$  in the farm soils. The outdoor radiation exposure to a farmer to farming operations in these mining territories and the probable-related radiological health risks were viewed as low and practically inconsequential.

Jwanbot *et al.* (2012) assessed the activity levels of natural radionuclides in some food crops developed in high foundation zones in Jos-Level utilizing gamma spectrometric investigation. The activity concentrations of the natural radionuclides in the food crops was found to be between  $12.36 \pm 0.82$  and  $56.92 \pm 8.84 \text{ Bqkg}^{-1}$ ;  $1.46 \pm 0.05$  to  $10.42 \pm 0.04 \text{ Bqkg}^{-1}$  and  $1.53 \pm 0.08$  to  $6.85 \pm 0.42 \text{ Bqkg}^{-1}$  for  $^{40}\text{K}$ ,  $^{226}\text{Ra}$  and  $^{232}\text{Th}$  respectively. The moderately high values of the activity concentrations was attributed to the history of tin-mining activities that have occurred in these regions for a long time. Nonetheless, the determined dose taken from intake of these radionuclides in the food crops was found to be low and that harmful effects were not expected.

Investigations of the social and economic impacts of tin mining in Rayfield of Jos Plateau was completed by Onwuka *et al.* (2013). The result of the first analysis showed that there is a significant difference between the social components resulting from tin mining, while the subsequent examination revealed that there is a huge distinction between the economic variables resulting from tin-mining activities.

The work demonstrated that tin-mining activities impacted on the environment significantly, deserting such a lot of social and economic scars that the administration needs to consider and take measures to ameliorate.

Odusote *et al.* (2014) estimated the radionuclides in the Tin mining soil from the Jos Plateau, Nigeria, and assessed the effect of radiation on the environment where the soils are used as building materials. Gamma spectrometry was use by means of a NaI(Tl) detector to decide the activities of the radionuclides  $^{40}\text{K}$ ,  $^{238}\text{U}$  and  $^{232}\text{Th}$  in ten (10)

samples from points within a distance of 20 km along the mining trail. The consequences of estimations in soil samples show that the concentrations of  $^{238}\text{U}$ ,  $^{232}\text{Th}$  and  $^{40}\text{K}$  went between 1.51 – 4.98, BDL - 8.64 and 10.3 – 35.2 Bqkg<sup>-1</sup> with mean concentrations of 3.20 ±1.16, 1.31 2.75 and 25.60 ± 8.89 Bqkg<sup>-1</sup>, respectively. The external hazards extended between 0.008 – 0.044 with mean estimation of 0.019 while the internal hazards went between 0.014 – 0.048 with mean estimation of 0.028. These hazard values are less than 1. The annual gonadal dose equivalent (AGDE) extended between 10.28 – 55.87 Svy<sup>-1</sup> with mean estimation of 24.22 12.16 Svy<sup>-1</sup>. The radium-proportional exercises extended from 3.07 – 16.23 Bqkg<sup>-1</sup> with a mean estimation of 7.04 Bqkg<sup>-1</sup>. The external absorbed dose rate ranged from 5.35–18.76 Gyh<sup>-1</sup> with a mean estimation of 12.95 4.26 Gyh<sup>-1</sup>.

While trying to examine the use of abandoned tin mining sites as residential areas, Wapwera *et al.* (2015) researched the ionizing radiation and heavy metal burden in the soils of abandoned tin mine sites in rock heaven, Zaria road, Jos city and Kufany town all situated in plateau state of Nigeria. The primordial radionuclide and heavy metal concentrations in the soils and water in the zones were measured however a NaI (TI) detector and X-ray fluorescence spectroscopy. Radionuclide concentration in water and soil in the area are found to be high. Moreover, they detailed the presence of colombite, zirconium, and other heavy-metal-bearing ores in the collected soil and water samples. The area it was concluded not safe for human residence Wapwera *et al.* (2015).

The level of natural radioactivity of  $^{238}\text{U}$ ,  $^{232}\text{Th}$  and  $^{40}\text{K}$  concentration in mine tailings and soil samples collected from Awo and Ede territories of Osun state in Nigeria was researched in 2015. The norm-activity concentration in the samples was estimated with a NaI(TI) detector and they were found to differ from 316.67 to 1487 Bqkg<sup>-1</sup>; 13.11 to 8.8 Bqkg<sup>-1</sup>; and 9.26 to 55.81 Bqkg<sup>-1</sup> for  $^{40}\text{K}$ ,  $^{238}\text{U}$ , and  $^{232}\text{Th}$  respectively. It was concluded that the activity concentration of the NORM in the territory were lower than the safely

limit exception  $^{40}\text{K}$  thus the determined radiation dose indices were all within a safe limit. Adewale *et al.* (2015).

### **2.15.2 Heavy metals toxicology**

The heavy metal that will be considered in this research are (Chromium (Cr), copper (Cu), zinc (Zn), lead (Pb), cobalt (Co), arsenic (As), cadmium (Compact disc), and nickel (Ni)). Copper is a reddish metal with a face-centered cubic crystalline structure. It reflects red and orange light and assimilates different frequencies in the visible spectrum because of its band structure, so it has a decent reddish colour. Copper is malleable, ductile, and an extremely good conductor of both heat and electricity. It is softer than iron however harder than zinc and can be polished to a bright finish. It is found in group IV of the periodic table, together with silver and gold. Copper has low compound reactivity. It slowly forms a greenish surface film called patina; this coating protects the metal from further attack.

Nickel is silvery-white, hard, malleable, and ductile metal. It is of the iron group and takes on a high polish. It is a genuinely good conductor of heat and electricity. Nickel is bivalent in its commonplace mixes despite the fact that it accepts different valences. It likewise forms various complex compounds. Most nickel compounds are blue or green. Nickel breaks down gradually in weak acids yet like iron becomes passive when treated with nitric corrosive.

Tin is a delicate, flexible, ductile, and highly crystalline silvery-white metal, when a bar of tin is bowed, a breaking sound known as the tin cry can be heard from the twinning of the crystals. Tin melts at low temperatures of about 232 °C (450 °F), the most minimal in group 14.

Lead is a somewhat blue-white shiny metal. It is delicate, exceptionally flexible, ductile, and a moderately poor conductor of electricity. It is very resistant to corrosion but

tarnishes upon exposure to air. Lead isotopes are the final results of every one of the three series of naturally occurring radioactive elements

Zinc is a radiant somewhat blue-white metal. It is found in group IV of the periodic table. It is fragile and crystalline at common temperatures, however it becomes ductile and malleable when heated between 110°C and 150 °C. It is a genuinely receptive metal that will join with oxygen and other non-metals, and will react with dilute acids to release hydrogen (www.lentech.com, 2010).

The assessment of heavy metals in soil and plant samples and furthermore plant samples are significant in checking ecological contamination. Metals are toxic even in traces. The capacity of the plant to assimilate heavy metals can cause human health or ecological become most exceedingly terrible. For instance, human take their meal (especially crops) that contain a lot of toxic heavy metals will cause them lung cancer. The soils at the landfill and nursery soil broadly used in agricultural activities but we do not know about the quality of both soil. The soils are containing a great deal of essentials metals that significant in biological system cause human attracted to use the contaminant soils as their fertilizer for their farming activity. The Table 2.8 portrays the toxicology of heavy metals that are expressed previously:

**Table 2.8:** Toxicology of some heavy metals

<b>Heavy Metal</b>	<b>Toxicology</b>
Copper (Cu)	The following May cause liver and kidney damage: Headaches, Stomach aches, Dizziness, Vomiting, and Diarrhoea
Nickel (Ni)	Higher probabilities of development of lung cancer, nose cancer, larynx cancer and prostate cancer, Sickness and dizziness after exposure to nickel gas, Lung embolism, Respiratory failure, Birth defects, Asthma and chronic bronchitis, Allergic reactions like skin rashes, mainly from jewellery, Heart disorders
Lead (Pb)	Disturbance of the biosynthesis of haemoglobin and anaemia, rise in blood pressure, Kidney damage, Miscarriages and subtle abortions, interference with nervous systems, Brain damage, Declined fertility of men through sperm damage, Reduced learning abilities of children, Behavioural disturbance of children, such as aggression, impulsive behaviour and hyperactivity
Zinc (Zn)	Vomiting, Nausea, Anaemia, Stomach cramps, Skin irritations, Damage the pancreas, interrupt the protein metabolism, Cause arteriosclerosis
Tin (Sn)	Severe sweating, Breathlessness, Urination problem, Depressions, Liver damage, Eye and skin irritations, Headaches, Stomach-aches, Sickness and dizziness, Brain damage (causing anger, sleeping disorders, forgetfulness and headaches) Malfunctioning of immune systems, Chromosomal damage, Shortage of red blood cells.

Source: [www.lentech.com](http://www.lentech.com) (2010)

## CHAPTER THREE

### 3.0 MATERIALS AND METHODS

#### 3.1 Materials

The major materials utilised for carrying out this research include the following:

1. Hand trowel,
2. Hand glove
3. Masking tape
4. Polythene bags
5. Marker
6. Sieve (500  $\mu\text{m}$  mesh size)
7. Marinell beakers (500g)
8. GPS map (Garmin CSx 76)
9. RDS- 30 multi-purpose survey meter (Mirion Rados)
10. EDXRF Spectrometer (Minipal4, Serial No. DY-1055, Made: PANALYTICAL, Year Installed: 2008).
11. Pellet beakers (30g)
12. HPGe Detector (Canberra coaxial n-type) calibrated for energy and efficiency and accessories coupled with a multichannel analyser.

#### 3.2 Methods

##### 3.2.1 Site survey

A preliminary survey of the location area (mining site at Rayfield-Du, Jos Plateau State) was carried out in order to ascertain major activities going on in the mine. Furthermore, the survey was intended to delineate the field into safe and unsafe areas. A tour of the site revealed the safe areas (though well distributed across the mine) where measurement and sampled soils were to be collected. Some of the different areas and activities going on in

them are depicted in Plates I and II. A total of sixty two (62) locations were identified as sampling or measurement points. Of all the 62 points of measuring, 42 were chosen in the processing and mining areas. These area include mining and processing points having waste (tailing) heaps. The remaining 20 points were chosen in the administrative and areas where no active mining was taking place. The map of the study area with the sampling points identified is shown in Figure 3.1.

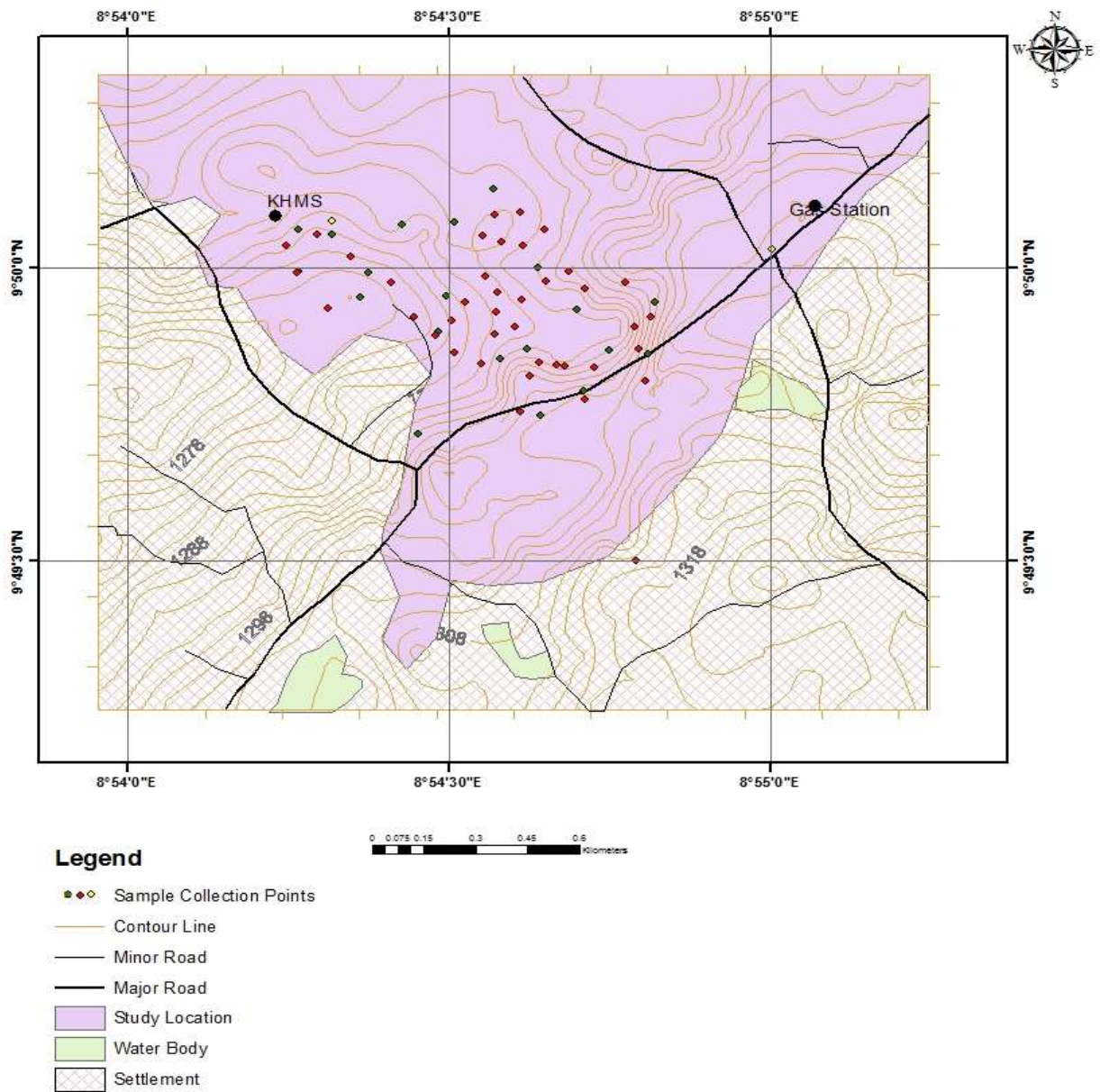


**Figure 3.1: Location map of the study area with sampling points identified**

### **3.3 *In-situ* Gamma Radiation Measurement**

The measurement of background and mining induced gamma radiation dose rate at the active mine was carried out by adopting an *in-situ* measurement approach. The *in-situ* data was collected with a pre-calibrated Geiger Mueller based multipurpose survey meter (RDS – 31 MIRION) (Plate I) at the initially identified 62 points as indicated in Figure 3.1. The survey meter is a battery operated digital hand held unit of dimension 100 x 67 x 33 mm and weighs about 175 g. The detector's  $\gamma$ -ray energy response and dose measurement capacity is in the range of 48 keV to 3 MeV and 0.01  $\mu$ Sv to 10 Sv respectively. The calibration of the detector was verified at radiation facility of the Nigerian Nuclear Regulatory Authority (NNRA) Ibadan, Nigeria.

At each of the identified measurement points, the survey meter was positioned at one meter (1 m) above the ground level with the aid of a constructed stand. The dose rate measurements were recorded at this height as this is the average position of the chest of adult population (Agbalagba, 2011; NCRP, 1990). The elevation above sea level together with each points location coordinated was taken and recorded with a Global Positioning System (GSP) unit (Garmin GPSMAP 76 CSx) (Plate II). All the measurement locations were distributed across the active and safe area of the mine. In order to ensure the accuracy of collected data, measurements were repeated five times at each of the sampling points and averaged. All *in-situ* measurements and sample collection at the site was carried out within two months in the dry season (November and December) and between 1200 and 1600 hr daily. This was done to minimise the effect of soil moisture attenuation of gamma ray intensity, uniformity of conditions and to avoid random error that could be attributed to variation in atmospheric parameters (NCRP, 1990).



**Plate I:** Multipurpose survey meter RDS-30



**Plate II:** GPSMap 76CSX

### 3.4 Gamma Spectrometric Analysis

The *ex-situ* procedure was adopted for this research i.e samples were collected from the area of origin and taken to the laboratory for gamma spectrometric measurement.

#### 3.4.1 Sample collection

Based on the preliminary results of the in-situ measurement, 42 locations with distribution covering both high and low dose rates were chosen for sample collection for  $\gamma$ -spectrometer analysis. A digger and hand trowel was used to dig where necessary and scoop the sand samples respectively. The scooped soils were put in polythene bags which were carefully labelled to reflect the uniqueness of each sample based on location (shown in Figure 3.2. The picture of collected samples is shown in Plates III.

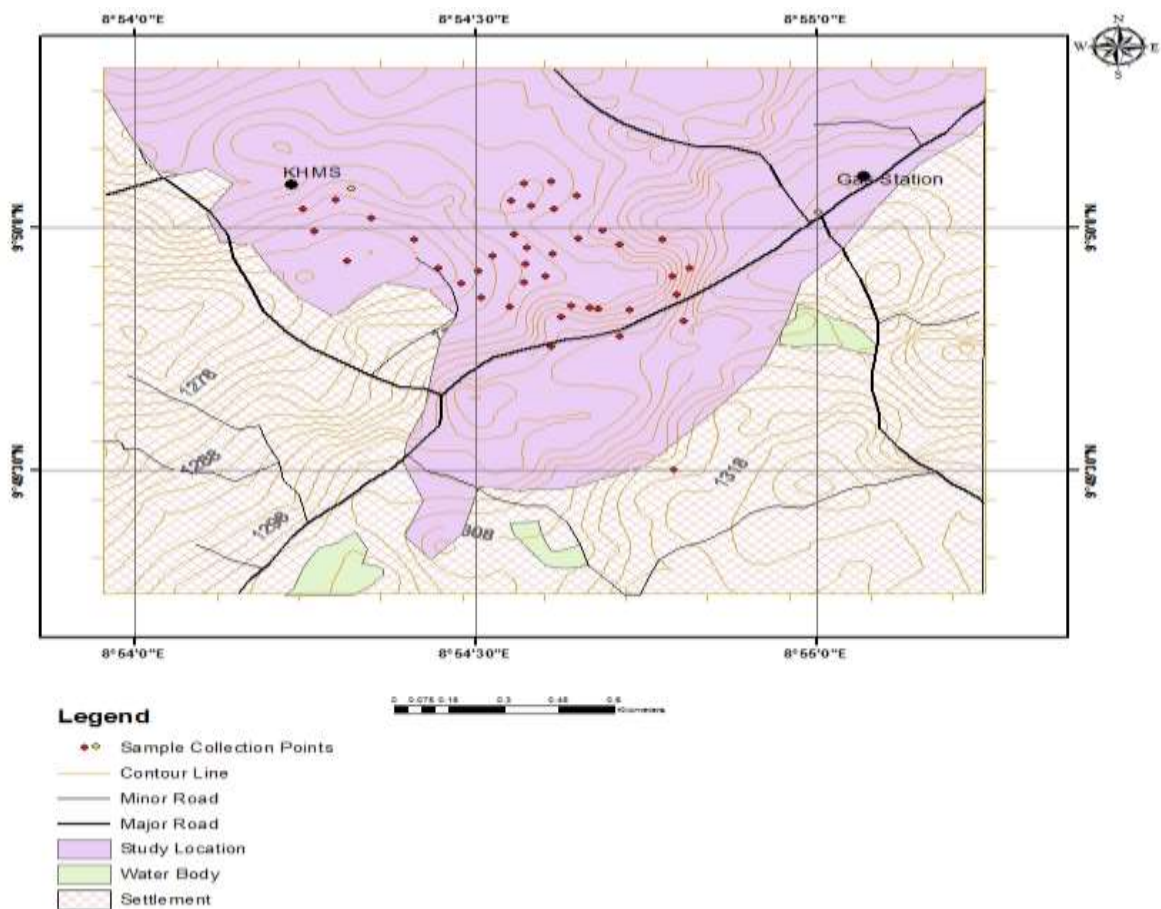


**Figure 3.2:** Soil, mineral soil, and tailing collection point

The labelled sealed samples were then transported to the laboratory where further preparations and analysis were carried out on them.



**Plate III:** Raw Soil sample

### **3.4.2 Sample preparation**

At the laboratory, the packed and labelled soil samples were un-packed sun-dried and weighed. The sun-drying removes moisture content from the soil samples. This is due to the fact that moisture content attenuate photon intensity emanating from radionuclides in the soil and consequently reduce the gamma energy flux during the spectrometric measurement leading to inaccuracy in the results (Moody, 2005; Reiley *et al.*, 1991). Thus the sun-drying and weighing continues until a constant soil weight is obtained (an indication that all soil water content has been removed) for each sample. The dried soil samples were then crushed using agate mortar and sieved using a sieve of 500  $\mu\text{m}$  mesh size (shown in Plates IV (a) and (b), respectively) to remove uncrushed stones, debris and organic materials.



a

**Plate IV (a)** agate mortar and pestle



b

**Plate IV (b)** sieve (500µm mesh)

500 g of the homogenize soil samples were then packed in Marinelli beakers (shown in Plate V) and sealed (air tight to avoid gaseous exchange between the sample and the environment). The sealed samples were then kept for 30 days to allow secular radioactive equilibrium between  $^{238}\text{U}$  and its short lived progenies ( $^{222}\text{Rn}$ ,  $^{214}\text{Pb}$ ,  $^{226}\text{Rn}$ ).



**Plate V: Marinelli beakers (500g)**

### 3.4.3 Gamma – activity measurement and spectra analysis

A High Pure Germanium (HPGe) detector which operates at liquid nitrogen temperature (77 K) was adopted in this research for  $\gamma$ -rays spectrometry of the soil samples. The HPGe detector used is shown in Plate VI.



**Plate VI: HPGe Setup at the National Institute of Radiation Protection and Research (NIRPR), Ibadan, Nigeria**

Prior to measurement, the detector was calibrated for energy and efficiency. The dimension of the crystal HPGe detector was 53.4 mm x 59 mm. The energy calibration was performed by matching the principal gamma ray peaks observed in the spectrum of the standard to the channel number. The match was related through the equation 3.1

$$E = A_0 + A_1 C \quad (3.1)$$

where E and C are the energy and channel numbers respectively,  $A_0$  and  $A_1$  are the calibration constants. The calibration curves are shown in Figure 3.3 and 3.4.

Furthermore, the efficiency calibration of the detector was performed by acquiring a spectrum of the standard sources until the count rate of total absorption could be calibrated

with a statistical uncertainty of <1% at a confidence level of 95%. The obtained efficiency calibration curve and equations are shown in Figure 3.4.

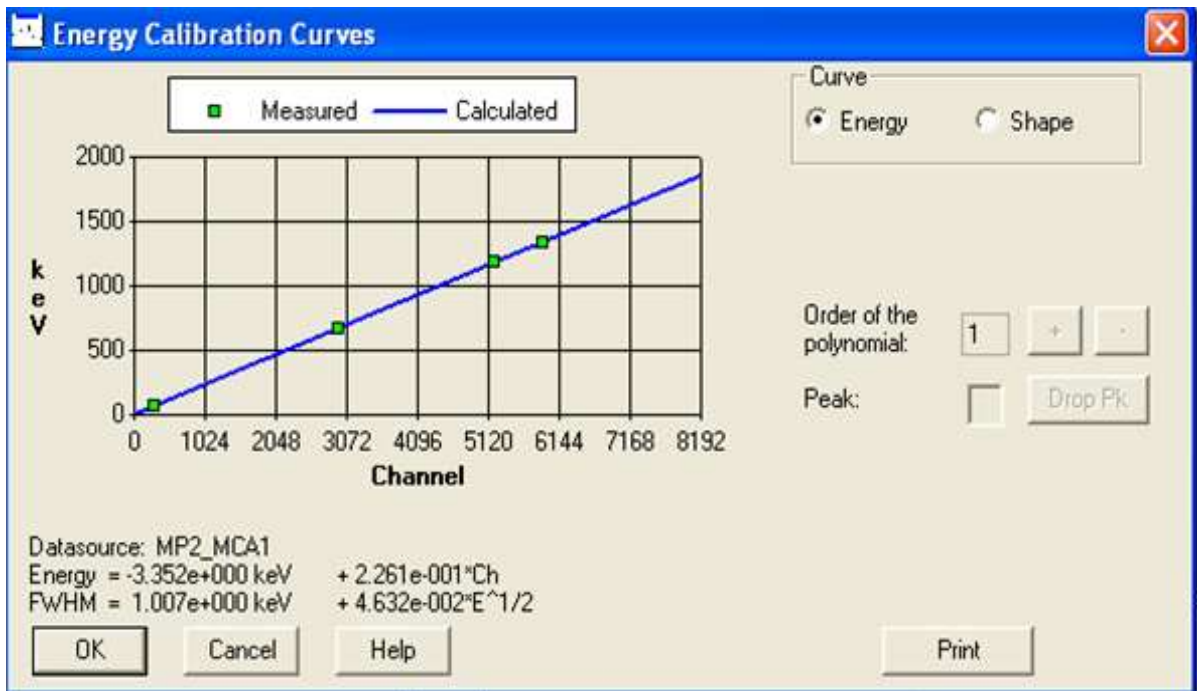


**Figure 3.3:** Energy calibration curve of the detector

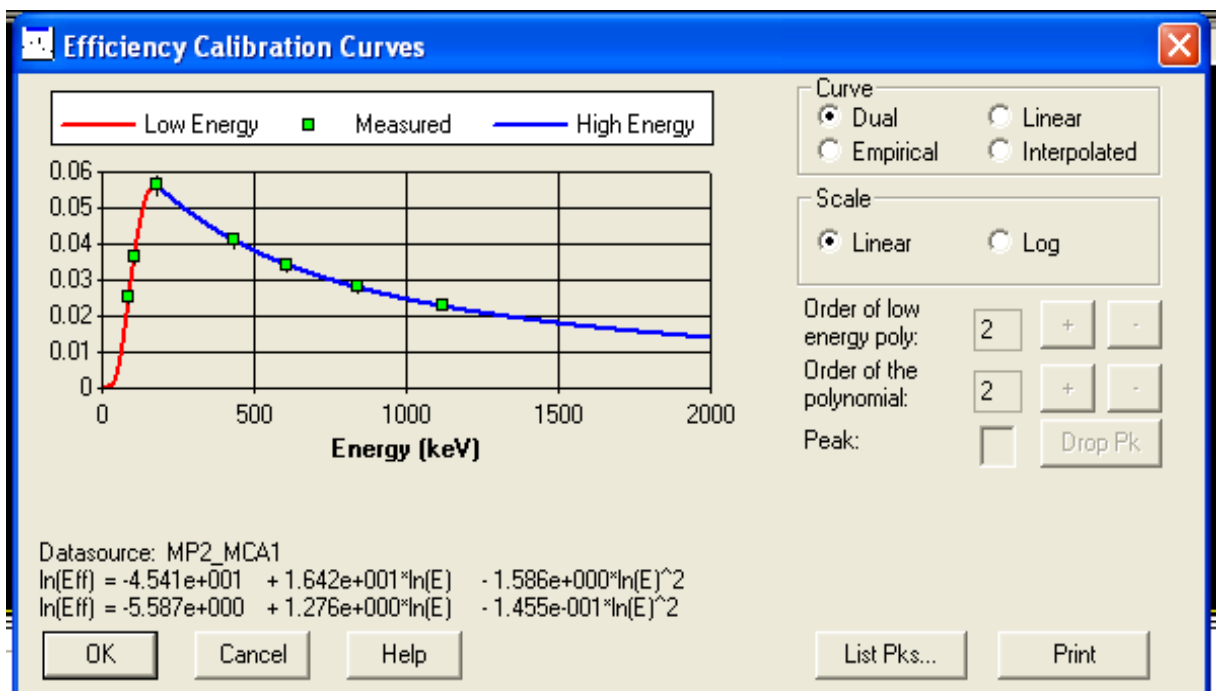


**Figure 3.4:** Efficiency calibration curve of the detector system

The detector was shield by a cylindrical lead of 5 cm thickness with internal diameter of 24 cm and height of 60 cm. the lead shield was lined with layers of cadmium and Plexiglas of 3 mm thick each as part of the set-up shield, to suppress external background radiation that may come from other sources.

The radioactivity concentrations of  $^{238}\text{U}$ ,  $^{232}\text{Th}$  and  $^{40}\text{K}$  was then determined using (HPGe) crystal detector (Canberra Co-axial (n-type) with an energy resolution of 0.0024 MeV (FWHM) at gamma energy of 1.33 MeV of  $^{60}\text{Co}$  and a relative efficiency of 50%. The detector was calibrated using standard IAEA referenced source soil (RG U- 238), RG Th- 332, R9G K-40 with same geometry and density as that of the prepared soil samples was placed on the detector. The detector coupled to a Multichannel analyzer, gamma energy spectra of the sample were accumulated for each of the soil samples using a counting time of 20000s. The  $^{238}\text{U}$  activity concentration was calculated using the 609.3 keV peak from  $^{214}\text{Bi}$  decay, while the 2.614 MeV peak of  $^{208}\text{Tl}$  was used to determine the concentration of  $^{232}\text{Th}$  and the single 1.46 MeV gamma line of  $^{40}\text{K}$  was also used to determine the concentration of  $^{40}\text{K}$  in the soil samples. The gamma-ray spectrum was accumulated analysed using a Genie 2000 software.

The activity of the radionuclides was determined using the equation (Isikalu *et al.*, 2011):

$$A_i = \frac{C_n}{E_\gamma M_s I_\gamma} \quad (3.2)$$

where  $A_i$  is the activity concentration of radionuclides ( $^{235}\text{U}$ ,  $^{232}\text{Th}$  and  $^{40}\text{K}$ ) in the soil sample,  $C_n$  is the net count per second of the sample under the corresponding photo peak,  $E_\gamma$  is the efficiency of the detector at the specific gamma ray energy of interest,  $M_s$  is the mass of soil sample and  $I_\gamma$  is the intensity of the gamma rays at desire energy being counted.

### 3.5 Evaluation of Radiological Dose and Risk Parameters

As part of radiological impact assessment of NORM concentration radiation dose and risk parameters are usually calculated. This will reveal if NORM concentration and radiation dose are within safe limits or otherwise.

#### 3.5.1 Absorbed Dose Rate ( $D$ )

The absorbed dose rate ( $D$ ) in air associate with the activity concentrates of  $^{238}\text{U}$ ,  $^{232}\text{Th}$  and  $^{40}\text{K}$  present in each of soil sample was evaluated using equation (3.2) (UNSCEAR, 2000, Abba *et al.*, 2018).

$$D(\text{nGyh}^{-1}) = \sum_{i=1}^3 A_i C_i \quad (3.3)$$

where  $A_i$  is the measured activity concentrations (Bq/kg) of  $^{238}\text{U}$ ,  $^{232}\text{Th}$  and  $^{40}\text{K}$  and  $C_i$  are their conversion factor to dose rate given as 0.462, 0.604 and 0.0417 nGyh<sup>-1</sup> per Bqkg<sup>-1</sup> respectively.

#### 3.5.2 Radium equivalent ( $R_{eq}$ )

The radium equivalent ( $R_{eq}$ ) is a radiological safety parameter which is calculated using equation (3.3) (Berekta and Mathew, 1985; UNSCEAR, 2000, Odoh *et al.*, 2018).

$$Ra_{eq} = A_U + 1.43A_{Th} + 0.077A_K \quad (3.4)$$

$A_U$ ,  $A_{Th}$  and  $A_K$  are the activity concentration as defined in equations (3.0) and (3.1). Equation (3.3) is based on the fact that 1 Bqkg<sup>-1</sup> of  $^{238}\text{U}$ , 1.43 Bqkg<sup>-1</sup> of  $^{232}\text{Th}$  and 0.077 Bqkg<sup>-1</sup> of  $^{40}\text{K}$  yield equal adsorbed gamma radiation dose rates. Thus the  $R_{eq}$ , acts as a single and simple index which can be used to compare the specific activity concentrations in materials containing different amount of  $^{238}\text{U}$ ,  $^{232}\text{Th}$  and  $^{40}\text{K}$ . Equation 3.3 was used to evaluate  $R_{eq}$  of U soil samples.

### 3.5.3 Annual outdoor effective dose rate ( $E_{out}$ (mSv/y))

In order to assess the long term hazard due to exposure to radiation, the outdoor annual effective dose rate at 1m above the ground level in air was estimated via equation 3.4 (UNSCEAR, 2000; ICRP, 2008).

$$E_{out} \left( \frac{mSv}{y} \right) = D \left( \frac{nGy}{h} \right) \times 8760 \left( \frac{h}{y} \right) \times 0.2 \times 0.7 \times 10^{-6} \left( \frac{mSv}{nGy} \right) \quad (3.5)$$

### 3.5.4 The external hazard index

The external hazard index was estimated using equation (3.5)

$$H_{ex} = \frac{A_u}{370} + \frac{A_{Th}}{259} + \frac{A_k}{4810} \leq 1 \quad (3.6)$$

### 3.5.5 Excess life cancer risk

The  $H_{ex}$  should be  $\leq 1$  in order for the external dose rate not to exceed 1.5 mGy. It also ensure that the maximum permissible level of  $Ra_{eq}$  does not exceed 370 Bqkg<sup>-1</sup> i.e.

$$H_{ex} = \frac{R_{acq}}{370(B)} (Bq/kg). \quad (3.7)$$

## 3.6 Method of Radiological Impact Assessment

In recent time standard have been set in order to protect non-human species from the harmful effect of uncontrolled exposure to ionizing radiation (UNSCEAR, 2008; ICRP, 2009; IAEA, 2011; Aliyu *et al.*, 2015). The radiological effect of mining and milling in the studied area due to the radionuclide burden in terrestrial plants and animals such as shrubs, mammals (big and small burrowing); birds, and arthropods was evaluated through the use of user friendly integrated simulation software – ERICA. The risk coefficients and dose rates to these organisms were estimated using the activity concentrations of the two measured primordial radionuclides (<sup>235</sup>U, and <sup>232</sup>Th) in the soil, tailings and mineral soils.

The ERICA assessment tool developed in Java is a stand-alone software which was designed to aid development of an integrated structure for scientific and managerial decisions with respect to environmental effect of radioisotope contamination. The software allows user to make impact assessment to the non-human biota due to ionizing radiation exposure (Beresford *et al.*, 2007; Torrud and Sactic, 2013). It allows estimation of risk to organisms in three tiers.

In the first tier, the soil concentrations were entered and compared with predefined Screening level called the environmental concentration limits (EMCL) from which risk quotients (RQ) was estimated according to equation 3.8 (UNSCEAR, 2008)

$$RQ_n = \frac{A_n}{EmcL_n} \quad (3.8)$$

where  $A_n$  is the measured activity concentration for nuclide n. For  $RQ < 1$ , the probability of exceeding the benchmark is low (<5%) and the risk calculation is terminated at this tier. But for  $RQ > 1$ , the assessment was continued to the second and third tier. In the second tier external dose rate was estimated using the equation 3.9 (Jibril *et al.*, 2009)

$$D_{ext} = \sum_x v_x \sum_i C_i^j F_{ext,i}^j \quad (3.9)$$

where  $C_i^j$  is the average concentration of radioisotope i – organism j ( $Bqkg^{-1}$ ) using fresh weight and  $F_{ext,i}^j$  is the radioisotope specific dose conversion coefficient for external exposure ( $\mu Gyh^{-1} Bq^{-1}kg$ ) and V is the occupancy factor of the organism at location X. Since the activity concentration of organism at the site was not measured, the activity ratio was rather used in the calculations. The RQ (expected and conservatives) was obtained at the end of this assessment. The total RQ was calculated.

while for high RQ, calculation proceeded to the third tier. This third tier is a probability assessment of risk where uncertainties within the results were determined using sensitivity analysis. The Graphic user interface (GUI) of ERICA is shown in Figure 3.5.

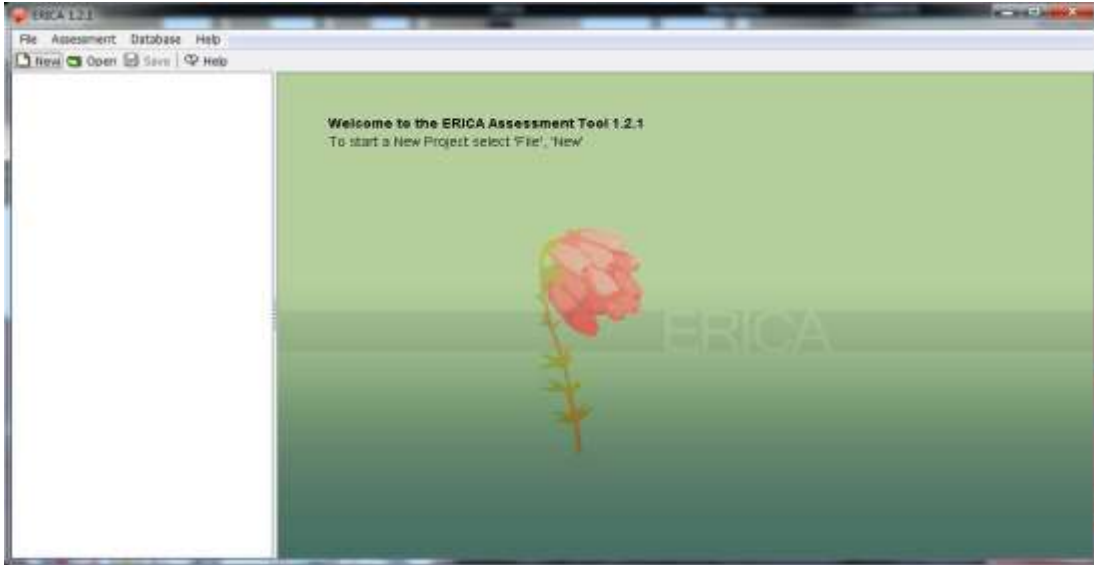


**Figure 3.5: ERICA (Version 1.2.1) Graphic User interface**

### **3.7 Heavy Metal Measurement**

Soil were collected from ten (10) of the selected 42 points for assessment of heavy metal concentration using EDXRF spectroscopy. The samples were pulverized (grind to fine powder) using pulverizing machine (planetary micro mill pulverise 7). The grinded samples were ensured to pass 150 micro mesh sieves to ensure homogeneity of the samples. Then the samples were transferred into 20g Pellet Beakers (shown in Plate VII).



**Plate VII: Pellet Beaker 20g**

For the EDXRF analysis 20g of homogenized dried sample of sand and tailing was separately used. Binder made up of pvc dissolved in toluene was added to the sample carefully and compressed with a hydraulic system to form pellets. The resulting pellets of 20g were then loaded into the sample chamber of the XRF spectrometer for quantitative and qualitative heavy metal content analysis. The EDXRF was a Minipal4 with a Model No DY-1055 and was made by PAN ANALYTICAL which was installed August, 2008 at National Geosciences Research Laboratory (NGRL) Kaduna, Nigeria. The qualitative analysis determine the type of heavy metal presents in the sample while the quantitative analysis used the net intensities in the spectrum of the heavy metal to evaluate their respective concentrations. The major heavy metals of interest were (Chromium (Cr), copper (Cu), zinc (Zn), lead (Pb), cobalt (Co), arsenic (As), cadmium (Cd), and nickel (Ni)).

### **3.7.1 Energy Dispersive X-ray Fluorescence Analysis**

The concentrations of heavy metals in the Tin mine site Rayfield – Du Jos, Plateau were determined through the Energy Dispersive X-ray Fluorescence (EDXRF) spectrometric Analysis. For this analysis, the pulverised soil samples were sundried for 96 hours until a near constant weight was obtained. Weighed 0.01 kg of the pulverised and dried soil were carefully pressed into circular pellets in a hydraulic press under a pressure of about 20 tonne. The pellets each of diameter about  $30 \pm 3$  mm were then loaded into the sample chamber of a PAN analytical Minipal4 model PW1055 EDXRF spectrometer for trace and major elemental oxide analysis.

### **3.7.2 Sample analysis**

Energy Dispersive X-ray fluorescence (EDXRF) spectrometer of model “Minipal 4” was used for the analysis. The EDXRF machine used is shown in Plate VIII. 10 g of the

powder sample were measured into sample cups and were carefully placed in the respective measuring positions on a sample changer of the machine.



**Plate VIII:** EDXRF Machine

The following condition sets were made as the machine was switched on.

- (i) Oxides/Elemental composition determination
- (ii) Nature of the samples to analyzed as press powder (pellet)
- (iii) The current used as 14 kv for major oxides, 20 kv for the trace elements/rare earth metals.
- (iv) Selected filters were “kapton” for major oxides, Ag/Al-thin for the trace elements/rare earth metals.

The selection of filters was guided by a given periodic table used for oxides/elemental analysis. Time of measurement for each sample was 100 seconds and the medium used was air throughout. The machine was then calibrated by the machines gain control measurement, after which the respective samples were measured by clicking the respective positions of the sample changer. Loss on ignition ( $H_2O^+$ ) was determined gravimetrically by heating 1g of the powdered sample in a cleaned weighed crucible at  $1000^{\circ}c$ . After which the crucible and the content was weighed to get the difference in weight before and after heating.

$$\text{Loss on Ignition (LOI)} = (a - b/1) \times 100\% = \text{H}_2\text{O}^+ \quad (3.10)$$

where, a = weight of crucible + 1g of the sample before heating

b = weight of crucible + 1g of the sample after heating

### 3.7.3 Determination of Analytes of interest using EDXRF Spectrometric analysis

The heavy metals, Chromium (Cr), Copper (Cu), Zinc (Zn), Lead (Pb), Cobalt (Co), Arsenic (As), Cadmium (Cd), and Nickel (Ni).were determined using Energy Dispersive X-ray Fluorescence (EDXRF) spectrometric Analysis.

### 3.7.4 Calculation of concentrations

The actual concentration of the analyte in the sample was calculated using the relation:

$$C_{Sam\_Actual} = \frac{C_{Sam\_Calib} * D_f * V_n}{M_{Sam}} \quad (3.11)$$

where;

$C_{sam\_actual}$  – Actual –Actual concentration of sample

$C_{sam\_calib}$  – Sample concentration (calibration curve)

$D_f$  – Dilution factor

$V_n$  – Nominal volume

$M_{sam}$  – Mass of sample

## CHAPTER FOUR

### 4.0

### RESULTS AND DISCUSSION

#### 4.1 *In-Situ* Gamma Radiation Level

The location coordinates, elevations above sea level, values of the measured absorbed dose rate in air are presented in Table 4.1 and 4.2 for both administrative areas (S) and mining and processing areas (TM). The values of the calculated AEDR and ELCR are also presented in Tables 4.1 and 4.2.

**Table 4.1: Measured ADR, elevation, coordinate and calculated dose parameters of contaminated soil**

Sample point ID	Latitude	Longitude	Elevation (m)	ADR ( $\mu\text{Sv/h}$ )	AEDR (mSv/y)	ELCR ( $\times 10^{-3}$ )
S1	9°49'45.2"N	8°54'36.6"E	1290	0.21	0.37	1.29
S2	9°50'3.3"N	8°54'17.7"E	1276	0.27	0.47	1.66
S3	9°50'8"N	8°54'34.2"E	1270	0.27	0.47	1.66
S4	9°49'59.5"N	8°54'22.4"E	1280	0.27	0.47	1.66
S5	9°50'1.8"N	8°55'0.2"E	1302	0.27	0.47	1.66
S6	9°50'4.6"N	8°54'30.5"E	1268	0.28	0.49	1.72
S7	9°50'3.4"N	8°54'19"E	1280	0.32	0.56	1.96
S8	9°50'4.7"N	8°54'19"E	1280	0.32	0.56	1.96
S9	9°50'4.4"N	8°54'25.6"E	1279	0.33	0.58	2.02
S10	9°50'3.2"N	8°54'33.1"E	1259	0.36	0.63	2.21
S11	9°50'3.8"N	8°54'95.9"E	1278	0.38	0.67	2.33
S12	9°49'48.4"N	8°54'48.3"E	1299	0.39	0.68	2.39
S13	9°49'43"N	8°54'27.1"E	1287	0.45	0.79	2.76
S14	9°50'1.1"N	8°54'20.8"E	1271	0.46	0.81	2.82
S15	9°50'5.3"N	8°54'34.3"E	1263	0.47	0.82	2.88
S16	9°49'56.4"N	8°54'49.2"E	1278	0.48	0.84	2.94
S17	9°49'50.2"N	8°54'33"E	1269	0.54	0.95	3.31
S18	9°50'2.2"N	8°54'14.8"E	1271	0.54	0.95	3.31
S19	9°49'51.1"N	8°54'48.6"E	1279	0.54	0.95	3.31
S20	9°49'51.7"N	8°54'37.3"E	1261	0.54	0.95	3.31

**Table 4.2: Measured ADR, elevation, coordinate and calculated dose parameters in tailing areas**

<b>Sample point ID</b>	<b>Latitude</b>	<b>Longitude</b>	<b>Elevation (m)</b>	<b>ADR (<math>\mu\text{Sv/h}</math>)</b>	<b>AEDR (mSv/y)</b>	<b>ELCR (<math>10^{-3}</math>)</b>
TM1	9°49'48.9"N	8°54'37.5"E	1265	0.56	0.98	3.43
TM2	9°49'51.3"N	8°54'30.5"E	1265	0.58	1.02	3.56
TM3	9°49'57.1"N	8°54'29.7"E	1261	0.58	1.02	3.56
TM4	9°49'59.6"N	8°54'15.9"E	1269	0.61	1.07	3.74
TM5	9°50'5.6"N	8°54'36.6"E	1263	0.64	1.12	3.92
TM6	9°49'50.6"N	8°54'34.8"E	1272	0.64	1.12	3.92
TM7	9°49'58.5"N	8°54'24.6"E	1275	0.65	1.14	3.99
TM8	9°50'2.2"N	8°54'36.9"E	1263	0.68	1.19	4.17
TM9	9°49'54.9"N	8°54'48.8"E	1276	0.68	1.19	4.17
TM10	9°49'44.9"N	8°54'38.6"E	1271	0.69	1.21	4.23
TM11	9°50'2.6"N	8°54'34.9"E	1259	0.70	1.23	4.29
TM12	9°49'49.9"N	8°54'40.8"E	1280	0.71	1.24	4.35
TM13	9°49'50.3"N	8°54'38.4"E	1263	0.73	1.28	4.48
TM14	9°49'53.4"N	8°54'29.0"E	1267	0.74	1.30	4.54
TM15	9°49'51.5"N	8°54'45.0"E	1277	0.79	1.38	4.84
TM16	9°49'53.9"N	8°54'36.1"E	1259	0.80	1.40	4.91
TM17	9°49'56.4"N	8°54'31.5"E	1261	0.81	1.42	4.97
TM18	9°49'55.7"N	8°54'41.9"E	1267	0.87	1.52	5.33
TM19	9°50'3.9"N	8°54'38.9"E	1262	0.88	1.54	5.40
TM20	9°49'54.5"N	8°54'30.3"E	1261	0.90	1.58	5.52
TM21	9°49'59.6"N	8°54'41.2"E	1266	0.92	1.61	5.64
TM22	9°49'59.1"N	8°54'33.4"E	1262	0.94	1.65	5.76
TM23	9°49'30.1"N	8°54'47.4"E	1280	0.96	1.68	5.89
TM24	9°49'57.4"N	8°54'34.5"E	1256	0.98	1.72	6.01
TM25	9°49'58.6"N	8°54'39.0"E	1267	1.00	1.75	6.13
TM26	9°49'51.7"N	8°54'47.7"E	1278	1.03	1.80	6.32
TM27	9°49'56.9"N	8°54'21.7"E	1264	1.03	1.80	6.32
TM28	9°50'0.00"N	8°54'38.3"E	1266	1.03	1.80	6.32
TM29	9°49'46.5"N	8°54'42.7"E	1287	1.04	1.82	6.38
TM30	9°49'47.4"N	8°54'42.6"E	1270	1.05	1.84	6.44
TM31	9°49'53.0"N	8°54'28.7"E	1263	1.06	1.86	6.50
TM32	9°49'53.9"N	8°54'47.3"E	1273	1.14	2.00	6.99
TM33	9°49'59.4"N	8°54'15.8"E	1268	1.41	2.47	8.65
TM34	9°49'50.0"N	8°54'40.0"E	1282	1.44	2.52	8.83
TM35	9°49'55.8"N	8°54'18.7"E	1264	1.49	2.61	9.14
TM36	9°49'49.8"N	8°54'43.6"E	1281	1.68	2.94	10.30
TM37	9°49'58.4"N	8°54'46.5"E	1271	1.70	2.98	10.42
TM38	9°49'53.2"N	8°54'34.3"E	1257	1.71	3.00	10.49
TM39	9°49'55.4"N	8°54'34.4"E	1257	1.75	3.07	10.73
TM40	9°49'54.9"N	8°54'26.7"E	1276	1.90	3.33	11.65
TM41	9°49'56.7"N	8°54'36.8"E	1262	1.93	3.38	11.83
TM42	9°49'57.8"N	8°54'42.7"E	1269	2.14	3.75	13.12

From the results, the ADR values of the administrative areas (Table 4.1) varied from 0.21 to 0.54  $\mu\text{Sv.h}^{-1}$  with a mean of 0.39  $\mu\text{Sv.h}^{-1}$ . While for the active mining and processing areas. (Table 4.2), the ADR was between 0.56 to 2.14  $\mu\text{Sv.h}^{-1}$  with a mean value of 1.04  $\mu\text{Sv.h}^{-1}$ . For the entire mining site, the total average ADR for both soil and tailing points was 0.83  $\mu\text{Sv.h}^{-1}$ . The AEDR varies from 0.37 to 3.75  $\mu\text{Sv.y}^{-1}$  with a mean of 1.45  $\mu\text{Sv.y}^{-1}$ . ELCR values for the mine area  $1.29 \times 10^{-3}$  to  $13.12 \times 10^{-3}$  with a mean of  $5.07 \times 10^{-3}$ . The elevation of the 62 survey points varies from 1256 to 1302 m with an average value of 1271 m.

The spatial distribution of the elevation ADR, AEDR, and ELCR for the mine are depicted in Figures 4.1 to 4.4. From the Figures, a strong correlation between ADR, AEDR and ELCR could be observed as expected from the computation expressions (equations 4.1 and 4.2). However, area with higher ADR, AEDR, and ELCR can be observed to correspond to lower elevation points. Consequently, there is an inverse correlation between each of ADR, AEDR, and ELCR, and elevation above sea level. Places with low elevations mostly corresponds to places on the mine field where mine pits have been dug for the collection of unprocessed soil and rock for mining and milling. The dug pits also have in some cases heaps of both processed (tailings) and unprocessed rocks and soils. These explain the elevated values of measured absorbed dose in these areas. The high ADR areas are located around the North – Western part of the mine (as seen in Figure 4.1b). Another feature that can be attributed to the high ADR in the mining pits is the fact that excavation exposes mineral and radionuclide rich rocks which could have been attenuated by surface soils.

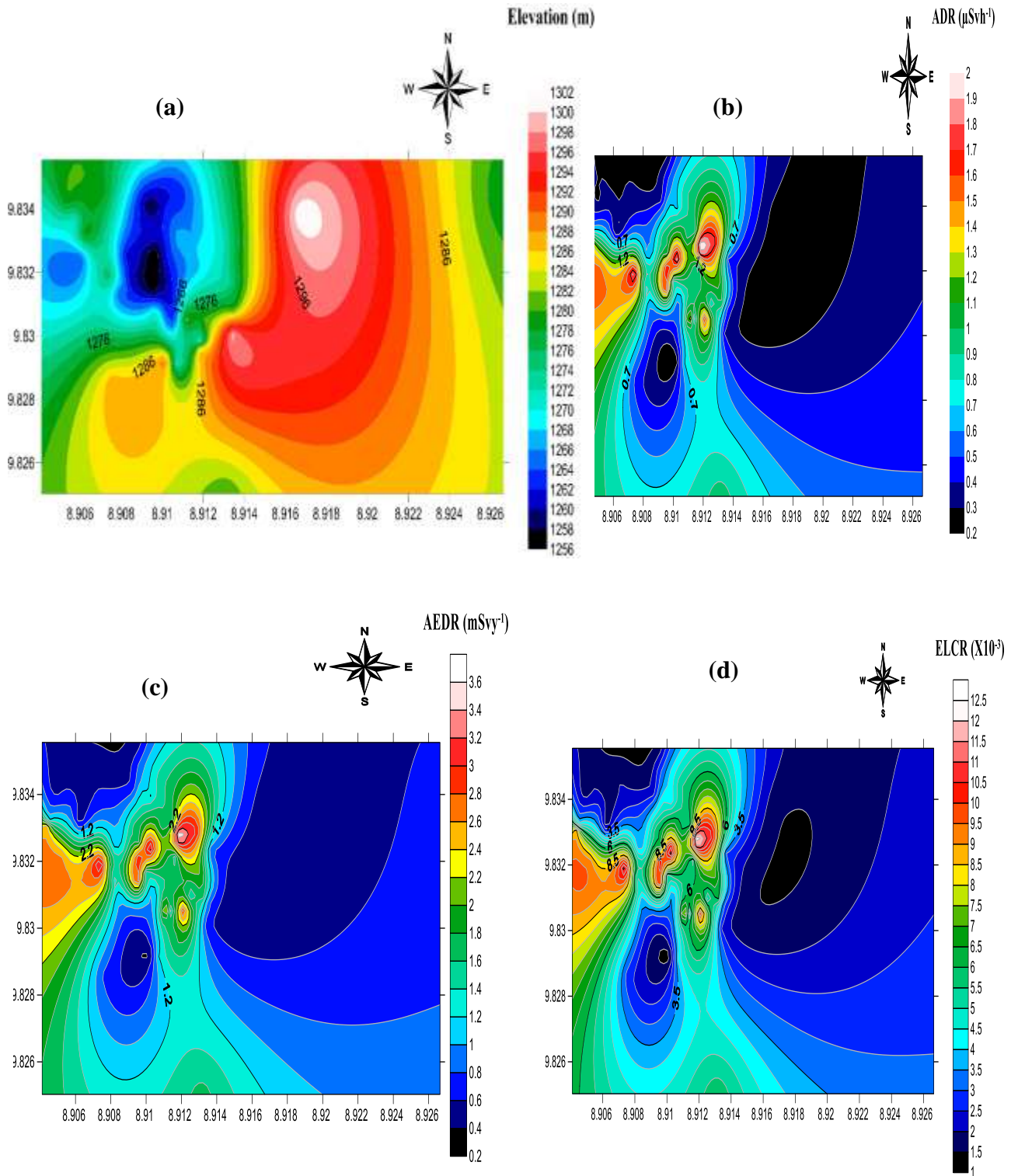


**Figure 4.1:** Spatial distribution of (a) elevation, (b) ADR, (c) ELCR, (d) AEDR across the mine

The exposure of such rocks and their radiation and radionuclide bearing minerals such as monazite contributed to the higher ADR values measured at those places.

Generally, the measured radiation level of administrative areas was lower compared to places where mining and processing were taking place. Tailings and mineral soils have been proven to contain high level of primordial radionuclides and thus high gamma radiation doses (Ibeanu, 2003; Arogunjo, 2009; Ademola, 2008; Aliyu, *et al.*, 2015). This automatically accounts for the observed higher dose rates in air in the active mining areas. The mean measured AED, AEDR, and ELCR for the mine were all higher than their corresponding world average according to UNSCEAR (2000) and safety limit according to the ICRP (1990). The mean measured AED value of  $0.83 \mu\text{Svh}^{-1}$  was about 17 times greater than the world average value of  $0.05 \mu\text{Svh}^{-1}$ . On the other hand, the mean AEDR of  $1.44 \text{mSvy}^{-1}$  was 24 times greater than the outdoor world average value of  $0.07 \text{mSvy}^{-1}$  UNSCEAR (2000). Compared to the occupational and public exposure limit of  $1.5 \text{mSvy}^{-1}$  and  $1.0 \text{mSvy}^{-1}$  respectively recommended by the ICRP (1990), the average computed AEDR falls between both values.

The average calculated ELCR value for the mine ( $5.07 \times 10^{-3}$ ) was extremely higher than the world average value of  $0.29 \times 10^{-3}$  documented in the UNSCEAR, (2000) report. This implies that anyone (miners, dwellers and others) staying or working in the mine field has more chances of developing cancer by a factor of about 17 years if they spent all their lives around the mine and live up to 70 years old.

The geology of the mine area (Jos) and the presence of mineral ores of columbite, tin, monazite and other NORM rich minerals are majorly responsible for the relatively high measured and calculated radiological parameters in the mine area. The higher values of AED and other radiological safety parameters in TM compared to S areas could also be

attributed to their richer mineral content which have been reduced due to mining processes or attenuated by surface soils in the S areas.

Effective doses received by the different organs ( $D_o$ ) of the body of the people living or working in the mine was estimated from the annual effective dose rate (AEDR) according to the equation 4.1 (Ibeanu 2003):

$$D_o \text{ (mSvy}^{-1}\text{)} = OF \times AEDR \text{ (mSvy}^{-1}\text{)} \times F \quad (4.1)$$

where, OF (=0.2) is the occupancy factor, and F is the organ of interest.

Equation 4 estimates the  $D_o$  as the amount of radiation dose the different organs of the human body are exposed to. The organs of interest and their corresponding organ conversion factor are lungs (0.64), ovaries (0.58), bone marrow (0.69), testes (0.82), kidney (0.62), and liver (0.46) (ICRP, 1996). The values of the organ doses of the six different human organs of interest calculated via equation 4.4 is presented in Table 4.3. From the results, the values of the organ doses for the administrative area are generally lower than those obtained from tailing points. Of all the organs considered, the testicles received the highest organ dose value of 0.3 mSvy<sup>-1</sup> and 0.11mSvy<sup>-1</sup> for TM areas and S areas respectively. While the lowest dose was found in liver with a value of 0.06 and 0.17 mSvy<sup>-1</sup> for S and TM areas respectively. The total organ dose values for both S and TM areas varies from 0.047 to 0.061 mSvy<sup>-1</sup>. The variation in the organ doses can be attributed to their different organ conversion factors ( $F$ ) which is a measure of their radio-sensitivity to ionising radiation.

The summary of the measured ADR and the calculated radiation safety parameters for the S and TM areas with respect to safety limits and world average values are also shown in Table 4.4. The comparison of the ADR measured in this research and other mining areas in Nigeria, Ghana and those of high background area in Malaysia is presented in Table

4.4. From the table, the range of ADR obtained in this research though higher than the world average value and safety limits, it was however lower than the values obtained at mining sites in Bukuru, Jos area and Ede all in Nigeria. Ademola (2008), though obtained higher values for Jos where the present research was conducted.

**Table 4.3: Summary of measured *in-situ* ADR, AEDR, ELCR and effective organ doses**

Location Description	Number of Locations	ADR ( $\mu\text{Sv/h}$ )	AEDR ( $\text{mSv/y}$ )	ELCR ( $10^{-3}$ )	Mean organ Effective Dose ( $\text{mSv/y}$ )					
					Lungs	Ovaries	Bone marrow	Testes	Kidney	Liver
TM	42	1.04	1.81	6.36	0.09	0.08	0.09	0.11	0.08	0.06
S	20	0.38	0.67	2.36	0.23	0.21	0.25	0.29	0.23	0.17
Total	62	0.83	1.45	5.10	0.19	0.17	0.20	0.24	0.18	0.10
Minimum		0.21	0.37	1.29	0.05	0.04	0.05	0.06	0.04	0.03
Maximum		2.14	3.75	13.12	0.48	0.43	0.52	0.61	0.46	0.34
World mean Value		0.05*	0.07*	0.29**						
Safety Limit			1.00**							

\*UNSCEAR (2000); \*\*ICRP (1990)

**Table 4.4: Comparison of ADR with earlier research in other places**

Location	Location description	<i>In-situ</i> ADR ( $\mu\text{Sv/h}$ )	Reference
Bukuru, Nigeria	Tine Mine	5 - 80	Funtua and Elegba, 2005
Jos, Nigeria	Tine Mine	6 - 28	Ademola, 2008
Ede, Nigeria	Columbite and Tantalite, Mine	0.02-11	Adewale <i>et al.</i> , 2015
Perseus, Ghana	Gold, Mine	0.04 -0.12	Faanu, <i>et al.</i> , 2016
Johor, Malaysia	High radiation area	0.07 - 1.44	Ramli <i>et al.</i> , 2005
Rayfield Du, Jos, Nigeria	Tin Mine	0.21 - 2.14	This study

The result presented here has further buttressed the fact that mining, in no small measure contribute to the terrestrial gamma radiation of an area. Furthermore, it has demonstrated that Jos and environs can be classified as high background radiation area in Nigeria. This is true as research had revealed that specific activities of natural radionuclides levels in Jos Plateau tin mines, exceed the mean values for areas designated as high background natural radiation areas (Arogunjo, 2009; Aliyu *et al.*, 2015, Forster *et al.*, 2002; Moller and Mousseau, 2013). The difference between ADR in this research and those obtained in Malaysia, Ghana and Ede could be attributed to variation in geological composition and classification of the different areas.

#### **4.2. Specific Activities Concentrations of NORM in Mine Soil Samples**

The results of the gamma spectrometric analysis of the soil samples collected from the mine together with the location coordinate of the points and elevation above sea level are given in Tables 4.5, 4.6 and 4.7. The results presented for the S samples (Table 4.5) showed that the specific activities of  $^{238}\text{U}$   $^{232}\text{Th}$  and  $^{40}\text{K}$  ranged from  $98.17 \pm 9.81$  to  $289.91 \pm 15.71$  Bqkg<sup>-1</sup>;  $229.06 \pm 14.58$  to  $965.09 \pm 55.75$  Bqkg<sup>-1</sup>; and  $59.94 \pm 4.93$  to  $1732.66 \pm 94.84$  Bqkg<sup>-1</sup> respectively. The mean concentration of the S samples was  $168.83 \pm 9.35$  Bqkg<sup>-1</sup>,  $436.08 \pm 26.31$  Bqkg<sup>-1</sup> and  $346.1 \pm 21.92$  Bqkg<sup>-1</sup> respectively for  $^{238}\text{U}$   $^{232}\text{Th}$  and  $^{40}\text{K}$ . For the tailing samples (T), the range of  $^{238}\text{U}$   $^{232}\text{Th}$  and  $^{40}\text{K}$  specific activities were  $77.44 \pm 4.76$  to  $195.45 \pm 10.82$  Bqkg<sup>-1</sup>,  $117.98 \pm 8.64$  to  $770.02 \pm 45.25$  Bqkg<sup>-1</sup> and  $2076.45 \pm 112.66$  Bqkg<sup>-1</sup>, with respective mean values of  $138.84$  Bqkg<sup>-1</sup>,  $469.31$  Bqkg<sup>-1</sup> and  $578.65$  Bqkg<sup>-1</sup>. The range of the three primordial radionuclides;  $^{238}\text{U}$   $^{232}\text{Th}$  and  $^{40}\text{K}$  in the mineral soils were  $176.34 \pm 9.79$  to  $617.61 \pm 33.16$  Bqkg<sup>-1</sup>,  $223.45 \pm 14.33$  to  $1915.41 \pm 110.82$  Bqkg<sup>-1</sup> and  $78.62 \pm 6.39$  to  $2719.18 \pm 148.04$  Bqkg<sup>-1</sup> respectively. The mean activity concentrations were found to be  $323.435$  Bqkg<sup>-1</sup>,  $877.63$  Bqkg<sup>-1</sup> and  $864.99$  Bqkg<sup>-1</sup> respectively for  $^{238}\text{U}$ ,  $^{232}\text{Th}$ , and  $^{40}\text{K}$ . Generally, the mean activity concentrations of the

classes of soil samples collected from the mine for Uranium-238, Thorium-232 and Potassium-40 were  $243.59 \text{ Bqkg}^{-1}$ ,  $677.96 \text{ Bqkg}^{-1}$  and  $680 \text{ Bqkg}^{-1}$  respectively.

**Table 4.5: Specific activities of NORM in S soils**

Sample point ID	Latitude	Longitude	Elevation (m)	$^{238}\text{U}$ (Bq/kg)	$^{232}\text{Th}$ (Bq/kg)	$^{40}\text{K}$ (Bq/kg)
S1	9°49'45.2"N	8°54'36.6"E	1290	130.5±7.36	323.29±20.14	59.94±4.92
S2	9°50'3.3"N	8°54'17.7"E	1276	148.82±8.2	270.52±16.63	148.55±10.6
S3	9°50'1.8"N	8°55'0.2"E	1302	171.86±9.47	306.03±18.89	170.7±12.42
S4	9°50'4.7"N	8°54'19"E	1280	289.91±15.71	263.97±16.99	124.96±10.91
S5	9°50'3.2"N	8°54'33.1"E	1259	145.65±8.13	285.16±17.84	130.64±11.27
S6	9°49'48.4"N	8°54'48.3"E	1299	174.12±9.81	965.09±55.75	139.31±13.91
S7	9°50'1.1"N	8°54'20.8"E	1271	98.17±5.62	229.06±14.58	220.02±14.89
S8	9°50'5.3"N	8°54'34.3"E	1263	163.32±8.99	393.31±23.7	183.21±13.4
S9	9°49'50.2"N	8°54'33"E	1269	202.08±11.17	749.98±44.53	1732.66±94.84
S10	9°50'2.2"N	8°54'14.8"E	1271	163.91±9.06	574.41±34.02	550.97±32.06
Min				98.17±5.62	229.06±14.58	59.94±4.92
Max				289.91±15.71	965.09±55.75	550.97±32.06
Mean				168.83±9.34	436.08±26.31	346.09±21.92

**Table 4.6: Specific activities of NORM in T soils**

Sample point ID	Latitude	Longitude	Elevation (m)	$^{238}\text{U}$ (Bq/kg)	$^{232}\text{Th}$ (Bq/kg)	$^{40}\text{K}$ (Bq/kg)
T1	9°49'48.9"N	8°54'37.5"E	1265	159.23±8.79	532.08±31.49	669.4±37.72
T2	9°49'51.3"N	8°54'30.5"E	1265	163.55±9.11	348.83±21.78	2076.45±112.66
T3	9°49'58.5"N	8°54'24.6"E	1275	123.12±6.93	244.41±15.57	96.71±8.84
T4	9°49'50.3"N	8°54'38.4"E	1263	136.73±7.56	321.94±19.47	223.29±14.81
T5	9°49'59.1"N	8°54'33.4"E	1262	77.44±4.76	117.98±8.64	290.27±17.81
T6	9°49'30.1"N	8°54'47.4"E	1280	113.98±6.37	423.58±25.51	109.41±10.22
T7	9°49'59.4"N	8°54'15.8"E	1268	155.14±8.7	770.02±45.25	391.91±24.67
T8	9°49'55.8"N	8°54'18.7"E	1264	195.45±10.82	730.41±43.2	1508.46±83.03
T9	9°49'49.8"N	8°54'43.6"E	1281	108.86±6.23	476.8±28.65	258.88±17.32
T10	9°49'55.4"N	8°54'34.4"E	1257	154.86±8.68	727.03±42.77	161.73±13.39
Min				77.44±4.76	117.98±8.64	96.71±8.84
Max				195.45±10.82	770.02±45.25	2076.45±112.66
Mean				138.84±26.23	469.31±26.33	578.65±34.05

**Table 4.7: Specific activities of NORM in M soils samples**

Sample point ID	Latitude	Longitude	Elevation (m)	<sup>238</sup> U (Bq/kg)	<sup>232</sup> Th (Bq/kg)	<sup>40</sup> K (Bq/kg)
M1	9°50'5.6"N	8°54'36.6"E	1263	376.92±20.22	467.08±27.39	78.62±6.39
M2	9°50'2.2"N	8°54'36.9"E	1263	306.14±16.65	699.52±41.58	593.7±35.45
M3	9°49'54.9"N	8°54'48.8"E	1276	241.47±13.23	727.2±42.99	142.3±12.57
M4	9°50'2.6"N	8°54'34.9"E	1259	241.08±13.20	543.91±32.64	637.04±36.93
M5	9°49'49.9"N	8°54'40.8"E	1280	205.23±11.30	1121.8±64.84	179.66±12.03
M6	9°49'53.9"N	8°54'36.1"E	1259	230.48±12.62	444.18±27.11	228.99±16.81
M7	9°49'56.4"N	8°54'31.5"E	1261	331.82±18.01	847.32±49.97	2091.4±114.09
M8	9°50'3.9"N	8°54'38.9"E	1262	472.79±25.46	562.97±34.14	252.91±19.28
M9	9°49'54.5"N	8°54'30.3"E	1261	233.46±12.78	537.15±32.32	1792.46±97.90
M10	9°49'59.6"N	8°54'41.2"E	1266	242.8±13.36	955.09±56.02	239.45±19.92
M11	9°49'57.4"N	8°54'34.5"E	1256	525.42±28.23	1178.4±68.81	2046.56±112.09
M12	9°49'58.6"N	8°54'39"E	1267	617.18±33.19	1744.33±101.16	2719.18±148.04
M13	9°49'51.7"N	8°54'47.7"E	1278	354.69±19.19	1158.48±67.68	372.48±25.98
M14	9°49'46.5"N	8°54'42.7"E	1287	280.1±15.17	974.96±56.87	189.94±14.91
M15	9°49'53"N	8°54'28.7"E	1263	237.94±13.03	723.23±42.10	1837.3±99.52
M16	9°49'53.9"N	8°54'47.3"E	1273	326.57±17.70	563.81±33.85	578.75±34.31
M17	9°49'50"N	8°54'40"E	1282	202.08±11.17	749.98±44.53	1732.67±94.84
M18	9°49'58.4"N	8°54'46.5"E	1271	617.61±33.16	1656.79±94.40	505.51±33.88
M19	9°49'53.2"N	8°54'34.3"E	1257	408.64±22.13	1915.41±110.82	1508.46±84.02
M20	9°49'54.9"N	8°54'26.7"E	1276	183.74±10.10	223.445±14.33	131.39±10.62
M21	9°49'56.7"N	8°54'36.8"E	1262	176.43±9.79	609.54±36.30	368±22.77
M22	9°49'57.8"N	8°54'42.7"E	1269	302.98±14.50	903.17±52.89	802.96±46.33
Min				176.43±9.79	223.445±14.33	78.62±6.39
Max				617.61±33.16	1915.41±110.82	2719.118±148.04
Mean				323.44±17.46	877.62±.51.49	864.97±49.01

The variation of the mean specific activity concentrations of the three primordial radionuclides in the three classes of collected and analysed soil samples are presented in Figure 4.2. Generally, all the radioisotopes under study had higher concentrations in the mineral soils (M) compared to the tailings (T) and normal soils (S) of the study area. The average concentration of <sup>40</sup>K was higher in the tailings compared to the normal some samples (S) while, <sup>232</sup>Th was slightly higher in tailings compared to the values in S. However, <sup>238</sup>U was found to be of higher concentration in the normal soil compared to the

tailings. For normal soil and mineral soils (M), the trend of activity concentration was  $^{232}\text{Th} > ^{40}\text{K} > ^{238}\text{U}$  while the trend in (T) samples was  $^{40}\text{K} > ^{232}\text{Th} > ^{238}\text{U}$ . The average specific concentration of  $^{238}\text{U}$ ,  $^{232}\text{Th}$  and  $^{40}\text{K}$  in all the three categories of soil samples collected in the mining site were all greater than their respective world average values of 33 Bqkg<sup>-1</sup>, 45 Bqkg<sup>-1</sup> and 420 Bqkg<sup>-1</sup> in normal soil (UNSCEAR, 2008). The average activity concentrations of  $^{238}\text{U}$  was about five, four and ten times the average value in soil for S, T, and M soils respectively. Also  $^{232}\text{Th}$  activity was about ten, ten and twenty times their world average values in soil while  $^{40}\text{K}$  was less than the world mean value in S – soil, slightly higher (1.4 times) in T- soils and about twice the world mean value in M – samples.

The variations in the distributions of the radioisotope in the different classes of soils collected, could be attributed to the geological (natural) and anthropological processes taking place in the area. The geological composition and description of an area has been confirmed to influence the radiological content in the soil and rocks found in such area (Olarinoye, 2010, Ademola, 2005, Arogunjo, 2009; Ramli, *et al.*, 2005). Consequently, the higher concentration of uranium, thorium and potassium in the study area could only have come from the geological and mineral composition of the soils and rocks in the area. The geology of the area has been described to be rich in minerals such as uranyl monazite, theorite, zirconium sand, cassiteite and columbite (Arogunjo, 2009, Ademola, 2008, Ibeanu, 2003, Dewet, 1996).

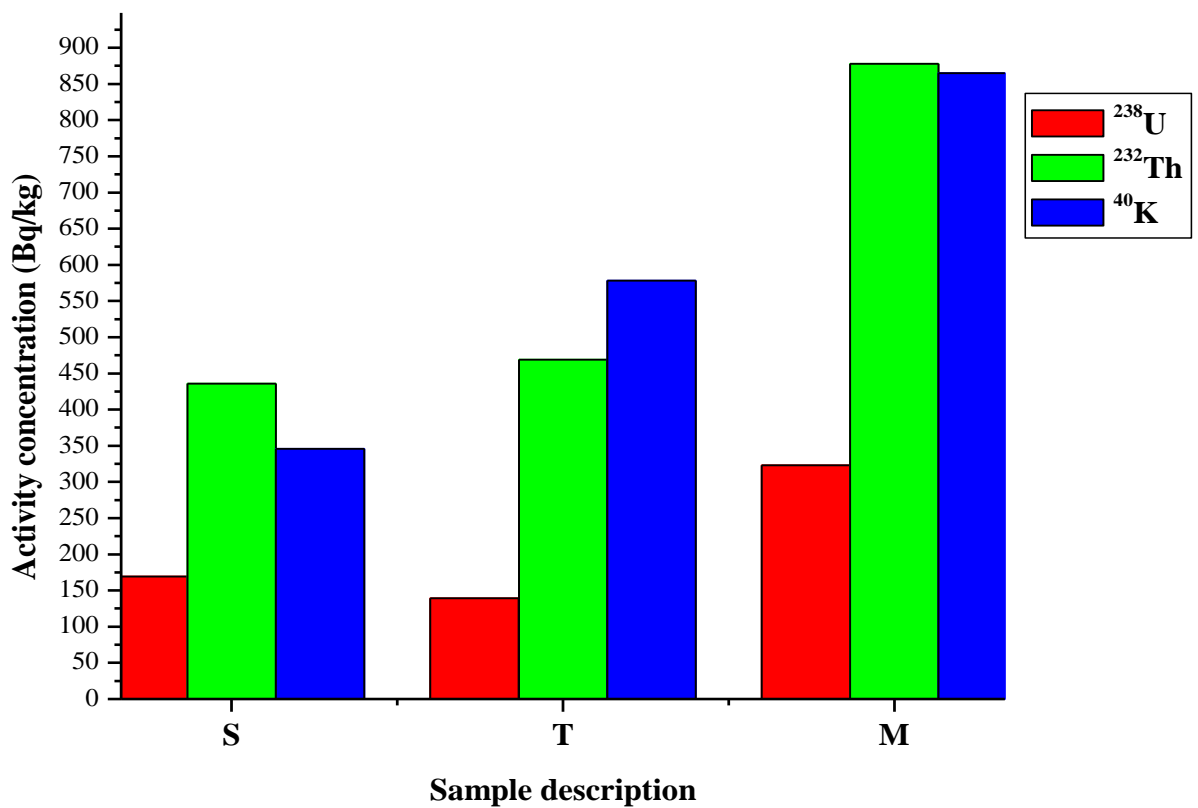


**Figure 4.2:** Mean distribution of  $^{238}\text{U}$ ,  $^{232}\text{Th}$  and  $^{40}\text{K}$  specific activity concentrations in soil samples

These minerals are rich in uranium, thorium, and potassium. This explains the elevated activity concentration of the radionuclide in the area under study. The higher radionuclide concentration in the mineral soil (M) compared to the other two categories of soils is in correlation with the fact that tin ore mineral soil is rich in minerals which contain more uranium, thorium and potassium and thus more radioactive isotopes of these nuclides (Arogunjo, 2009, UNSCEAR, 2008). This elevated radionuclide concentration of mineral soil is attributed to their delayed crystallisation in the magmatic differentiation processes which characterizes them (Olise *et al.*, 2014). This also explains why the radionuclide concentrations are higher in T soils than normal soil. Although, the T soil has been mined (stripped of their mineral content which host the radionuclides) however, complete mining

and isotope extraction cannot be guaranteed. This is possibly due to the crude mining methods adopted in the mining site. More so research conducted in the mine tailings all in the past has revealed higher radioisotope NORM burden compared to normal soils. The elevated NORM concentration of the soil collected from the administrative (with no mine activities) areas' soils (S) compared to natural distribution in soils in other areas as shown in Table 4.8 and world average values is an indication that the soil in the area is rich in radioisotope and the mine soil could not have been also contaminated by tailings and mineral soil as top soil was removed during the sample collection process. The measured NORM distribution in the undisturbed soil is purely an indication of the geochemical composition of the soil in the area.

Generally, the activity concentration of thorium -232 was always higher than those of uranium. This is different from the normal trend of non- contaminated environmental samples where uranium concentration values are always higher than those of thorium (Ademola *et al.*, 2015; Arogunjo 2009; Hartley 2001; Deng *et al.*, 1997; Haridason *et al.*, 2001; Mohanty *et al.*, 2003; Hofman, *et al.*, 2000). This trend has also been shown in previous research carried out in different mining areas of Jos, and its environs (Table 4.8). The higher specific activities of thorium compared to uranium and potassium could also be attributed to its low solubility in soil. Whereas uranium form uranyl complexes in soil water, it has been reported that uranium is potentially available biologically with high mobility potential compared to thorium (Lind, *et al.*, 2013). This is an indication that the ground water in the area could have been contaminated due to the mining activities. More so, that the mining process involves washing in water (open pit style). This further explains lower K and U content in T and S sample compared to M. Although potassium is relatively more abundant in natural soil, however radioactive potassium ( $^{40}\text{K}$ ) has lower mean activity concentration in T soils and M samples compared to  $^{232}\text{Th}$ . Again the higher

concentration of  $^{232}\text{Th}$  bearing mineral and the biomobility of  $^{40}\text{K}$  in ground (soil) water and mine processing could be used to explain this variation.

In order to trace the source of radioisotopes in soil sample the correlation of  $^{232}\text{Th}$  and  $^{238}\text{U}$  specific activities concentration could be used. Consequently, a linear regression analysis of the  $^{232}\text{Th}$  and  $^{238}\text{U}$  concentration in S, T, and M sample were done. A good linear correlation between  $^{232}\text{Th}$  and  $^{238}\text{U}$  exists for M and T sample respectively with a correlation coefficient (R) value of 0.72 and 0.66 respectively. However, the R value for the linear correlation analysis between  $^{40}\text{K}$  and  $^{238}\text{U}$  in M and T samples were 0.36 and 0.40, while R value for  $^{40}\text{K}$  and  $^{232}\text{Th}$  were 0.63 and 0.14 respectively. The better correlation between  $^{238}\text{U}$  and  $^{232}\text{Th}$  radioisotope in M and T samples indicated a common thorium and uranium bearing mineral sources such as monazites and zirconium (Mohanty *et al.*, 2004; Olise *et al.*, 2014; Arogunjo, 2009). The weaker correlation of Thorium and Uranium in the tailing samples compared to the M samples confirmed that the mining process actually perturbed the natural distribution of the uranium isotope in the mineral soils.

Furthermore, the mean  $^{232}\text{Th}$  and  $^{238}\text{U}$  activity ratio in S, T, and M samples were 2.57, 3.37 and 2.72 respectively. The  $^{232}\text{Th}$  and  $^{238}\text{U}$  ratio is higher in the T soil compared to the S and M soils and this also shows that the mining process actually alter the natural distribution of these radionuclide in soils. The process trend to enrich the soil with thorium compared to uranium. Similar uranium enrichment have been reported in mine soil in earlier research (Arogunjo, 1999; Ramli *et al.*, 2015; Olise *et al.*, 2014; Ibeanu, 2003).

The mean specific radioactivity of the NORM determined for S, T and M soils were compared with world average values and those obtained for similar investigations within and outside Jos in Table 4.8. As seen from the Table, terrestrial radionuclide concentration

varies from place to place and sample type. The obtained values in this research were all higher than their respective world average Figures, however, result for radionuclide concentrations were found to be lower than some previous research conducted around Jos. Furthermore, in comparison with Jos city soil as reported by Arogunjo *et al.* in 2009 (Table 4.8), the NORM concentration in the mine soil was greater- an indication of the impact of the mine activities. The Table also show that elevated NORM concentrations are highest in mineral sand, tin and Zircon samples. The variation observed in the NORM concentrations could be as a result of the different mineral ores deposit in the mines and the geotechnical definition of the different locations.

**Table 4.8: Summary of activity Concentrations in soil due to mining in Jos and other places in Nigeria**

<b>Location</b>	<b>Sample description</b>	<b>A<sub>k</sub> (Bq/kg)</b>	<b>A<sub>Th</sub> (Bq/kg)</b>	<b>A<sub>U</sub> (Bq/kg)</b>	<b>Study</b>
Akure, Nigeria	Soil	-	53	66	Arogunjo <i>et al.</i> , 2009
Jos, Nigeria	Soil	-	109	150	Arogunjo <i>et al.</i> , 2009
Bitsichi, Nigeria	Soil	-	16800	8700	Arogunjo <i>et al.</i> , 2009
Bitsichi, Nigeria	Tailing	-	30000	22000	Arogunjo <i>et al.</i> , 2009
Bitsichi, Nigeria	Mineral sand	-	92000	40000	Arogunjo <i>et al.</i> , 2009
Bitsichi, Nigeria	Tin	-	32000	11000	Arogunjo <i>et al.</i> , 2009
Bitsichi, Nigeria	Zircon	-	98000	51000	Arogunjo <i>et al.</i> , 2009
Bitsichi, Nigeria	Soil	350	451	-	Jibiri <i>et al.</i> , 2009
Bukuru, Nigeria	Soil	981	154	-	Jibiri <i>et al.</i> , 2010
Ropp, Nigeria	Soil	1062	147	-	Jibiri <i>et al.</i> , 2011
Jos, Nigeria	Mine Soil	-	8175	3779	Ibeanu, 2003
Jos, Nigeria	Mine Tailing	-	1680	722	Ademola, 2008
Bukuru, Nigeria	Mine Soil	35	3	776	Ajayi, 2008
Jos, Nigeria	Soil	346	436	169	This study
Jos, Nigeria	Tailing	578	469	139	This study
Jos, Nigeria	Mineral and	865	878	326	This study
World Average	Soil	420	45	33	UNSCEAR, 2008

The spatial distribution of the total mean specific activities of the NORM in the mine field for all the 42 soil samples analysed is shown in Figures 4.3, 4.4 and 4.5. The Figures show a strong positive correlation between  $^{232}\text{Th}$  and  $^{238}\text{U}$  spatial distributions compared to  $^{40}\text{K}$

confirming the regression analysis result. This further confirm that the radioisotopes ( $^{232}\text{Th}$  and  $^{238}\text{U}$ ) from the soil samples comes from common mineral source.

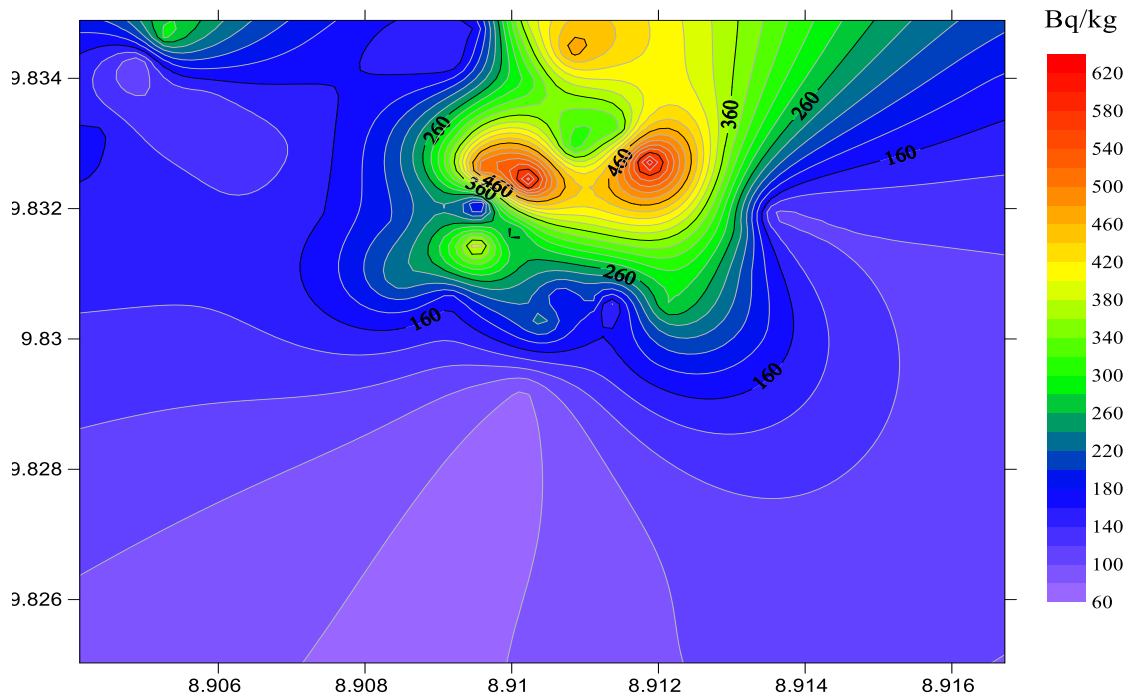


**Figure 4.3:** Spatial distribution of  $^{238}\text{U}$  activities for the sample location.

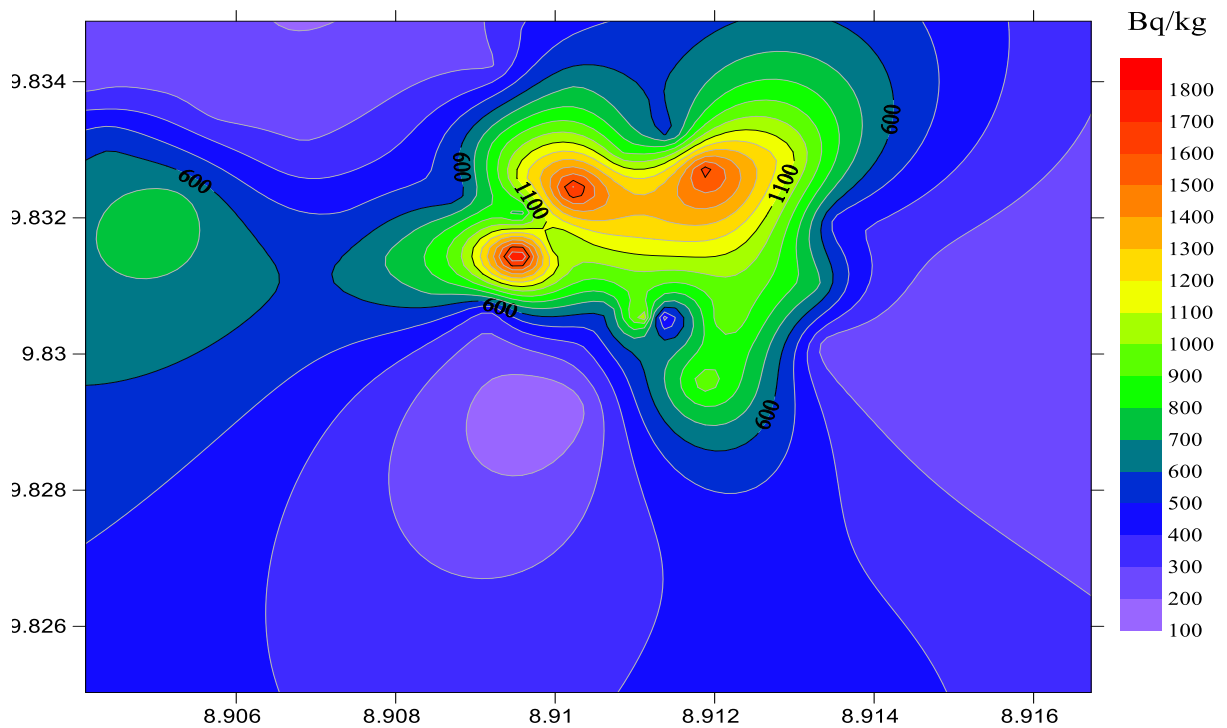


**Figure 4.4:** Spatial distribution of  $^{232}\text{Th}$  activity concentration of sampled location.

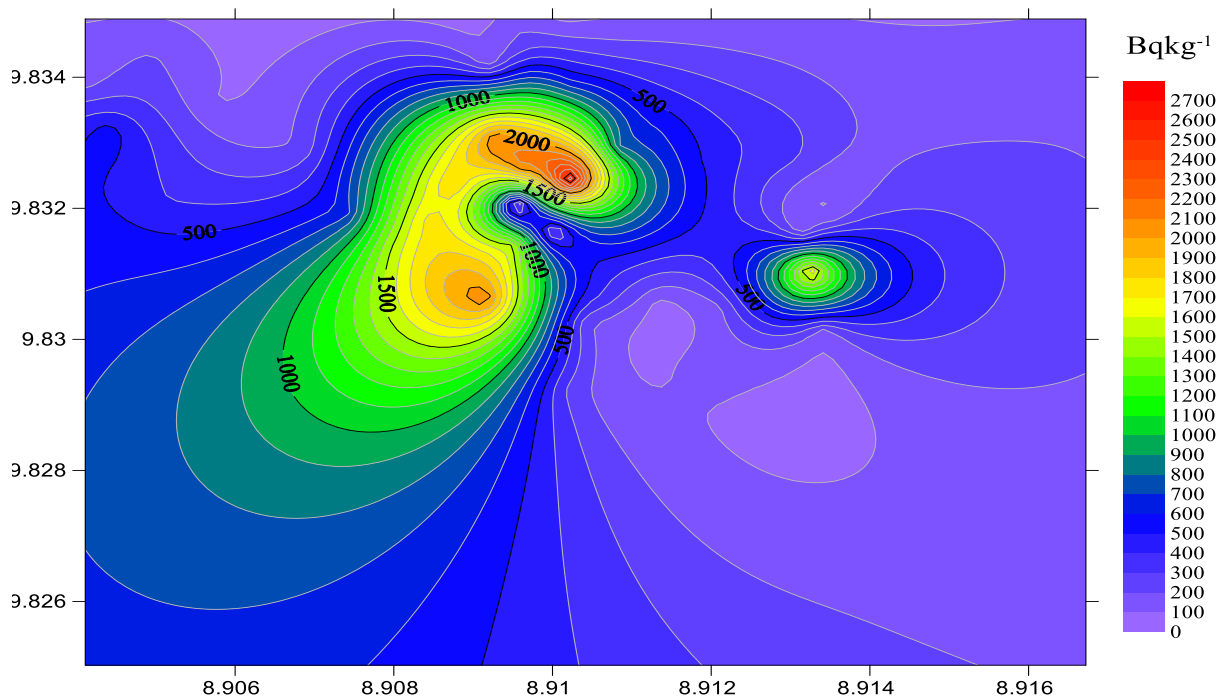


**Figure 4.5:** Spatial distribution of  $^{40}\text{K}$  activity concentration of sampled location

### 4.3 Assessment of Radiological Hazard Parameters due to NORM Concentration

The external absorbed dose rate ADR in air at the respective sample collection point containing the concentration of  $^{238}\text{U}$ ,  $^{232}\text{Th}$ , and  $^{40}\text{K}$  evaluated using equation 3.3 are presented with other evaluated radiological hazard indices (using equations 3.4 to 3.7) in Tables 4.9-4.11. The mean ADR obtained for the three classes of soil was 0.36, 0.46, and 0.76  $\mu\text{Gyhr}^{-1}$  respectively for S, T and M. The higher ADR of M with respect to S and T was due to the evaluated NORM content of M with respect to S and T. The mean radium equivalent ( $R_{eq}$ ) annual effective dose rate (AEDR), external hazard index ( $H_{ex}$ ), annual gonadal dose rate (AGDR) and the excess life cancer risk (ELCR) and other radiological hazard parameters calculated and their variation with soil type are also presented in Tables 4.9-4.11. The mean calculated  $R_{eq}$  in S, T and M were 819, 1057, and 1645  $\text{Bqkg}^{-1}$ .

respectively. These values were all greater than the world average value and safety limit of 370 Bqkg<sup>-1</sup> (UNSCEAR, 2000; Suleiman *et al.*, 2018; Kolo *et al.*, 2019).

**Table 4.9: Radiological hazard indices due to NORM concentration in S samples**

Sample point ID	D (nGy/hr)	R <sub>eq</sub> (Bq/kg)	AEDR (mSv/y)	H <sub>ex</sub>	AGDE	ELCR (×10 <sup>-3</sup> )
S1	258.06	597.42	0.32	1.61	1.77	1.11
S2	238.34	547.10	0.29	1.48	1.64	1.02
S3	271.36	622.63	0.33	1.68	1.86	1.16
S4	298.59	677.01	0.37	1.83	2.04	1.28
S5	244.97	563.49	0.30	1.52	1.68	1.05
S6	669.17	1564.93	0.82	4.23	4.62	2.87
S7	192.88	442.67	0.24	1.20	1.33	0.83
S8	320.65	739.86	0.39	2.00	2.21	1.38
S9	618.60	1407.97	0.76	3.80	4.30	2.66
S10	445.65	1027.74	0.55	2.78	3.08	1.91

**Table 4.10: Radiological hazard indices due to NORM concentration in T samples**

Sample point ID	D (nGy/hr)	R <sub>eq</sub> (Bq/kg)	AEDR (mSv/y)	H <sub>ex</sub>	AGDE	ELCR
T1	422.85	971.65	0.52	2.62	2.93	1.82
T2	372.84	822.26	0.46	2.22	2.62	1.60
T3	208.54	480.07	0.26	1.30	1.43	0.90
T4	266.93	614.30	0.33	1.66	1.84	1.15
T5	119.14	268.50	0.15	0.73	0.82	0.51
T6	313.06	728.12	0.38	1.97	2.16	1.34
T7	553.11	1286.45	0.68	3.47	3.82	2.37
T8	594.37	1356.09	0.73	3.66	4.13	2.55
T9	349.08	810.62	0.43	2.19	2.41	1.50
T10	517.42	1206.97	0.63	3.26	3.57	2.22

The AEDR were also highest in M samples, while its value in T were greater than that in S. The mean AEDR were 0.44, 0.56 and 0.88 mSvy<sup>-1</sup> for S, T and M respectively. The mean values of the AEDR were all greater than the mean value of 0.07mSvy<sup>-1</sup> in normal soil (UNSCEAR, 2000). Furthermore, these values exceed the 1 mSvy<sup>-1</sup> and 1.5mSvy<sup>-1</sup> recommended by ICRP (2008) for maximum annual public and occupational exposure

respectively. Therefore, the mining site is not safe in terms of exposure to NORM. The average AGDE were 2.45, 3.14 and 4.94 mSv<sup>-1</sup> respectively for S, T and M. These values are much higher than the average value of 0.30 mSv<sup>-1</sup> in soil (Ademola, 2008; Xinwei *et al.*, 2006).

**Table 4.11: Radiological hazard indices due to NORM concentration in M samples**

Sample point ID	D (nGy/hr)	R <sub>eq</sub> (Bq/kg)	AEDR (mSv/y)	H <sub>ex</sub>	AGDE	ELCR (×10 <sup>-3</sup> )
M1	459.53	1050.90	0.56	2.84	3.14	1.97
M2	588.70	1352.17	0.72	3.65	4.06	2.53
M3	556.72	1292.32	0.68	3.49	3.83	2.39
M4	466.47	1067.92	0.57	2.88	3.22	2.00
M5	779.88	1823.24	0.96	4.92	5.38	3.35
M6	384.32	883.29	0.47	2.39	2.64	1.65
M7	752.29	1704.53	0.92	4.60	5.22	3.23
M8	569.01	1297.31	0.70	3.50	3.89	2.44
M9	507.04	1139.60	0.62	3.08	3.53	2.18
M10	699.03	1627.02	0.86	4.39	4.82	3.00
M11	1039.84	2368.12	1.28	6.40	7.19	4.46
M12	1452.10	3320.95	1.78	8.97	10.05	6.23
M13	879.12	2040.00	1.08	5.51	6.06	3.77
M14	726.20	1688.92	0.89	4.56	5.00	3.12
M15	623.37	1413.63	0.76	3.82	4.34	2.68
M16	515.55	1177.38	0.63	3.18	3.55	2.21
M17	618.60	1407.97	0.76	3.80	4.30	2.66
M18	1307.12	3025.74	1.60	8.17	8.99	5.61
M19	1408.60	3263.83	1.73	8.81	9.74	6.05
M20	225.33	513.38	0.28	1.39	1.54	0.97
M21	465.02	1076.41	0.57	2.91	3.21	2.00
M22	718.97	1656.34	0.88	4.47	4.96	3.09

For radiological safety,  $H_{ex}$  should be less than one (1). However,  $H_{ex}$  were all greater than one (1) for S, T and M. The mean value for the  $H_{ex}$  in S, T and M were 2.21, 2.84 and 4.44 respectively. These values are very high and they indicate that workers and inhabitant of the area where the mine is located who spend at least a fraction of 0.2 of their daily time in the mine have increase probability of having radiation induced disease such as cancer.

The probability of developing cancer for an adult who used all their lives in the area is measured by the magnitude of ELCR. The ELCR ( $\times 10^{-3}$ ) values for the mean concentrations of the three NORM were 1.52, 1.97 and 3.07 respectively for S, T and M. These averaged ELCR values were extremely higher than the world average value of  $0.29 \times 10^{-3}$  (UNSCEAR, 2000). This implies that anyone (miners, dwellers and others) staying or working in the mine field has more chances of developing cancer by a factor of at least 5 if they spent all their lives around the mine and live up to 70 years old.

The relative mean values for all the considered radiological parameters calculated for the soil classes are depicted in Figure 4.6. The observed differences in the hazard indices can be attributed to the NORM concentration in the different soil classes.

The linear correlation between NORM concentrations and all evaluated radiological hazard indices were analysed using the Pearson correlation coefficient. The Pearson's correlation coefficient is a statistical tool that measures the relationship between two continuous parameters. The coefficient assumes a number between -1 and 1 that indicates the level to which the variables are linearly associated. A value of 1 or -1 shows strong positive or negative linear correlation. The correlation of NORM concentration and hazard indices are presented in Table 4.12. From the Table, the hazard indices had strong linear and positive correlation with  $^{238}\text{U}$  and  $^{232}\text{Th}$  compared to  $^{40}\text{K}$ . The correlations are qualitatively shown in the spatial distribution of  $^{238}\text{U}$ ,  $^{232}\text{Th}$  and  $^{40}\text{K}$  (Figure 4.3-4.5) and that of ADR (Figure 4.7).

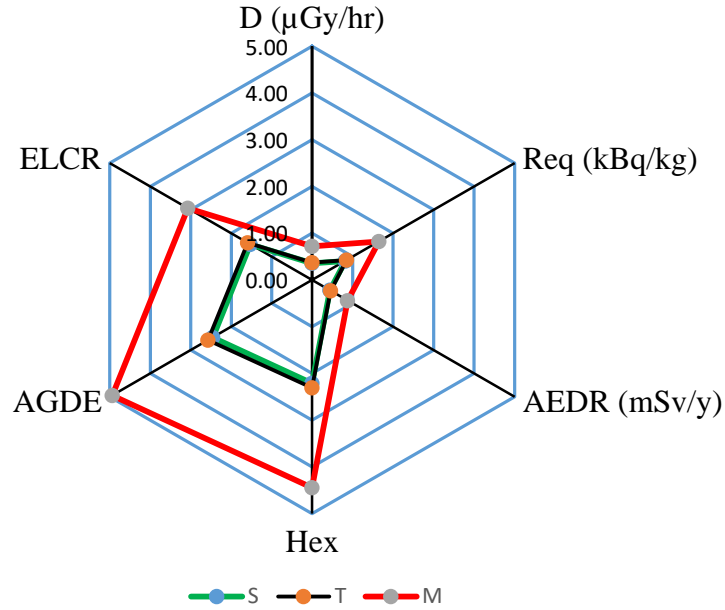


**Figure 4.6:** Variation of the mean radiological parameters of all the soil classes

**Table 4.12: Correlation coefficient between NORM and radiation safety indices**

	U-238	Th-232	K-40	ADR	Ra <sub>eq</sub>	AEDE	H <sub>ex</sub>	ELCR	AGDE
<sup>238</sup> U	1								
<sup>232</sup> Th	0.66	1							
<sup>40</sup> K	0.42	0.51	1						
ADR	0.77161	0.96	0.56	1					
Ra <sub>eq</sub>	0.7701	0.98	0.56	1	1				
AEDE	0.7716	0.98	0.56	1	1	1			
H <sub>ex</sub>	0.6663	0.98	0.56	1	0.99	0.99	1		
ELCR	0.7716	0.98	0.56	1	1	1	1	1	
AGDE	0.7716	0.98	0.56	1	1	1	1	1	1

Furthermore, linear regression analysis was depicted to show the correlation between in-situ and ex-situ (evaluated from NORM) ADR. A positive and good correlation was observed between the two ADRs. Figure 4.8 show the relationship between the ADRs with an R value of 0.74. The values of the *ex-situ* in comparison with the *in-situ* ADR were higher. The excess ADR from *ex-situ* data was attributed to high photon flux from <sup>238</sup>U, <sup>232</sup>Th and <sup>40</sup>K isotopes and sensitivity of the HPGe detector used compared to the survey meter. There are more uncertainties in field measurements (Rostron *et al.*, 2014).

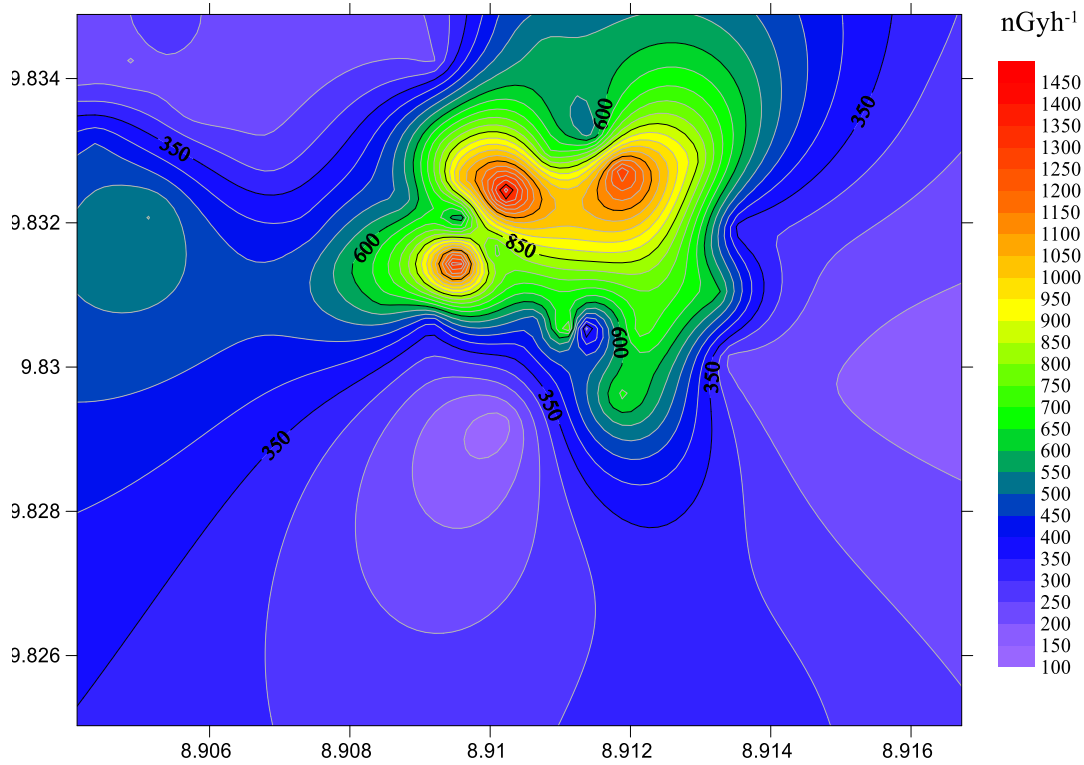


**Figure 4.7:** Spatial distribution of ADR due to NORM concentration in the mine

The spatial distribution of the absorbed dose rate in the study area is depicted in Figure 4.7. The high correlation observed between calculated ADR from radionuclide concentrations and uranium and thorium concentration was also observed. The spatial distribution of uranium and thorium presented in Figures 4.3 and 4.4 qualitatively correlated with the distribution map of ADR (Figure 4.7).

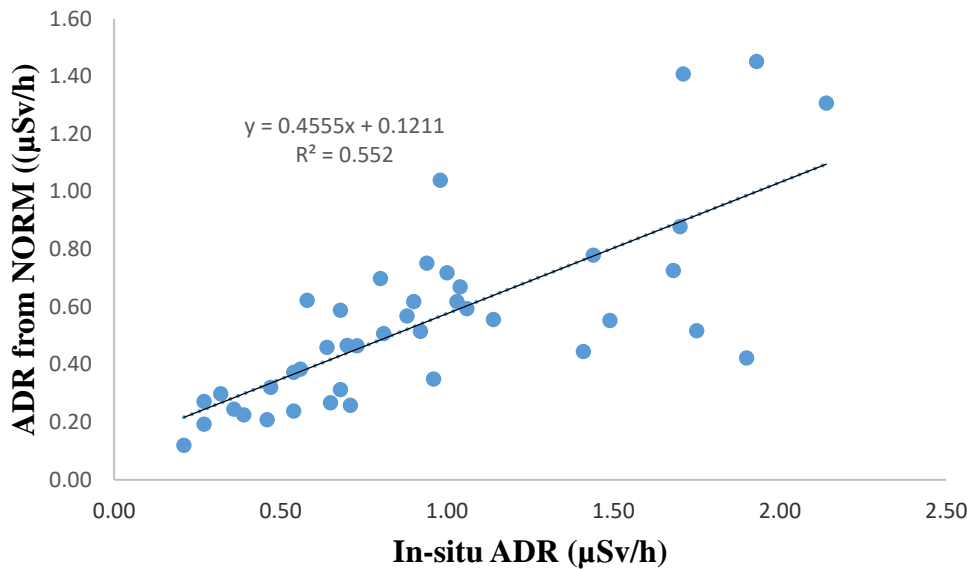


**Figure 4.8:** Relationship between *in-situ* ADR and *ex-situ* ADR

#### 4.4 Radiological Impact of NORM Concentration on Non- human Biota

The measured mean concentrations of NORM in this work are comparable to those of areas designated as high natural radioactive backgrounds (HINARs) such as the Niev Island in South Pacific (Mandery, 1960), Pecosde-Caldes in Brazil (Asmaral *et al.*, 1992). Other areas include sites of nuclear accidents such as the Fukushima and Chernobil areas. However, research on the populations of the HINARs (Fustes *et al.*, 2002; Mather and Moussesal 2013, Aliyu and Ramli, 2015) has revealed that the human, animal and plant populations suffer from radiation induced health defects. Such defects include point mutation, high frequency of diseases, change in immunology and physiology. Consequently, the ICRP (2009), IAEA (2011) and the UNSCEAR (2008) have set standard for the protection of non-human species in the environment from harmful effect of radiation.

In an attempt to access the radiological impact of tin mining at the Rayfield – Du tin mining field the ERICA (Version 1.2.1) computer code was adopted. In an earlier research

(Beresferd *et al.*, 2008), the exposure of small mammals situated in the designated exclusive zones of Chernobyl nuclear plant were evaluated using the ERICA tool. The obtained doses were found to be in good approximations to external doses obtained with thermo luminescent dosimeters. Consequently, result produced from the ERICA tool are reliable. In order to be consistent with regulating standards, the maximum value of the NORM concentration for all soil samples (S, T and M) was used to run a second tier ERICA impact assessment analysis. The TIER 2 procedure was used to evaluate the dose rate and risk quotients for amphibian, annelid, arthropod – detritivorous, bird, flying insect, grasses and herbs, lichen and bryophytes, mammals- large, mammals- small burrowing, mollusc – gastropod, reptile, shrub and trees. The limiting dose adopted for the assessment was the generally accepted screening dose of  $10 \mu\text{Gyh}^{-1}$  (Mather and Moussesal 2013; Aliyu and Ramli, 2015). Results of the second Tier ERICA analysis are presented in Figure 4.9 The risk quotient (expected and conservative are given in Table 4.13. The total dose rate per organism was 0.10, 0.91, 0.38, 0.04, 0.38, 8.96, 30.41, 0.09, 0.09, 0.91, 0.17, 3.60 and 0.15 for amphibian, annelid, arthropod – detritivorous, bird, flying insect, grasses and herbs, lichen and bryophytes, mammals- large, mammals- small burrowing, mollusc – gastropod, reptile, shrub and trees respectively.

All obtained dose rates were low compared to the  $40 \mu\text{Gyh}^{-1}$  often considered as a dose rate of significance to terrestrial animals according to the International Atomic Energy Agency (IAEA, 1992); UNSCAER (1996) and the United States Department of Energy (USDoE, 2002). This dose rate is often generally adopted by government and nongovernmental organisations for dose limit criterion for terrestrial organisms. Recent research has however shown that for lesser doses, terrestrial animal populations have produced measurable defects (Moller *et al.*, 2014; Moller and Mouseau, 2011). Thus the ERICA dose limit of  $10 \mu\text{Gyh}^{-1}$  was adopted for dose rate limit for the non-human biota in

this research. From the result, only one reference group (lichens and bryophytes) is predicted to have dose rate above the regulatory  $10 \mu\text{Gy h}^{-1}$  limit (shown as screening value in Figure 4.9).

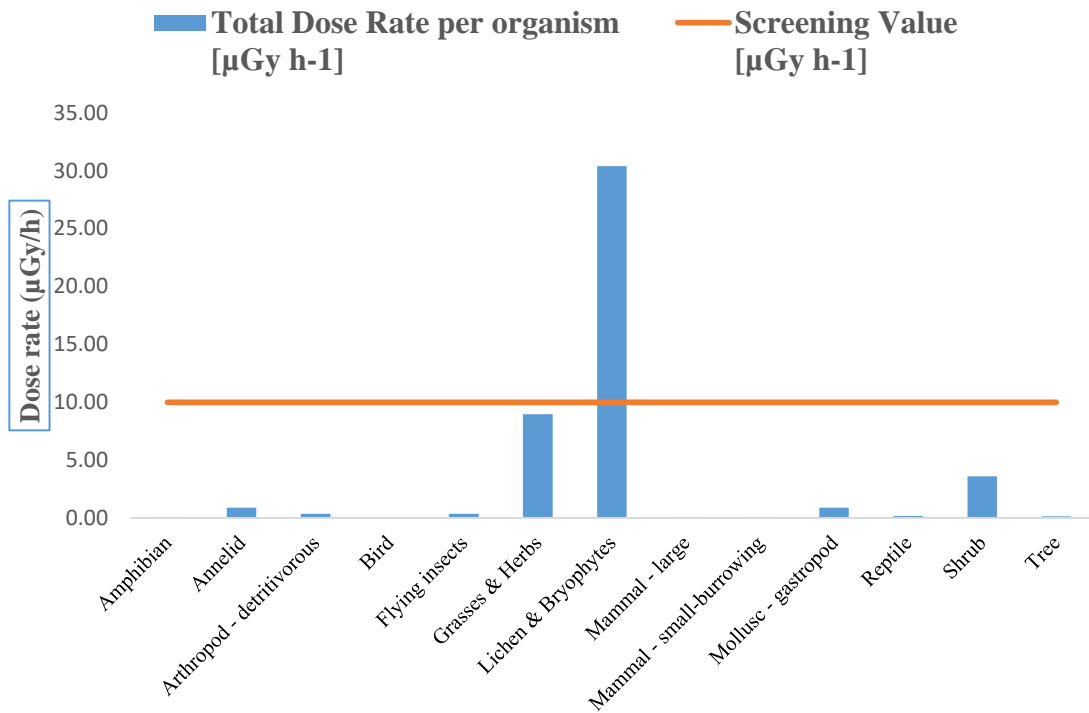


**Figure 4.9:** Total dose rate per organism calculated from ERICA

The dose rate of lichens and bryophytes is more than three times the high risk level. Consequently, this group of animals are considered at risk and of radiological concern. Next in the line of high dose rate exposure are the grasses and herbs followed by the shrubs. Although their dose rates are not in excess of the dose limit. All other groups are of no radiological risk of concern as indicated on Table 4.13. For organisms in which both the conservative and expected risk quotients are less than 1 (coloured in green), it implies the screening level was not exceeded and thus the risk to them are considered trivial. However, if one of the risk quotients is greater than 1 (coloured yellow), then there is potential risk to the non-human biota. Only the organism in which the two risk quotients are greater than 1 (coloured in red) are of considerable risk since their absorbed doses rate are higher than the screening level. It must however be noted that these estimates are

conservative and underestimated since radiation from other nuclides whose concentrations were not measured were ignored. If their radioactive level is considerable, then the dose presented in the simulation could be higher. The result of the dose received by non-human biota in this study has been found to be consistent with earlier result obtained using reported radionuclide data by Ibeanu (2003) and simulated by Aliyu *et al.* (2015).

**Table 4.13: Risk quotients for considered terrestrial organisms**

<b>Organism</b>	<b>RQ<sub>exp</sub></b>	<b>RQ<sub>Cons</sub></b>
Amphibian	0.01	0.03
Annelid	0.09	0.27
Arthropod – detritivorous	0.04	0.11
Bird	0.00	0.01
Flying insects	0.04	0.11
Grasses & Herbs	0.90	2.69
Lichen & Bryophytes	3.04	9.12
Mammal – large	0.01	0.03
Mammal - small-burrowing	0.01	0.03
Mollusc – gastropod	0.09	0.27
Reptile	0.02	0.05
Shrub	0.36	1.08
Tree	0.02	0.05

#### 4.5 Heavy Metals Concentrations and Pollution Indices

Heavy metals (HM) have been associated with the mineral ores found and mined in the Jos Plateau area (Aduke-Brown and Ngozi, 2004). The HM analysis of the ten (10) soil: S (3), M (4), and T (3) (representing normal soil, tailing and mineral soils respectively) collected from the mine under study are presented in Table 4.14. The total average concentrations of the HM for all soils collected are given in Table 4.14 as well. Of all the metals investigated only Cr, Cu, Zn and Pb was commonly detected above the detection level (<0.01 mg/kg) in all the soil samples, while the concentrations of the remaining HM (Co, As, Cd, and Ni) were below detection level (BDL) in some soil samples.

**Table 4.14: Mean Heavy metal concentration in S, M and T soil samples and pollution indices**

Soil Category	Heavy Metal Concentration $\pm 0.01$ (mg/kg)							
	Cr	Cu	Zn	Pb	Co	As	Cd	Ni
S5	12.00	260.45	600.30	21.00	3.80	1.84	0.01	0.02
S6	40.30	380.00	320.00	88.87	BDL	BDL	2.56	0.84
S8	55.00	250.00	160.00	44.41	BDL	BDL	BDL	BDL
M1	387.54	200.24	104.40	450.20	BDL	BDL	BDL	BDL
M3	486.33	350.24	70.87	87.76	BDL	BDL	BDL	1.20
M4	2.43	180.00	130.46	680.00	7.48	0.88	BDL	BDL
M8	246.00	160.00	258.12	150.78	0.35	0.88	BDL	0.38
T1	58.34	21.00	4.64	450.45	BDL	BDL	2.11	0.05
T4	53.46	170.00	130.21	85.00	BDL	BDL	2.85	BDL
T8	170.00	330.12	583.77	300.00	BDL	4.12	BDL	2.60
Mean (All)	151.14	230.21	236.28	235.85	3.88	1.93	1.88	0.85
TV (DPR)	100	36	140	85	20	1	0.8	35
$CI_i$ (All)	1.51	6.39	1.69	2.77	0.19	1.93	2.35	0.02
$T_i$	2	5	1	5	5	10	30	5
$E_i$ (All)	3.02	31.97	1.69	13.87	0.97	19.30	70.59	0.12

BDL-Below detection level; TV- Target Value; DPR- Department of Petroleum Resources

The concentration of Cr, Cu, Zn, Pb, Co, As, Cd, and Ni in S Sample is 35.77, 296.82, 360.82, 51.43, 3.80, 1.84, 1.29, and 0.43 mg/kg. The corresponding mean concentration of these HM in M soils is 280.58, 222.62, 140.96, 342.19, 3.91, 0.88, <0.01 and 0.79 mg/kg while that of T soil is 93.93, 173.71, 239.54, 278.48, 4.12, 2.48, <0.01 and 1.33 mg/kg accordingly.

#### 4.5.1 Soil heavy metal pollution indices

In order to assess the level of contamination of each species of metals, soil and the entire mining area, the HM contamination (CI), pollution load (PI), ecological risk index (E), and the total potential ecological risk indices were adopted.

The contamination index  $CI_i$  of the  $i^{th}$  metal was computed according to the equation (Curlik and Sevcik, 1999):

$$CI_i = C_i / C_{0i} \quad (4.2)$$

where  $C_i$  is the measured concentration of the  $i^{th}$  HM and  $C_{0i}$  is the concentration of background/reference value of the  $i^{th}$  HM. For this research, the reference value adopted for the HM was the Department of Petroleum resources (DPR, 2002) reference values for maximum allowable concentration HM in Nigerian soil. The DPR background values are given in Table 4.14. Also, the values for the concentration index of the HM are given in the Table 4.14. The values showed that all the HM considered have concentrations in excess of the reference value (i.e.  $CI > 1$ ), except for Co and Ni.

The pollution load index for all the heavy metals in each soil samples were evaluated via the equation (Edori and Kpee, 2017; Suleiman *et al.*, 2018):

$$PI = (\prod_{i=1}^n CI_i)^{\frac{1}{n}} \quad (4.3)$$

where  $n$ , is the number of associated metals considered. The value of  $PI$  is used to classify the HM pollution according to the following categories:

- i. For  $PI < 1$                       no pollution
- ii.  $1 \leq PI < 2$                     moderate pollution
- iii.  $PI > 2$                          extreme pollution

The  $PI$  is the index that is commonly used for comparing the level of HM pollution for a given site. From Figure 4.10, the  $PI$  of the considered HM were low in both normal soil (S) and mineral soil (M) while in the tailings samples, the HM pollution was moderate. This also is an indication of possible concentration of heavy metal in the tailings during

the mineral extraction processes. For the mine, the PI is slightly below 1 and thus, it is concluded that there is no heavy metal pollution of the mine.

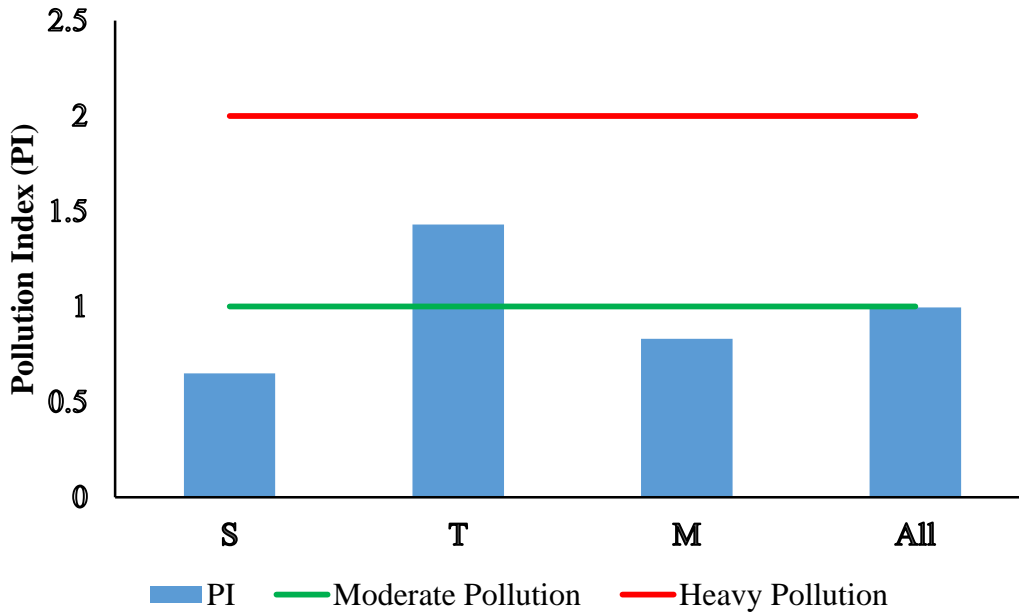


**Figure 4.10:** Pollution index of HM in the S, T and M soils

The ecological risk factor ( $E_i$ ) due to a particular heavy metal pollution refers to concentration level that might affect soil biological processes, and plant functional structure. According to Hakanson (1980); and Edori and Kpee (2017), the  $E_i$  can be calculated via the equation:

$$E_i = T_i C_i \tag{4.4}$$

here,  $T_i$  is the toxic response factor for a specific HM. The values of the toxic factors of all the metals considered are presented in Table 4.14, the  $E_i$  values are categorized according to the following tiers: for  $E_i < 40$ , the potential ecological risk is regarded as low; for  $40 \leq E_i < 80$ , the risk is said to be moderate; for  $160 \leq E_i < 320$ , the risk is said to be very high. The ecological risk of the considered heavy metals in each category of soil and site can be assessed via the use of the total potential ecological risk index ( $RI$ ). The  $RI$  can be calculated according to the equation (Curlik and Sefcik, 1999):

$$RI = \sum_{i=1}^n E_i \quad (4.5)$$

The RI are graduated also according to the following rules: for  $RI < 150$ , the risk is low;  $150 \leq RI < 300$ ; the ecological risk is moderate; while for  $300 \leq RI < 600$ , the risk is considerable and for  $RI > 600$ , the risk is said to be very high.

The potential ecological risk of all the HM considered were found to be low except for Cd which has a moderate risk value Table 4.14. Also the total *PI* result (Figure 4.11), showed that its value in S and M samples can be categorised as low risk while, its value in the T sample can be categorized as moderate. Hence the potential ecological risk of the HM species considered can be regarded as low.

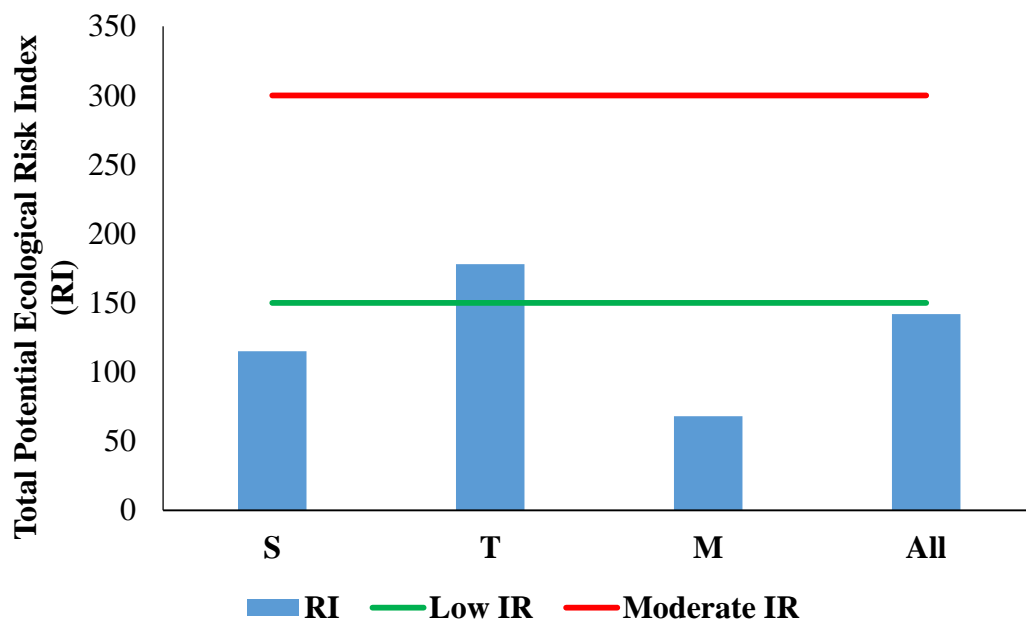


**Figure 4.11:** Potential ecological risk index of the HM in soil.

## CHAPTER FIVE

### CONCLUSION AND RECOMENDATIONS

#### 5.1 Conclusion

In this study, the level of terrestrial gamma radiation, NORM specific activities, absorbed dose to human and nonhuman components and other radiation hazard indices of soil, samples collected at Rayfield – Du area of Jos Plateau Nigeria were measured and analysed. The measured in-situ terrestrial background dose rate in the mine site were found to be above recommended safety limits. All derived radiological hazard index from the measured in-situ dose were mostly found to be in excess of world average and regulatory limits. In order to ascertain radioisotope distribution in the mine site, three groups of soil samples (soil, tailings and mineral) were collected and analysed for their  $^{40}\text{K}$ ,  $^{232}\text{Th}$  and  $^{238}\text{U}$  content using a well calibrated HPGe detector. The mean activity concentration of  $^{40}\text{K}$ ,  $^{232}\text{Th}$  and  $^{238}\text{U}$  together with their corresponding absorbed dose rate, annual effective dose rate, and estimated life cancer risk were greater than the world average and safety limits. The high value of radioisotopes and calculated mean value of radiological hazard indices were attributed to the geology, and geochemical definition of the area. The influence of the mining activities of the mine is another factor responsible for the evaluated radioisotope level. The activities of primordial radioisotope level obtained in the mine were comparable with those obtained in similar research in Jos area and areas designated as high background radiation areas by the UNSCEAR (2000). Furthermore, a strong correlation existed between  $^{232}\text{Th}$  and  $^{238}\text{U}$  in mineral soil, tailings and mine soil indicated common ore bearing sources.

The radio ecological dose rate estimated for non-human biota in the mine revealed that all non-human species except lichen and bryophyte had absorbed dose rate less than the 10

$\mu\text{Gyh}^{-1}$  screening dose. Consequently, all considered organisms except lichen and bigophytes are radiologically safe within the mining area from radiation induced defects.

Generally, the potential of developing radiation induced health defects (such as cataract and cancer) as a result of high absorbed dose rate to the miners, and other categories of people living or working in the mine is very high.

The analysis of eight heavy metals (Cr, Cu, Zn, Pb, Co, As, Cd, and Ni) concentrations showed that they are above the Nigerian reference level except for Co and Ni. Also employing the index model, the pollution and ecological risk indices of the heavy metals concentrations were classified as low for the Rayfield-Du mine in Jos, Nigeria.

## **5.2 Recommendations**

In view of the high level of radiation recorded within the mining field studied in this research, remedial actions towards reducing the absorbed radiation dose rates in the area by local authorities are urgently required. This would protect both man and the environment from the dangers associated with exposure to high level of ionising radiation. On the part of government, stakeholders, mine authorities, and regulatory bodies such as the Nigerian Nuclear Regulatory Authority (NNRA), the following recommendations are suggested:

- (i) Proper tailing management disposal should be encouraged at the mine sites to prevent local population around the mine who are presently using the waste (tailings) for building and farming from doing so.
- (ii) Due to weather and human factors, particles carrying significant amount of radioisotopes can be inhaled or deposited in food items. Thus mining activities in the area under study needs to be regulated by appropriate authorities with the

cardinal principles of reclamation, rehabilitation and restoration so as to ensure the retention of biodiversity and sustainability of public health.

Although the present study did not address the potential risk related to contamination of human diet in the area due to radionuclides, the high level of NORM and subsequent radiation level obtained in this research present such possibility. Consequently, further research on the impact of the mining activities on the food grown and consumed in the area is recommended. In addition to this, the following recommendations are also suggested for further research.

- (i) The extent of surface and underground water pollution by radionuclides, and heavy metal released and possibly leached from the mine soil needs to be investigated.
- (ii) In order to assess the radiological risk to dwellers around the mine, the internal absorbed dose rates in houses close to the mine and those built with tailings from the mine need to be evaluated.
- (iii) Mine workers and dwellers around the mine are potential candidate for high radon gas inhalation which is the leading cause of lung cancer among non-smokers. Since high uranium and thorium activities implies high radon gas concentration; thus radon gas measurement and inhalation is required within and around the mine so as to evaluate the level of internal radiological contamination of the public.
- (iv) Because of the high level of radiation in the mine, as a matter of urgency, epidemiological study of radiation induced sickness is recommended to be carried out on the population of Rayfield-Du area of Jos.

## REFERENCES

- Abba, H. T., Hassan, W. M., & Saleh, M. A. (2018). Evaluation of environmental natural radioactivity levels in soils and ground water of Baarkin Ladi, Plateau State. *Malaysian Journal of Fundamental and Applied Science*, 14(3), 338-342.
- Abdulahi, M. A. (2009). Gamma-ray spectrometry of naturally occurring radioactive materials (NORM) from Birnin Gwari artisanal goldmine of Kaduna State, Nigeria. M. Sc. Thesis, Department of Physics, Ahmadu Bello University, Zaria, Nigeria. <http://kubanni.abu.edu.ng/jspui/handle/123456789>
- Adegboye. M. A. (2012). Effect of mining on farming in Jos South Local Government Area of Plateau State. *Journal of soil science and Environment Management* 3(4); 77- 83.
- Adekoya, J. A. (2003). Environmental effect of solid minerals mining in Kenya. *Journal of Physical Science*. PP 625-640.
- Ademola, J. A., & Farai, I. P. (2006). Gamma activity and radiation dose in concrete building blocks used for construction of dwellings in Jos, Nigeria. *Radiation Protection Dosimetry* 121 (4), 395–398.
- Ademola, J. A. (2008). Exposure to high background radiation level in the tin mining area of Jos, Plateau, Nigeria. *Journal of Radiation Protection* 28, 93 – 99.
- Adewale, O. O., Tubosun, I. A., & Go, J. O. (2015). Assessment of terrestrial naturally occurring radioactive material in soil and mine tailings of Awo and Ede, Osun – State, Nigeria. *Ife Journal of Science* 17(1), 199 – 209.
- Adiuku-Brown, M. E., & Ogezi, A. E. (2004). The utilization of mill tailings on Jos Plateau: A need to exercise some restraint. *African Journal of Natural Science* 7: 1-8.
- Agbalagba, E. O., & Onoja, R. A. (2011). Evaluation of natural radioactivity in soil, sediment and water samples of Niger Delta (Biseni) flood plain lakes, Nigeria. *Journal of Environmental Radioactivity*, 102(7), 667–71.
- Ajayi, I. R. (2008). An evaluation of the equivalent dose due to natural radioactivity in the soil around the consolidated tin mine in Baukuru-Jos, plateau state of Nigeria. *Iran Journal of Radiation Research*. 5:203–206.
- Akanbi, E. S. (2014). Map Integration to Locate Potential Cassiterite Deposits in Parts of North Central Nigeria. Naraguta Sheet 168, PhD Thesis, University of Jos, Nigeria.
- Aliyu, A. S., & Ramli, A. T. (2015). The world's high background natural radiation areas (HBNRAs) revisited: A broad overview of the dosimetric, epidemiological and radiobiological issues. *Radiation Measurements* 73: 51–59.
- Amaral, E. C. S., Rochedo, E. R. R., Paretzke, H. G. & Franca, E. P. (1992). The radiological impact of agricultural activities in an area of high natural radioactivity. *Radiation Protection Dosimetry* 45: 289–292.
- Arogunjo, A. M., Hollriegl, V., Gusseni, A., Leopold, K., Gesstmaan, U., Veroneses I., & Deh, U. (2009). Uranium and thorium in soils, mineral sands, water and food

- samples in a tin mining area in Nigeria with elevated activity. *Journal of Environmental Radioactivity* 100, 232-240
- Badejo, T. A. (1975). Evidence of magmatic differentiation in the origin of the younger granites of Nigeria *Journal of Mining Geology*. 10, 67.
- Beir, V. (1970). Health effects of exposure to low level of ionizing radiation committee on the Biological Effects of Ionizing Radiation National Research Council National Academy Press Washington, DC.
- Bek-Uzarov G. N., Teterin, Y. A. & Vukchevich, K. E. (2003). Human body internal radionuclide contamination measurement protocol. *Rom Journal of Physics* vol. 48, No. 1 – 4: 59 – 66.
- Beresford, N. A., Gaschak, S., Barnett, C. L., Howard, B. J. Chizhevsky, I., Strømman, G., ... Copplestone, D. (2008). Estimating the exposure of small mammals at three sites within the Chernobyl exclusion zone—A test application of the ERICA Tool. *Journal of Environmental Radioactivity* 99, 1496–1502.
- Beretka, J., & Mathew, P. J. (1985). Natural radioactivity of Australian building materials, industrial wastes and by-products. *Health Physics*. 48 87–95
- CDC. (2015). Centres for Disease Control and Prevention reviewed December 7, 20015
- Cember, H. (1996). *Introduction to Health Physics* (3rd Edition). New York: McGraw–Hill Medical.
- Choppin, G, Liljenzin, J. O, & Rydberg, J. (2006). *Radiochemistry and Nuclear Chemistry*. United Kingdom: Elsevier Press, Oxford.
- Cooper, N. (2002). Tin mining in the Jos Plateau. Open educational resources 230. <http://scholarworks.uni.edu/oermaterials/230>. Accessed 24<sup>th</sup> May, 2019).
- Deng, W., Tian, K., Zhang, Y., & Chen, D. (1997). Radioactivity in zircon and building tiles. *Health Physics* 73, 369–372.
- De-Wet, P. D. (1996). The occurrence and bio-accumulating of Selected metals and radionuclides in aquatic and terrestrial ecosystem on the water sand, Unpublished PhD. Thesis, and Africans University, Johannesburg.
- Douglas, M. N. (2008). Measurement of heavy metals and natural radioactivity levels in soils around the titanium mining site in Kwale district. M.Sc. Thesis, Institute of Nuclear Science and Technology, University of Nairobi.
- Dowdall, M., Vicat, K., Frearson, I., Gerland, S., Lind, B., & Shaw, G. (2004). Assessment of the radiological impacts of historical coal mining operations on the environment of Ny-Alesund, Svalbard. *Journal of Environmental Radioactivity* 71(2): 101-114
- DPR (2002). Environmental guidelines and Standards for the petroleum industries in Nigeria. Department of Petroleum Resources, Ministry of Petroleum and Mineral Resources Abuja, Nigeria
- Eric, J. H. (1984). *Radiation and Life* (2<sup>nd</sup> Edition). New York: Pergamon Press.
- Falconer, J. D. (1921): The Geology of Plateau Tin Fields. Geological Survey of Nigeria

- Falconer, J. D., Raeburn, C., & Bain, A. D. (1926). The Southern Plateau Tin Fields.
- Felix, B. M., Paulus, L. M., & Jwanbot, I. D. (2015). Natural radioactivity concentration and effective dose rate from Jos tin mining dumpsites in Rayfield, Nigeria; *Journal of Environment and Earth Science* 5, 12-25.
- Forster, L., Forster, P., Lutz-Bonengel, S., Willkomm, H. & Brinkmann, B. (2002). Natural radioactivity and human mitochondrial DNA mutations. *Proceedings of the National Academy of Sciences* 99: 13950–13954.
- Fred, A. M., & Robert, D. M. (1985). *Medical Effect of Ionizing Radiation*. Orlando, Florida: Grune and Stratton.
- Funtua, I. I., & Elegba, S. B. (2005). Radiation exposure from high-level radiation area and related mining and processing activities of Jos Plateau, Central Nigeria. *International Congress Series* 1276: 401-412
- Geological Survey of Nigeria (1963). Geology map of Naraguta, sheet 168.
- Hakonson-Hayes, A. C., Fresquez, P., & Whicker, F. (2002). Assessing potential risks from exposure to natural uranium in well water. *Journal of Environmental Radioactivity*, 59(1), 29-40.
- Haridasan, P. P., Paul, A. C., & Desai, M. V. M. (2001). Natural radionuclides in the aquatic environment of a phosphogypsum disposal area. *Journal of Environmental Radioactivity* 53, 155–165.
- Hartley, B. M. (2001). The measurement of radiation levels in Australian zircon milling plants. *Health Physics*, 80(1), 16–23.
- Herman, C. (1996). *Introduction to Health Physics* (3rd Ed.). New York: Megrano.
- Hiroshima and Nagasaki committee for the compilation of materials on damage caused by the atomic Bombs in Hiroshima and Nagasaki, Ed, Hiroshima and Nagasaki. (1981) (Basic Books, New York)
- Hodder, B. W. (1959). Tin mining in the Jos Plateau of Nigeria. *Economic Geography*, 35 (2), 109 – 122.
- Hofman, J., Leicht, R., Wingender, H. J., Worner, J. (2000). Natural radionuclide concentrations in materials processed in the chemical industry and the related radiological impact. *Report EUR 19264*.
- [Http://www.jsttor.org/stable/142.394](http://www.jsttor.org/stable/142.394). Accessed on October, 30, 2015, 15:20 UTC.
- IAEA (1974) Activities of the International Laboratory of Marine Radioactivity Report IAEA.
- IAEA (1983b). Safety Standards Series Occupational Radiation Protection Technical Document Pp. 100 No. RS-G1.1 *Vienna*.
- IAEA (1996). International Basic Safety Standard for protection against Ionising Radiation and for the safety of radiation sources, safety series No 115, *IAEA Vienna*.

- IAEA (1992). Effects of ionising radiation on plants and animals at levels implied by current radiation protection standards. Technical Reports Series No. 332. Vienna: International Atomic Energy Agency.
- IAEA (2006 b). Remediation of Sites with Dispersed Radioactive Contamination Technical Reports Series No 424.
- IAEA (2005). Naturally occurring radioactive materials (iv), Proceedings of an International Conference held in Szezyrk, *IAEA TEC DOC-1472, Poland*.
- IAEA (2011). Basic Safety Standard. Vienna: International Atomic Energy Agency.
- IAEA (2012). Modelling Radiation Exposure and Radionuclide Transfer for Non-human Species Report of the Biota Working Group of EMRAS Theme 3.
- IARC (2012). A specific spectrum of Pp53 Mutations in Lung Cancer from non-smokers. *Science Publication No. 161*.
- Ibeanu, I. (1999). Assessment of radiological hazards of tin mining and ore processing in Jos, Nigeria. International Symposium on Restoration of Environments with Radioactive Residues. *International Atomic Energy Agency SM-359*, 86-91.
- Ibeanu, I. (2003). Tin mining and processing in Nigeria: Cause for concern. *Journal of Environmental Radioactivity* 64, 59–66.
- ICRP (1977). Radiation Protection in Uranium and other mines, Vol. 1, No. 1, Pergamon Press, Oxford. Pp. 71-90.
- ICRP (1991). 1990 recommendations of the International Commission on Radiological Protection, ICRP Publication 60, Pergamon Press, Oxford.
- ICRP (1996) International Commission for Radiation Protection Age-dependent doses to members of the public from intake of radionuclides. Ingestion and inhalation coefficients, ICRP Publication 72 (Ann. ICRP 26 (1)) (Oxford: Pergamon), 1996.
- ICRP (2003). Dose Coefficients for Non-human Biota Environmentally Exposed to Radiation. ICRP Publication IXX.
- ICRP (2003). A framework for assessing the impact of ionising radiation on non-human species. Publication 91. Amsterdam: Elsevier.
- ICRP (2007). 2006 Recommendations of the International commission on Radiological protection, ICRP publication 103, pergamon press, Oxford.
- ICRP (2009). Environmental protection: The concept and use of reference animals and plants [dosimetry and effects]. Publication 108. Amsterdam: Elsevier.
- Idowu, O. O. (2013). Mineral Prospecting and Exploration; Resource Mining Utilization and Disaster, Disaster Risk Management University of Ibadan Pp 1- 9.
- International Atomic Energy Agency, (IAEA) (1982). Generic Models and Parameters for Assessing the Environmental Transfer of Radionuclides from Routine Releases, Exposure of Critical Groups. Safety Series No. 57, IAEA, Vienna.
- International Commission for Radiation Protection (ICRP) (1990). Annual limits of intake of radionuclides by workers based on the 1990 recommendations. A report from

- Committee 2 of the ICRP, ICRP Publication 61 (Ann. ICRP 21 (4)) (Oxford: Pergamon).
- International Commission for Radiation Protection (ICRP). Report of task group on reference man, ICRP Publication 23 (Ann. ICRP 4 (3-4) p III) (Oxford: Pergamon), 1975.
- Isikalu, M. R., Anoka, O. C., & Balogun, F. A. (2011). Radioactivity measurements of the Jos tin mine tailing in Northern Nigeria. *Archives of Physics Research* 2(2) 80-86.
- Jacobson, R.R.E., Webb, J.S., 1946. The pegmatites of central Nigeria. Geological Survey of Nigeria Bulletin 17.
- James, E. T. (1995). *Atoms Radiation and Radiation Protection* (2nd Edition). Weinheim: John Wiley and Sons.
- Jibiri, N. N., Alausa, S. K., & Farai, I. P. (2009). Assessment of external and internal doses due to farming in high background radiation areas in old tin mining localities in Jos-Plateau, Nigeria. *Radioprotection*, 44 (2), 139 -151.
- Jibiri, N. N., Alausa, S. K., Owofolaju, A. E., & Adeniran, A. A. (2011). Terrestrial gamma dose rate and physico-chemical properties of soil from ex-tin mining locations in Jos-Plateau, Nigeria. *African Journal of Environmental Science and Technology* 5(12), 9-17.
- Jibiri, N. N., Farai, I. P., & Alausa, S. K. (2007) Estimation of annual effective dose due to natural radioactive elements in ingestion of foodstuffs in tin mining area of Jos Plateau, Nigeria. *Journal of Environmental Radioactive*, 94, 31–40.
- Jwanbot, D. I., Izam, M. M., & Gambo, M. (2012). Measurement of Indoor Background Ionizing Radiation in Some Science Laboratories in University Of Jos, Jos – Nigeria; *Science World Journal*, 7 (2), 5-8
- Knoll, G. F. (2010). *Radiation Detection and Measurement* John Wiley and Sons Incorporation Fourth Edition PP 219, 365.
- Kolo, M. T., Khandaker, M. U., & Shuaibu, H. K. (2019). Naturally radioactivity in soils around mega coal-fired cement factory in Nigeria and its implication on human health and environment. *Arabian Journal of Geosciences*, 12(15), <https://doi.org/10.1007/s12517-019-4607-6>
- Loveland, W., Morrissey, D. J., & Seaborg G. T. (2006). *Modern Nuclear Chemistry*, Wiley, New Jersey.
- Lind, O. C., Stegnar, P., Tolongutov, B., Rosseland, B. O., Strømman, G., Uralbekov, B., ... B. Salbu. (2013). Environmental impact assessment of radionuclide and metal contamination at the former U site at Kadji Sai, Kyrgyzstan. *Journal of Environmental Radioactivity* 123: 37–49.
- Mackay, R. A., Greenwood, R., & Rockingham J. E. (1949). *The Geology of the Plateau Tinfields*. Kaduna: Geological Survey of Nigeria.
- Macleod, W. N., Turner, D. C., & Wright, E. P. (1971). *The Geology of the Jos Plateau*. Lagos: Geological Survey of Nigeria.

- Mangset, W. E., & Sheyin, A. T. (2009). Measurement of radionuclide in processed mine tailings in Jos, Plateau State. *Bayero Journal of Pure and Applied Science* 2(2) 56-60.
- Masok, F. B., Ike-Ogbonna, M. I., Dawam, R. B., Jwanbet, D. I., & Yenle, N. M., (2015). Cancer risk due to radionuclide concentration in tin ore and sediments at Barkin Ladi, Plateau State, North Central, Nigeria. *International Journal of Environmental Monitoring and Analysis* 3(5), 260-264.
- Masok, F. B., Paulus, L. M., & Jwanbot, I. D. (2015). Natural radioactivity concentration and effective dose rate from Jos tin mining dump sites in Rayfield, Nigeria. *Journal of Environment and Earth Science* 5(12): 33-39
- Marsden, E. (1960). Radioactivity of soils, plants and bones. *Nature* 187: 192–195.
- Mohanty, A. K., Sengupta, D., Das, S. K., Saha, S. K., & Van, K. V. (2004). Natural radioactivity and radiation exposure in newly discovered high background radiation area on the easter coast of Orissa, India. *Radiation Measurement* 38: 153-165.
- Moller, A. P., Bonisoli-Alquati, A., Mousseau, T. A., & Rudolfson, G. (2014). Aspermy, sperm quality and radiation in Chernobyl birds. *PLoS ONE* 9: e100296.
- Moller, A. P., & Mousseau, T. A. (2011). Efficiency of bio-indicators for low-level radiation under field conditions. *Ecological Indicators* 11: 424–430.
- Moller, A.P., & Mousseau, T. A. (2013). The effects of natural variation in background radioactivity on humans, animals and other organisms. *Biological Reviews* 88: 226–254.
- Moody, K. J., Hutcheon, I. A., & Grant, P. M. (2005). *Nuclear Forensic Analysis*. Boca Raton: CRC Press.
- Musa, H. D., & Jiya, S. N. (2011). An assessment of mining activities impact on vegetation in Bukuru Jos Plateau State Nigeria using normalised differential vegetation index (NDVI). *Journal of Sustainable Development* 4(5), 150-159.
- National Research Council Committee on the Biological Effect of Ionising Radiation (1990). *Health Effects of Exposure to low level of Ionising Radiation*, Beirv, and National Academy Press, Washington. D.C.
- NCRP (1971). Basic radiation protection crieteria, Report Number 39. (NCRP Publications, 7910 Woodmont Avenue, Bethesda, MD 20814).
- NCRP (1990). Report No 107 – Implementation of the Principle of As low As Reasonably Achievable (ALARA) for Medical and Dental Personnel.
- NCRP (National Council on Radiation Protection and Measurements). (1975). *Natural Background Radiation in the United States*. *NCRP Report No.45*. NCRP, Washington, D.C
- Odoh, R., Ogah, E., Oko, O. J., Yebpella, G. G., & Magomya, A. M. (2018). Assessment of some physico-chemical parameters of drinking water sources, in Okpokwu and Ogbadibo areas of Benue State. *Sci-Afric Journal of Scientific Issues, Research and Essays* 5(1), 001-005.

- Odusote, O. O., Alausa, S. K., & Gyang, B. N. (2014). Radionuclide concentration and impact assessment of the Jos tin mining soil residues. *The Nucleus* 51 No. 1 (1-7).
- Olarinoye, I. O., Sharifat, I., & Kolo, M. T. (2010). Heavy Metal content of soil samples from two major dumpsites in Minna. *Natural and Applied Science Journal*, 11(1), 13-21.
- Olise, F. S., Oladejo, O. F., Almeida, S. M., Owoade, O. K., Olaniyi, H. B., & Freitas M. C. (2014). Instrumental neutron activation analyses of uranium and thorium in samples from tin mining and processing sites. *Journal of Geochemical Exploration*. 142, 36-42.
- Olise, F. S., Owoade, O. K., Olaniyi, H. B., & Obiajunwa, E. I. (2010). A complimentary tool in the determination of activity concentrations of naturally occurring radionuclides. *Journal of Environmental Radioactivity*, 101, 910-914.
- Onwoka, S. U., Duluora, J. O., & Okoye, C.O. (2013). Socio-economic impacts of tin mining in Jos Plateau State Nigeria. *International Journal of Engineering and Science Invention* 2(7), 30-34.
- Onyeanauna, G. C. (2016). Interpretation of ring structures in Jos Plateau using Nigeria Sat 1 imagery. *International Journal of mathematics and physical sciences Research*, 4(2), 95-104.
- Paul, T., Michael, J. P., & Monika, F. (1999). Combined effects of space flight factors and radiation on humans. *Mutation Research* 430: 211–219.
- Patel, J. P. (1991b). Environmental Radiation Survey of the Area of High Natural Radiation of Mrima Hill of Kenya, M.Sc. Thesis, University of Nairobi.
- Patterson, G. (1986). Lake Pidong. A preliminary survey of a Volcanic Crater Lake Durham! Department of Geography. University of Durham.
- Reilly, D., Ensslin, N. & Smith, H. (1991). Non-destructive Assay of Nuclear Materials, *National Technical Information services*, Springfield. VA.
- Ramlia, T., Wahab, A., Hussein, M. & Wood, A., (2005). Environmental <sup>238</sup>U and <sup>232</sup>Th concentration measurements in an area of high level natural background radiation at Palong, Johor, Malaysia. *Journal Environmental Radioactivity*. 80, 287–304.
- Rostron, P. D., Heathcote, J. A., & Ramsey, M. H. (2014). Comparison between in situ and ex situ gamma measurements on land areas within a decommissioning nuclear site: a case study at Dounreay. *Journal of Radiation Protection*, 34(3): 495-508
- Sato, J. & Endo, M. (2001). Activity ratios of uranium isotopes in volcanic rocks from Izumariana-Island-Arc volcanoes, Japan. *Journal of Nuclear and Radiochemical Sciences* Vol. 2, No. 1-2, pp. 1-3.
- Sulaiman, M. B., Saturaki, A. H., & Babayo, A. U, (2018). Ecological risk assessment of some heavy metals in roadside soil at traffic circles in Gombe, Northern Nigeria. *Journal of Applied Science and Environmental Management*, 22(6), 999-1003.
- Suleiman, I. K., Agu, M. N., & Onimisi, M. Y. (2018). Evaluation of naturally occurring radioactivity in soil samples from Erena mining sites in Niger State, Nigeria. *Current Journal of Applied Science and Technology*, 27(6), 1-12, <https://doi.org/10.9734/cjast/2018/41562>

- SIPRI (1981). *World Armaments and Disarmament Year Book*. No 4 John Street London: Taylor & Francis Ltd.
- Geoscience Survey of Nigeria Publication. Tin Fields-Resurvey 1945-1948. *Bulletin Geological Survey, Nigeria*, no. 19.
- Torudd, J., & Saetre, P. (2013). Assessment of long-term radiological effects on plants and animals from a deep geological repository: No discernible impact detected. *Ambio* 42:506–516.
- Turner, D. C. (1976). *Structure and Petrology of the Younger Granite Ring Complexes of Nigeria*. In *Geology of Nigeria* edited by Kogbe, C.A. Lagos Nigeria: Elizabethan Publication Company, Lagos Nigeria.
- UNSCEAR (1988). *Source and Effects and Risks of Ionizing Radiation*, UNSCEAR Report to the General Assembly, with scientific annexes. United Nations, New York.
- UNSCEAR (2000). *Exposures from Natural Sources of Radiation 2000 Report to General Assembly Annex B*, New York.
- UNSCEAR (2000). *Sources and Effects of Ionizing Radiation*, United Nations Scientific Committee on the Effect of Atomic Radiation Report Vol.1 to the General Assembly, with Scientific Annexes. United Nations Sales Publication, United Nations, New York,
- UNSCEAR (1996). *Sources and effects of ionizing radiation. Report to the general assembly with scientific annex A/AC.82/R.54*. Vienna: United Nations.
- UNSCEAR (2008). *Effects of ionizing radiation on non-human biota*. New York: United Nations Scientific Committee on the Effects of Atomic Radiation.
- USDoe (2002). *A graded approach for evaluating radiation doses to aquatic and terrestrial biota*. Technical Standard DoE-STD-1153-2002. Washington DC, USA.
- Wapwera, S. D., Ayanbimpe, G. N., & Odita, C. E. (2015). Abandoned mine, potential home for the people: A case study of Jos Plateau tin – mining region. *Journal of Civil Engineering and Architecture* 9, 429 – 445.
- Weekly Trust Newspaper, (Saturday 3rd December, 2011). Nigeria.
- WHO (1972). *World Health Organization, Health Hazards of the Human Environment* WHO, Geneva. Pp 273.
- Wright, J. B. (1976). *A Critical Review of the Geology of Nigeria*. Edited by Kogbe, C.A Elizabethan, Publisher Company, Lagos Nigeria, Pp309 – 317.
- www.lentech .com, September, 2010.
- Xinwei L, Lingquig W, Xiaodan J, Leipeng & Y, Gelian D (2006). Specific activity and hazards of Archeozoic–Cambrian rock samples collected from the Weibei area of Xhaanxi, China. *Radiation Protection Dosimetry* 118 (3):352–359.

APPENDIX A



Appendix A1 Active Mining site 1



Appendix A2 Residential house 150 m away from active mine site.2



Appendix A3 Active mine site 3



Appendix A4 Extracted tin mined



Appendix A5 Abandoned mine Site



Appendix A6 Goggle earth map of the study area



Appendix A7 Active mine site 4



Appendix A8 Active mine site 5